INFORMATION TO USERS

This reproduction was made from a copy of a document sent to us for microfilming. While the most advanced technology has been used to photograph and reproduce this document, the quality of the reproduction is heavily dependent upon the quality of the material submitted.

The following explanation of techniques is provided to help clarify markings or notations which may appear on this reproduction.

1. The sign or "target" for pages apparently lacking from the document photographed is "Missing Page(s)". If it was possible to obtain the missing page(s) or section, they are spliced into the film along with adjacent pages. This may have necessitated cutting through an image and duplicating adjacent pages to assure complete continuity.

2. When an image on the film is obliterated with a round black mark, it is an indication of either blurred copy because of movement during exposure, duplicate copy, or copyrighted materials that should not have been filmed. For blurred pages, a good image of the page can be found in the adjacent frame. If copyrighted materials were deleted, a target note will appear listing the pages in the adjacent frame.

3. When a map, drawing or chart, etc., is part of the material being photographed, a definite method of "sectioning" the material has been followed. It is customary to begin filming at the upper left hand corner of a large sheet and to continue from left to right in equal sections with small overlaps. If necessary, sectioning is continued again—beginning below the first row and continuing on until complete.

4. For illustrations that cannot be satisfactorily reproduced by xerographic means, photographic prints can be purchased at additional cost and inserted into your xerographic copy. These prints are available upon request from the Dissertations Customer Services Department.

5. Some pages in any document may have indistinct print. In all cases the best available copy has been filmed.

University Microfilms International
300 N. Zeeb Road
Ann Arbor, MI 48106

FUKUMORI, EIJI

WELLS IMAGED ABOUT AN INTERFACE: A MATHEMATICAL MODEL.

THE UNIVERSITY OF ARIZONA, M.S., 1982

WELLS IMAGED ABOUT AN INTERFACE:
A MATHEMATICAL MODEL

by

Eiji Fukumori

A Thesis Submitted to the Faculty of the

DEPARTMENT OF CIVIL ENGINEERING AND ENGINEERING MECHANICS

In Partial Fulfillment of the Requirements
For the Degree of

MASTER OF SCIENCE

In the Graduate College

THE UNIVERSITY OF ARIZONA

1 9 8 2

STATEMENT BY AUTHOR

This thesis has been submitted in partial fulfillment of requirements for an advanced degree at The University of Arizona and is deposited in the University Library to be made available to borrowers under rules of the Library.

Brief quotations from this thesis are allowable without special permission, provided that accurate acknowledgment of source is made. Requests for permission for extended quotation from or reproduction of this manuscript in whole or in part may be granted by the head of the major department or the Dean of the Graduate College when in his judgment the proposed use of the material is in the interests of scholarship. In all other instances, however, permission must be obtained from the author.

SIGNED: Eiji Fukumori

APPROVAL BY THESIS DIRECTOR

This thesis has been approved on the date shown below:

E. M. Laursen

E. M. LAURSEN
Professor of Civil Engineering
and Engineering Mechanics

8/2/82
Date

ACKNOWLEDGMENTS

The author wishes to express his most sincere gratitude and indebtedness to Professor Emmett M. Laursen for his supervision and guidance throughout the period of this study.

Sincere appreciation is extended to Professor Ralph M. Richard for supporting computer accounts and Mr. Sami A. A. Abed for providing experimental support for this study.

The author wishes to express his gratitude to Professor Akio Wake for manuscript review and enlightening discussions.

This study has been supported by the Department of Civil Engineering, the University of Arizona.

TABLE OF CONTENTS

TABLE OF CONTENTS -- Continued

LIST OF ILLUSTRATIONS

LIST OF ILLUSTRATIONS -- Continued

LIST OF ILLUSTRATIONS -- Continued

LIST OF TABLES

ABSTRACT

A mathematical model and numerical techniques were developed for analyzing the flow characteristics of aquifer with wells imaged about the interface of two immiscible fluids. The mathematical model is based on the concept of mass conservation and Darcy's law.

As a preliminary study, a two-dimensional steady state condition is considered. The finite element method and the boundary element method are employed to obtain the numerical solutions.

To demonstrate the numerical models, three types of domains in x-z plane are examined with different boundary conditions. In the boundary element method, wells are treated as point sources. One of the domains is bounded by a free surface and an impervious layer with a single well. The other domains consist of a free surface, an interface, an impervious layer, and two wells imaged about the interface. The computed results are compared with equations approximated by Dupuit theory.

CHAPTER 1

INTRODUCTION

The objective of this study is to develop a mathematical model and numerical solution techniques for simulating the flow behavior aquifer in response to simultaneous pumping of two stratified fluids from both sides of the interface. A typical application can be found in coastal aquifers where water supply wells are often contaminated by sea water because of the uncontrolled upconing of the interface. Conceptually, it can be envisioned that a simultaneous withdrawal of the underlying salt water by an additional well placed in the saline region under the fresh water well would result in an equal tendency for downconing with a net effect of the interface not being displaced. Despite its practical applicability and theoretically intriguing concepts, only a few groundwater investigators have touched on this solution to the problem to date. All of the previous work in this area is descriptive in nature and no mathematical modeling effort has been made.

One of the difficulties in modeling this problem is in the treatment of the interface between the two fluids. Except for the cases of petroleum-water interface, the

location of the interface cannot be clearly defined. There is always a transition zone of finite thickness between the fresh and saline waters. The thickness of the zone is a function of various local aquifer characteristics and the rates of pumpage themselves. The complete mathematical formulation and subsequent numerical treatment would be excessive for the present purposes. Furthermore, in view of the limited computer resources, such an approach would be prohibitively uneconomical. For the analysis of salinity intrusion in coastal aquifers, the assumption of a sharp interface is a widely accepted practice and is known to produce reasonable results.

In the present study which is a preliminary stage of a possible continued study of the two-well system, the existence of the transition zone is neglected and the two fluids are assumed to be immiscible, forming a sharp interface.

Even with this simplifying assumption, the mathematical formulation for the problem is highly nonlinear and solutions can be obtained only by a numerical approximation technique. Two well-known numerical methods, the finite element method and the boundary element method, have been tried in the present study.

CHAPTER 2

HISTORICAL DEVELOPMENT OF TWO-WELL SYSTEM

The interest at the University of Arizona in the two-well system imaged about the fresh/salt water interface began with a suggestion by Professor Emmett M. Laursen in the search for a master's thesis topic for a graduate student from Saudi Arabia, Sami A. A. Abed. Abed's thesis (1982), which was completed recently, tested the notion by means of a Hele-Shaw model; the concept worked with the indication that at least ten times as much fresh water could be obtained as from a single fresh-water well. The investigation reported upon herein is the second step in the investigation of the imaged wells: a mathematical model of the flow system. Another thesis is planned for the immediate future which will use a sand model to investigate the effect of the mixed transition zone between the fresh and salt water.

In the literature search for mathematical techniques which have been successful in this type of problem, several papers were found which describe something like the same idea. Most of the previous work dealt with the ordinary vertical wells in aquifers having fresh-saline interfaces. No mathematical modeling effort on the topic, however, was discovered.

Fader (1957) provided a comprehensive study of the groundwater level in southwestern Louisiana. The study included measurements of chloride content in the Chicot artesian aquifer. Using about 600 electrical logs of oil-test holes, Fader indicated that saltwater-freshwater interface was moving northward at a rate of about 50 feet per year and the chloride content in the water from one well increased from about 128 ppm to 530 ppm within a period of about 4 months because of heavy pumping. In order to prevent the migration of salt water into the supply well, Fader suggested the use of a scavenger well installed next to the supply well. The purpose of the scavenger well is to pump salt water or bracking water under the interface so that the chloride content in water from the supply well can be reduced and maintained at a fixed level. Fader also introduced an application of the scavenger well. The well, which is deeper than the supply well, does not penetrate into the salt water section. The benefit of the system will reduce the construction of the scavenger well.

Long (1965) continued to investigate the scavenger-well system, whose idea was introduced by Fader. His experiments at the town of Gonzales in Louisiana started with a single well. His report shows that the original chloride content was 10 to 12 ppm, and with a pumping rate of 400 to 500 gpm the concentration reached about 400 ppm after about

4 years. Also the report shows that the concentration was gradually increasing and reached 620 ppm at the end of the test. His report introduced a two-well system which consists of two pumps in one well. Fresh water and salt water in the well are effectively divided by making use of a packer between the pumps. Long indicated that chloride concent of water from the supply well ranged from 14 to 238 ppm, and from the scavenger well from 700 to 1,450 ppm. Long also indicated that it was possible to produce water, within yield limitations, of any desired chloride content between the minimum and maximum chloride of the water in the aquifer.

Underhill and Atherton (1964) discussed a double-pumping technique whose idea is similar to Fader's scavenger-well system. Their problem is to maintain the transition zone of fresh water/salt water in a coastal aquifer. If a transition zone is thick, then the upconing on the zone by pumping fresh water will be larger than on a thin transition zone since the density of the fluid of the upper part of the thick transition zone is thin, and the flow zone of the part is thicker than that in the thin transition zone. They also mentioned that the flow lines in the transition zone were maintained unchanged by adjusting the ratio of the fresh water/salt water pumping rates.

An interesting well system (doublet well) was invented by C. E. Jacob (1965) and was reviewed by Wickersham

(1977). The well consists of two pumps. One of the pumps, located in a fresh water region in an aquifer, the lower half of which contained saline water, is used for supplying water. The other pump, located right above the normal static interface, withdraws saline water and releases it from the bottom of the well so that the saline water will circulate between the outlet and the intake. As can be seen in many fluid mechanics texts, the concept of the doublet (sink and source) is used for making an imaginary body in a flow. It seems, therefore, that the salt water may still upcone and flow into the fresh water intake. The flow in the doublet well system may distort the streamlines as if there were a roughly spherical bulb of impermeable clay in this case. Mathes (1982) mentions a multi-well system for recovering spilled petroleum products trapped on top of the groundwater. The exact procedure of the system is not mentioned in the paper, but two pumps in the fresh water region are designed to depress the water table (pertoleum-water interface) in order to maintain the migration of petroleum products toward the well. The concept does not seem to be exactly the same as the imaged wells being studied here, but the effect on the flows might be rather similar.

The imaged-well system investigated mathematically in this study, and experimentally in Abed's study, consists of two horizontal wells in a symmetrical two-dimensional

domain. This system was chosen because of its relative simplicity both mathematically and experimentally. However, as Abed pointed out, it is the model of a possible real system of long horizontal wells buried in the beach parallel to the sea. It also approximates the near field around a modified Ranney well system in which the horizontal well points radiating out from large-diameter caisson are imaged by another set below the interface.

These kinds of systems would be advantageous in comparison to the usual vertical well because the piezometric head gradients near the well do not become as large. Smaller gradients (and smaller drawdowns) near the wells should result in more easily controlled flow behavior.

If the fresh-water table and the interface are considerably below the ground surface, it may be necessary to use the standard vertical well. The two-dimensional solution should still give insight into the axisymmetric or three-dimensional cases. Therefore, this situation being studied is a good starting point.

With the advent of the finite element method, numerous papers have been published on subjects of various groundwater flow problems. One of the difficulties in the groundwater analysis is the proper handling of the free surface. This becomes even more difficult when a seepage face is considered. Neuman and Witherspoon (1970) presented a unique

approach to such problems. An application of the boundary element method for predicting the location of the interface between fresh water and salt water has been dealt with by Lee (1981). A fundamental numerical approach for the application of the boundary element method to general potential problems can be found in Brebbia (1978).

CHAPTER 3

THEORETICAL CONSIDERATION

Law of Conservation of Mass

The mechanism of flow in aquifers is not as readily apparent as is the mechanism of laminar fluid flows in a pipe or channel because of the complexity of geometry of the void space of the aquifers. In spite of this fact ground-water flow can be analyzed by taking the law of conservation of mass into consideration with Darcy's law.

Consider mass being taken out of by velocities from the boundary of an arbitrary three-dimensional domain, as shown in Figure 3.1. The integral form of the continuity equation (Potter and Foss, 1975) can be written as

$$\iiint \frac{\partial \rho}{\partial t} dV + \iint \rho \vec{V} \cdot d\vec{A} = 0 \qquad (3.1)$$

The right side of the above equation is always zero for any three-dimensional domain because mass can be neither created nor destroyed. However, the right side of Equation (3.1) will have neither a positive or a negative value as source or sink if the integration is carried out over one- or two-dimensional domains. The sources and sinks are, however,

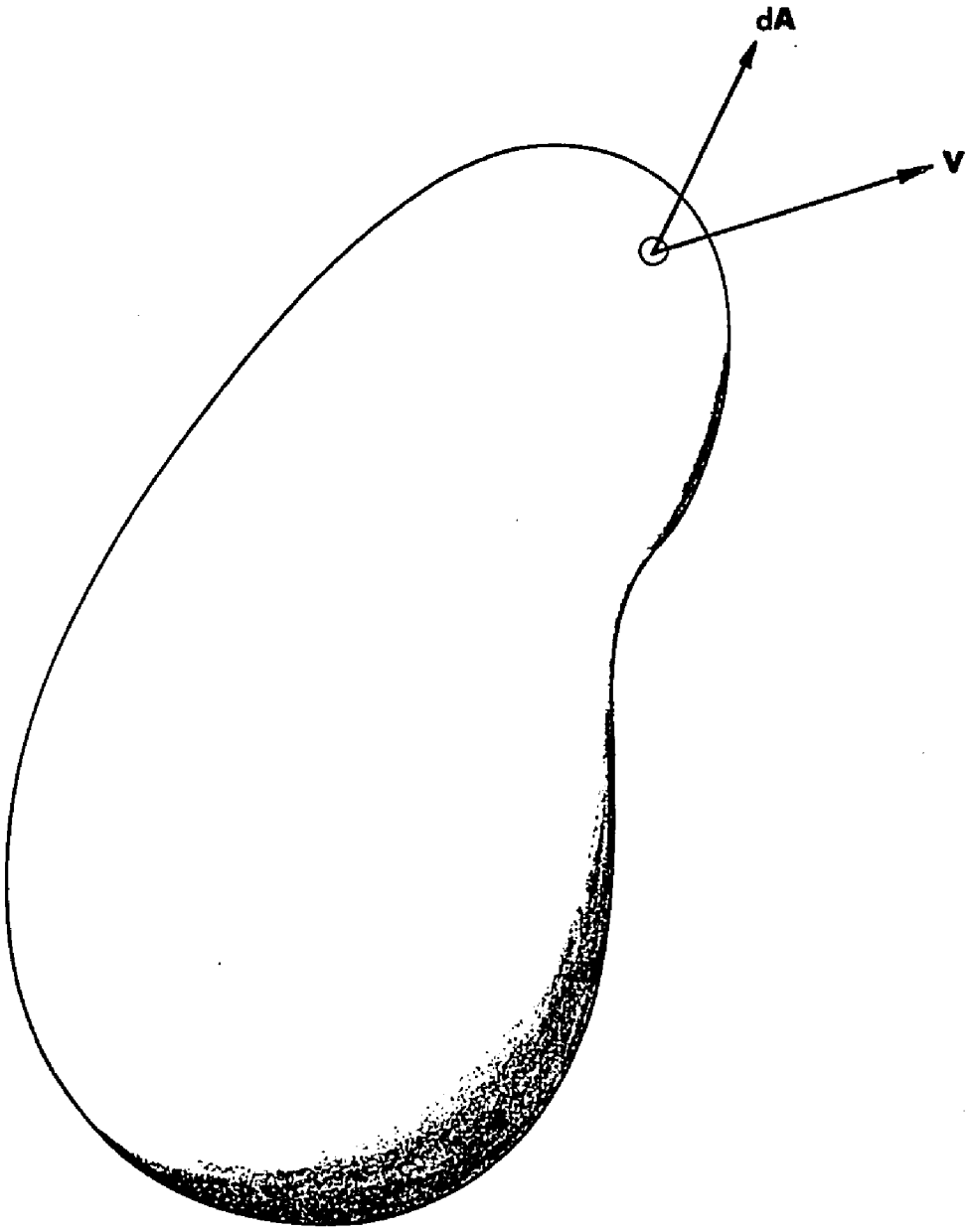

Figure 3.1. Flow around three-dimensional domain.

flows on the boundary whose area vector $d\vec{A}$ is parallel or antiparallel to the coordinate which has been eliminated by the purpose.

Employing the divergence theorem, the surface integral is transformed into a domain integral. Equation (3.1) then becomes

$$\iiint [\frac{\partial \rho}{\partial t} + \text{div}(\rho \vec{V})] d\forall = 0 \qquad (3.2)$$

Because the limits of the integral are chosen to be arbitrary, the integrand must equal zero, yielding the differential form of the continuity equation.

$$\frac{\partial \rho}{\partial t} + \frac{\partial (\rho u)}{\partial x} + \frac{\partial (\rho v)}{\partial y} + \frac{\partial (\rho w)}{\partial z} = 0 \qquad (3.3)$$

This can be written also as

$$\frac{d\rho}{dt} + \rho \vec{\nabla} \cdot \vec{V} = 0 \qquad (3.4)$$

where the first term in the above equation is defined as

$$\frac{d\rho}{dt} = \frac{\partial \rho}{\partial t} + \vec{V} \cdot \vec{\nabla} \rho \, .$$

If the compressibility of water is assumed negligible, the continuity equation can be simplified as

$$\vec{\nabla} \cdot \vec{V} = 0 \qquad (3.5)$$

or in Cartesian coordinates

$$\frac{\partial u}{\partial x} + \frac{\partial v}{\partial y} + \frac{\partial w}{\partial z} = 0 . \qquad (3.6)$$

Although water may be considered as an incompressible fluid, density varies with temperature or by solute substances. For cases in which the density variation is pronounced, Equation (3.4) must be considered.

Darcy's Law and its Development

In 1856 Henry Darcy investigated and reported on the flow of water in isotropic and homogeneous sand. He showed that the specific discharge, V, is proportional to the slope of the piezometric (hydraulic) head. Darcy's law can be then written as, in differential form,

$$V = -K\frac{dh}{d\ell} \qquad (3.7)$$

where h is hydraulic or piezometric head, and the constant K, is the constant of proportionality between the specific discharge and the slope of hydraulic head. The constant K is called the hydraulic conductivity and has units of velocity [L/T]. The specific discharge is defined as discharge from a unit area of seepage face; i.e., including the area taken up by the sand grains. A true average velocity of flow in an aquifer is given by $V_s \simeq V/n$ where n is the porosity or void ratio of the aquifer.

According to observations by Hubbert (1940), the constant, K, in the Darcy's law is a function not only of

the porous matrix but also of the fluid. Applying his observations, the Darcy's constant (Freez and Cherry, 1979) can be written as

$$K = \frac{k\gamma}{\mu}$$

where γ is the specific weight of fluid, μ is the viscosity of fluid, and k is normally called the intrinsic permeability having units of $[L^2]$. In the above equation, γ and μ are functions of the fluid alone and the permeability, k, which characterizes the size and shape of grains, is a function of the medium alone. Although k describes the characteristics of grains, the intrinsic permeability k, or the hydraulic conductivity K must be determined experimentally for each aquifer system. K, or k will be larger for larger void ratio, for larger voids, and for void geometry which results in less loss for the laminar flow in the voids. Only approximate notions of the value of K, or k, exist and these are based on past measurements in field or laboratory. For sands the value of K will range between 0.01 cm/sec and 0.005 cm/sec. In general, the real aquifer is not isotropic or homogeneous. It will usually have a greater conductivity along the formation of the stratum. It is, therefore, necessary to generalize the Darcy's law for two- or three-dimensional flow. In three dimensions the specific discharge V_i would be

$$V_i = - K_i \frac{\partial h}{\partial x_i} \tag{3.9}$$

where K_i is the hydraulic conductivity in i-coordinate, and the coordinate system for this case coincides with the principal axes. A more general form of Darcy's law, therefore, should be given for any coordinate system as

$$V_i = - K_{ij} \frac{\partial h}{\partial x_j} \tag{3.10}$$

where K_{ij} is the second-order tensor having nine components. For most aquifers, the hydraulic conductivity tensor is symmetric, i.e., $K_{ij} = K_{ji}$. Non-homogeneity can be handled by making the K's dependent on space, but this makes the computations somewhat more difficult and laborious.

Ground-Water Equations

The law of conservation of mass in a saturated porous medium requires that the net mass rate of fluid flow through the boundary of an arbitrary three-dimensional domain be equal to the time rate of change of fluid mass stored in the domain. This can be written, in Cartesian coordinates, as

$$\frac{\partial(\rho n)}{\partial t} + \frac{\partial(\rho V_i)}{\partial x_i} = 0 \tag{3.14}$$

Applying the concept of the specific storage and recognizing that terms of the form $\rho \text{div}\vec{V}$ are much greater than terms of the form $\vec{V}\cdot\vec{\nabla}\rho$, the density, ρ, may be cancelled from the both

terms of the above equation. Substituting Equation (3.10) into (3.11) yields

$$S_s \frac{\partial h}{\partial t} = \frac{\partial}{\partial x_i}(K_{ij} \frac{\partial h}{\partial x_j}) \ . \tag{3.12}$$

If an aquifer is isotropic and homogeneous, the above equation can be simplified as

$$\frac{\partial h}{\partial t} = \frac{K}{S_s} \nabla^2 h \tag{3.13}$$

Many applications in ground-water analysis are treated as two-dimensional flows in the horizontal or vertical plane. For these cases, the lack of a coordinate can be handled by considering an extra source term in Equation (3.12). Equation (3.12) then becomes, for x-y plane,

$$S \frac{\partial h}{\partial t} = \frac{\partial}{\partial x_i}(bK_{ij} \frac{\partial h}{\partial x_j}) + q \tag{3.14}$$

where the hydraulic conductivity tensor is now two by two.

One of the important tasks in this study is to predict the location of the interface between the two fluids. In many cases of practical interest, the transition zone between two miscible fluids flowing simultaneously in a porous medium is narrow relative to the dimensions of the regions occupied by each fluid alone. Under such conditions, it can be assumed that the fluids are immiscible and the lower flow domain can be treated as a confined aquifer with the interface as the upper boundary, and the upper flow domain as an unconfined

aquifer with a lower boundary of the interface. However, this assumption gives two more equations to solve simultaneously with the governing equations for locating the interface.

The interface line can be represented by

$$F(x,y,z,t) \equiv z - z_I = 0 \tag{3.15}$$

where z_i is the elevation of the interface. The hydraulic pressure of both sides of the interface must be the same, i.e.,

$$\gamma_2(h_2 - z_I) = \gamma_1(h_1 - z_I) \tag{3.16}$$

where the subscripts 1 and 2 indicate the upper and lower domains, respectively. Since the interface is a material surface, the following equations must be satisfied on the interface at any given time.

$$\left.\begin{aligned} &\frac{dF}{dt} \equiv \frac{\partial F}{\partial t} + \frac{1}{n}\vec{V}_1\cdot\vec{\nabla}F = 0 \\ &\text{and} \\ &\frac{\partial F}{\partial t} + \frac{1}{n}\vec{V}_2\cdot\vec{\nabla}F = 0 \end{aligned}\right\} \tag{3.17}$$

Substituting Equation (3.15) into (3.17) yields

$$n\left(\alpha_1\frac{\partial h_2}{\partial t} - \alpha_2\frac{\partial h_2}{\partial t}\right) + \alpha_1 K_1|h_1|^2 + \alpha_1 K_2\vec{\nabla}h_1\cdot\vec{\nabla}h_2 - \frac{\partial h_1}{\partial z} = 0 \tag{3.18}$$

and

$$n(\alpha_1 \frac{\partial h_1}{\partial t} - \alpha_2 \frac{\partial h_2}{\partial t}) + \alpha_1 K_1 \vec{\nabla} h_1 \cdot \vec{\nabla} h_2 - \alpha_2 K_2 |\vec{\nabla} h_2|^2$$

$$- \frac{\partial h_2}{\partial z} = 0 \qquad (3.19)$$

where $\alpha_1 = \gamma_1/\Delta\gamma$, $\alpha_2 = \gamma_2/\Delta\gamma$, and $\Delta\gamma = \gamma_2 - \gamma_1$. It is interesting to note that if $h_1 = 0$ and $\gamma_1 = 0$ in Equation (3.19), the equation becomes the boundary condition for a free surface. A more detailed treatment of this subject can be found in Bear (1972).

Sometimes, mathematics has provided solutions before the partial differential equations describing the physical phenomena are derived. In fluid mechanics, irrotational flows are describable by using the Laplace equation. A solution is called the velocity potential. Also there exists the orthogonal function to the solution which is called the stream function. The existence of both the velocity potential and the stream function had been known among mathematicians as an application of complex variable methods before engineers started using the technique, the flow net, for fluid mechanics. The flow net consists of the equipotential lines and the stream lines. The two lines are always orthogonal each other and the two sets of lines form squares. A flow over a sharp-crested weir can be described by the flow net technique since the flow is assumed to be irrotational, and in fact is almost irrotational. The technique had also been used for ground-water

analysis, especially for estimating the amount of seepage flow under or through dams before the computer age came because steady flows in isotropic media are described by Laplace equation. The graphical flow net has produced approximate solutions for cases for which closed mathematical solutions have not bee found. With the advent of computers, other techniques for finding approximate solutions have been developed. It is important to note that in ground-water analysis, the potential lines are not orthogonal to the stream lines if a medium is anisotropic; moreover, the describing equation is no longer the Laplace equation. The equation can be either an elliptic-type or a hyperbolic-type equation.

Imaged-Well System

The simplest two-well system can be constructed with two fully penetrating pipes (infinitely extended) installed horizontally near the interface, as shown in Figure 3.2. The flow behavior around the wells can then be described by the two-dimensional ground-water equation. An application of the two-well system such as in Figure 3.3 (a comprehensive study of this kind of well system can be seen in Abed, 1982) generally yields the three-dimensional flow pattern; however, in order to search what happens around a pair of the wells, the flow characteristics may be replaced by a two-dimensional flow domain, as in Figure 3.2. The aim of this study is to inves-

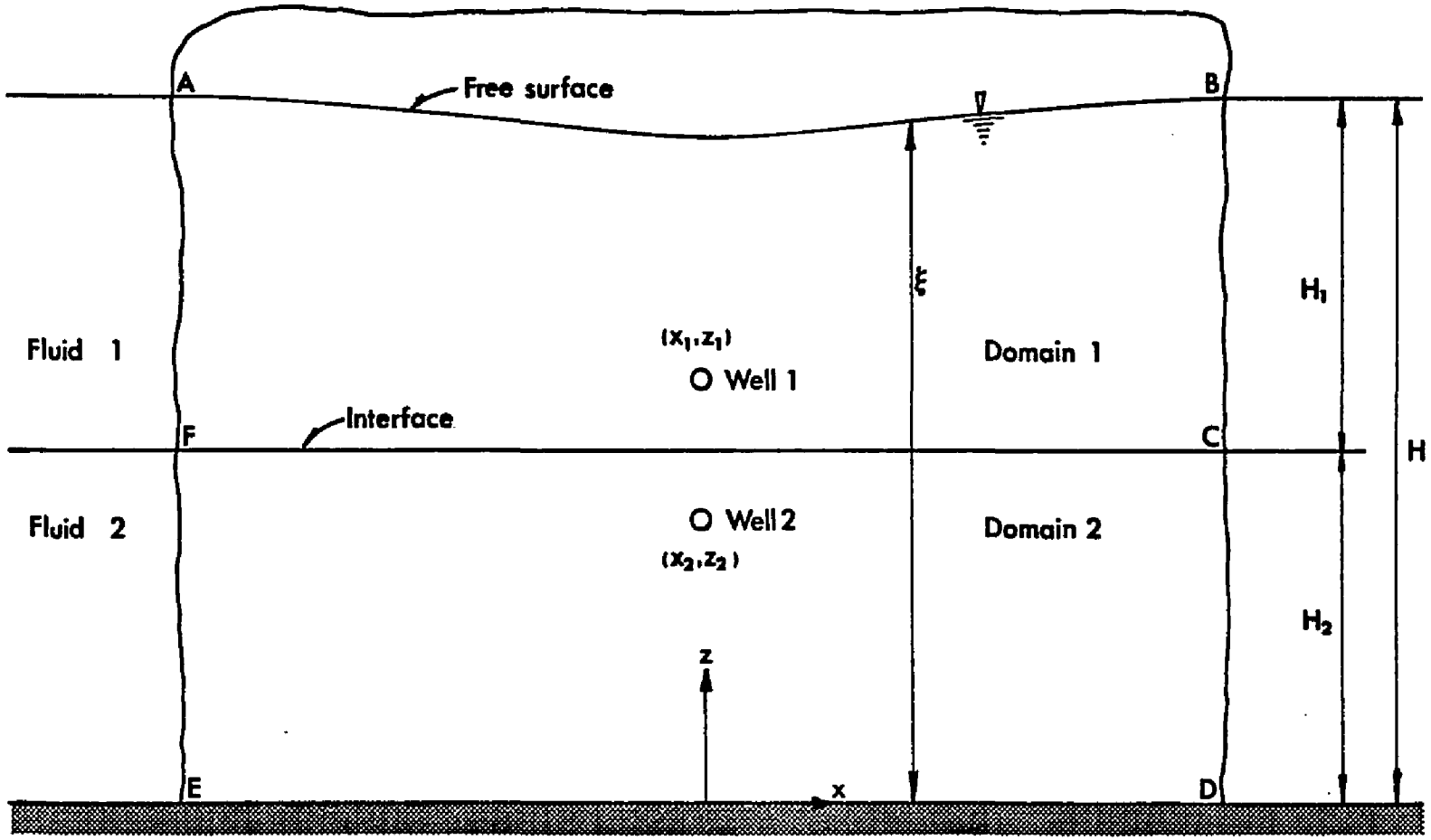

Figure 3.2. Multiple flows and two wells.

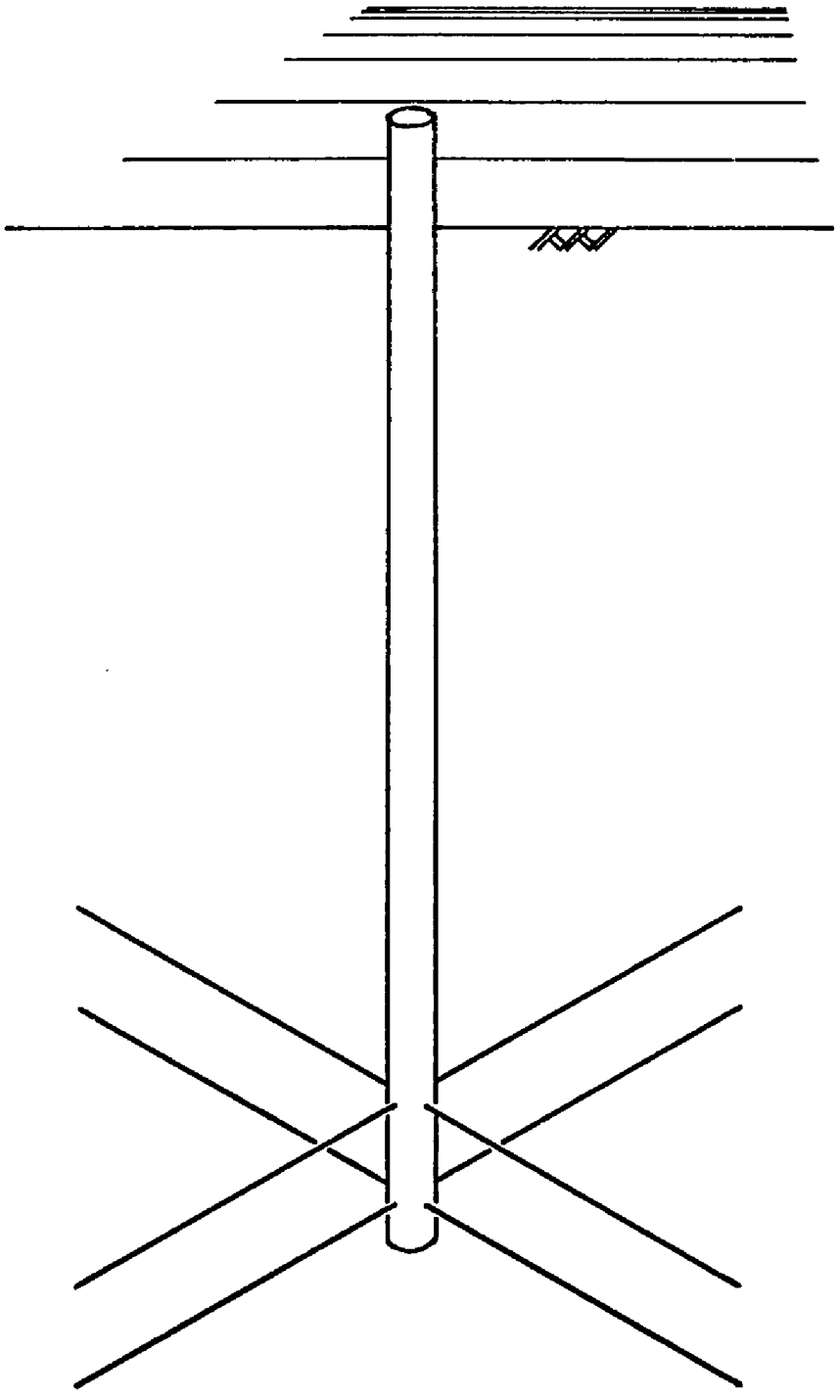

Figure 3.3. A double Ranny well.

tigate how the interface settles down with simultaneous pumping of two fluids from the wells. This clearly indicates the nonnecessity of solving the unsteady ground-water equations. As a preliminary study, the aquifer is assumed to be isotropic; therefore, Equation (3.12) can be reduced to, for the domain 1 in Figure 3.2,

$$\iint_{\Omega_1} \left[\frac{\partial^2 h_1}{\partial x^2} + \frac{\partial^2 h_1}{\partial z^2} - \frac{q_{p_1}}{K_1}\delta(\vec{r}_1 - \vec{r})\right] dA = 0 \qquad (3.20)$$

where the vector $\vec{r}_1$ indicates the location of the well whose discharge is q_{p_1} and δ is the delta function which gives infinite value if the argument of the function is zero; otherwise, it gives zero. Integrating the function yields unity. The above equation is written in the integral form because the integrand is valid only in the domain 1. If the limit of area to be integrated is understood, Equation (3.20) can be written as

$$\frac{\partial^2 h_1}{\partial x^2} + \frac{\partial^2 h_1}{\partial z^2} = \frac{q_{p_1}}{K_1}\delta(\vec{r}_1 - \vec{r}) \qquad (3.21)$$

The system shown in Figure 3.2 has not only the interface but also the free surface. This combination creates a strong nonlinear behavior for the mathematical model. For the steady state, the hydraulic pressure in the domain 1 must be equal to the pressure in the domain 2 on the interface, i.e.,

$$\gamma_1(h_1 - z) = \gamma_2(h_2 - z) \qquad (3.22)$$

where z is the elevation of the interface. It is assumed that there is no mixing zone at the interface.

Along the free surface the pressure is atmospheric; therefore, the piezometric head is equal to the elevation of the free surface, i.e., $h_1 = z$.

The entire system, as shown in Figure 3.2, can be written as,

$$\iint (\nabla^2 h_1 - \frac{Qp_1}{bK_1}\,\delta(\vec{r}_1 - \vec{r}))dA = 0 \text{ in } D_1 ,$$

$$\iint (\nabla^2 h_2 - \frac{Qp_2}{bK_2}\,\delta(\vec{r}_2 - \vec{r}))dA = 0 \text{ in } D_2 ,$$

$$h_1 = \xi \quad \text{and} \quad \frac{\partial h_1}{\partial n} = 0 \text{ A-B} ,$$

$$h_1 \doteq H \text{ on B-C and A-F} ,$$

$$\gamma_1(h_1 - z) = \gamma_2(h_2 - z) \text{ along F-C} ,$$

$$\frac{\partial h_2}{\partial z} = 0 \text{ on E-D} ,$$

and

$$h_2 = H^* \text{ on F-E and C-D} \qquad (3.23)$$

where H* must be uniquely determined so that the pressures in the domains 1 and 2 are the same at the point c where the interface line begins. At any point on the segment C-D the pressure is given by

$$P_2 = \gamma_1 H_1 + \gamma_2(H_2 - z) \qquad (3.24)$$

and the piezometric head is given as

$$H^* = \frac{P_2}{\gamma_2} + z$$

$$= \frac{\gamma_1}{\gamma_2} H_1 + H_2$$

$$= H - \frac{\Delta\gamma}{\gamma_2} H_1 \qquad (3.25)$$

where

$$\Delta\gamma = \gamma_2 - \gamma_1$$

and

$$H = H_1 + H_2 .$$

If the porous matrix in the domain 1 is assumed to be the same as that in the domain 2, the hydraulic conductivities are governed only by the properties of the two fluids. The specific viscosity of normal sea water at 20°C is about 1.07 (Abed, 1982) while the specific density is 1.025. If these conditions are held in the entire domain, the specific hydraulic conductivity (defined as K_s/K_f) becomes 0.96, indicating that the sea-water domain is less conductive than the fresh-water domain.

Momentum Equation for Newtonian Fluids

The general form of Newton's viscosity law is called Stoke's viscosity law and is restricted to laminar flows. The general equation of motion can be derived by considering

an infinitesimal element and Newton's second law as

$$df_i = \frac{d(\rho v_i)}{dt} d\forall . \tag{3.26}$$

which states that total applied forces on and in the element is equal to the total change in ρv_i in the element. The right side of the above equation is also equal to the sum of the following statements.

1. Partial change in ρv_i in the element with respect to time.
2. ρv_i carried away by velocities from the surface of the element, as shown in Figure 3.4.

Another way of viewing the above statements is to consider the conservation of quantity ρv_i if $df_i = 0$. Integrating Equation (3.26) over some arbitrary domain and applying the above statements, it yields

$$\iiint B_i d\forall + \oiint T_i^{(\nu)} dA = \iiint \frac{\partial \rho v_i}{\partial t} d\forall + \oiint \rho v_i v_j \nu_j dA \tag{3.27}$$

where $v_j \nu_j dA = \vec{v} \cdot d\vec{A}$, B_i is the body force applied in the domain, and $T_i^{(\nu)}$ is the traction applied on the boundary. Using Cauchy's formula and the divergence theorem, the surface integral on the left side of the above equation becomes

$$\iiint \frac{\partial \tau_{ij}}{\partial x_j} d\forall . \tag{3.28}$$

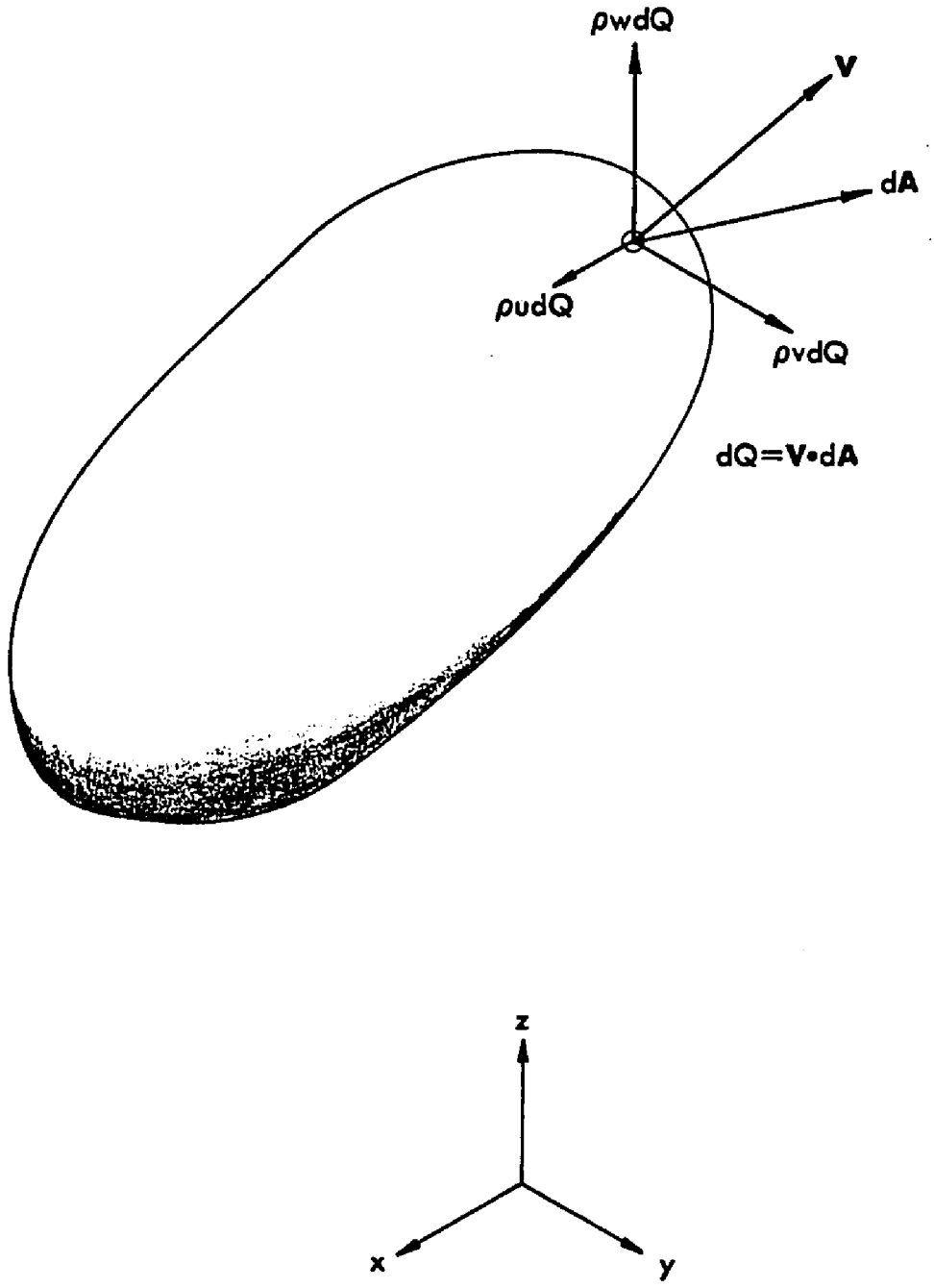

Figure 3.4. Momentum flux through boundary.

Using the divergence theorem again, the surface integral in the right side of Equation (3.27) can be transformed into a volume integral

$$\iiint \frac{\partial}{\partial x_j}(\rho v_i v_j)dV = \iiint (v_i \text{div}\rho\vec{v} + \rho\vec{v}\nabla v_i)dV \,. \tag{3.29}$$

Substituting Equations (3.28) and (3.29) into Equation (3.27), Equation (3.27) can be alternatively expressed as

$$\iiint [B_i + \frac{\partial \tau_{ij}}{\partial x_j} - \rho\frac{\partial v_i}{\partial t} - \rho\vec{v}\cdot\nabla v_i - v_i(\frac{\partial \rho}{\partial t} + \text{div}\rho\vec{v})]dV \tag{3.30}$$

The expressions in parentheses in the above equation is zero from the law of conservation of mass. Since the domain is arbitrary, it can be concluded that at any point the following must hold

$$B_i + \frac{\partial \tau_{ij}}{\partial x_j} = \rho\frac{\partial v_i}{\partial t} + \rho\vec{v}\cdot\nabla v_i \tag{3.31}$$

The above equation must be applicable not only for incompressible fluids but also for compressible fluids. For the Newtonian isotropic fluid the stress-rate of strain relations are given by Stokes' viscosity law as

$$\tau_{ij} = \mu(\frac{\partial v_i}{\partial x_j} + \frac{\partial v_j}{\partial x_i}) - (\frac{2}{3}\mu\text{div}\vec{v} + p)\delta_{ij} \tag{3.32}$$

where μ is the viscosity of fluid and δ_{ij} is the delta function which gives unity if i = j and zero otherwise.

In order to simluate the ground-water motion, the aquifer system is often replaced by an incompressible laminar flow such as flows in the Hele-Shaw model (Bear, 1972). For this case the expression $\text{div}\vec{v}$ is zero and Equation (3.29) becomes

$$\tau_{ij} = \mu\left(\frac{\partial v_i}{\partial x_j} + \frac{\partial v_j}{\partial x_i}\right) - \delta_{ij}P \tag{3.33}$$

The derivative of τ_{ij} with respect to x_j can be given, as for incompressible fluids (Shames, 1962),

$$\begin{aligned}\frac{\partial \tau_{ij}}{\partial x_y} &= \mu\frac{\partial^2 v_i}{\partial x_j^2} + \mu\frac{\partial^2 v_j}{\partial x_i \partial x_j} - \frac{\partial P}{\partial x_j}\delta_{ij} \\ &= \mu\nabla^2 v_i + \mu\frac{\partial}{\partial x_i}(\text{div}\vec{v}) - \frac{\partial p}{\partial x_i} \\ &= \mu\nabla^2 v_i - \frac{\partial p}{\partial x_i}\end{aligned} \tag{3.34}$$

If the gravity force is the major source for the body force, the B_i in Equation (3.31) can be expressible as

$$B_i = -\gamma\frac{\partial z}{\partial x_i} \tag{3.35}$$

where the minus sign indicates that the gravity force is acting vertically downward while z-coordinate is positive vertically upward, and γ is the specific weight of the fluid. Substituting Equations (3.34) and (3.35) into Equation (3.31), it finally yields

$$\rho\frac{\partial v_i}{\partial t} + \vec{v}\cdot\vec{\nabla}v_i = \mu\nabla^2 v_i - \frac{\partial}{\partial x_i}(p + \gamma z) \qquad (3.36)$$

This is the Navier-Stokes equation for incompresible fluids.

Hele-Shaw Model

As mentioned earlier, for physically stimulating the ground-water flow mechanism a laminar fluid flow whose Reynolds number ($\mathbb{R} = \rho vb/\mu$) is 700 or less is often used instead of building a sand box or similar one. The Hele-Shaw physical model, used for studying viscous flow, is a well known technique for vertical two-dimensional ground-water investigations. The model consists of two parallel plates placed in a vertical position.

Considering steady state viscous flow between the parallel plates, as shown in Figure 3.5, the equation for the flow can be derived from Equation (3.36) as

$$\mu\frac{\partial^2 v_i}{\partial y^2} = \frac{\partial}{\partial x_i}(p + \gamma z) \qquad (3.37)$$

where the free index is indicates the coordinate x or z. Integrating the above equation twice with respect to y and applying the boundary conditions of zero velocities on the surface of plates results in

$$v_i = \frac{1}{2\mu}(y^2 - \frac{b^2}{4})\frac{\partial}{\partial x_i}(p + \gamma z) \; . \qquad (3.38)$$

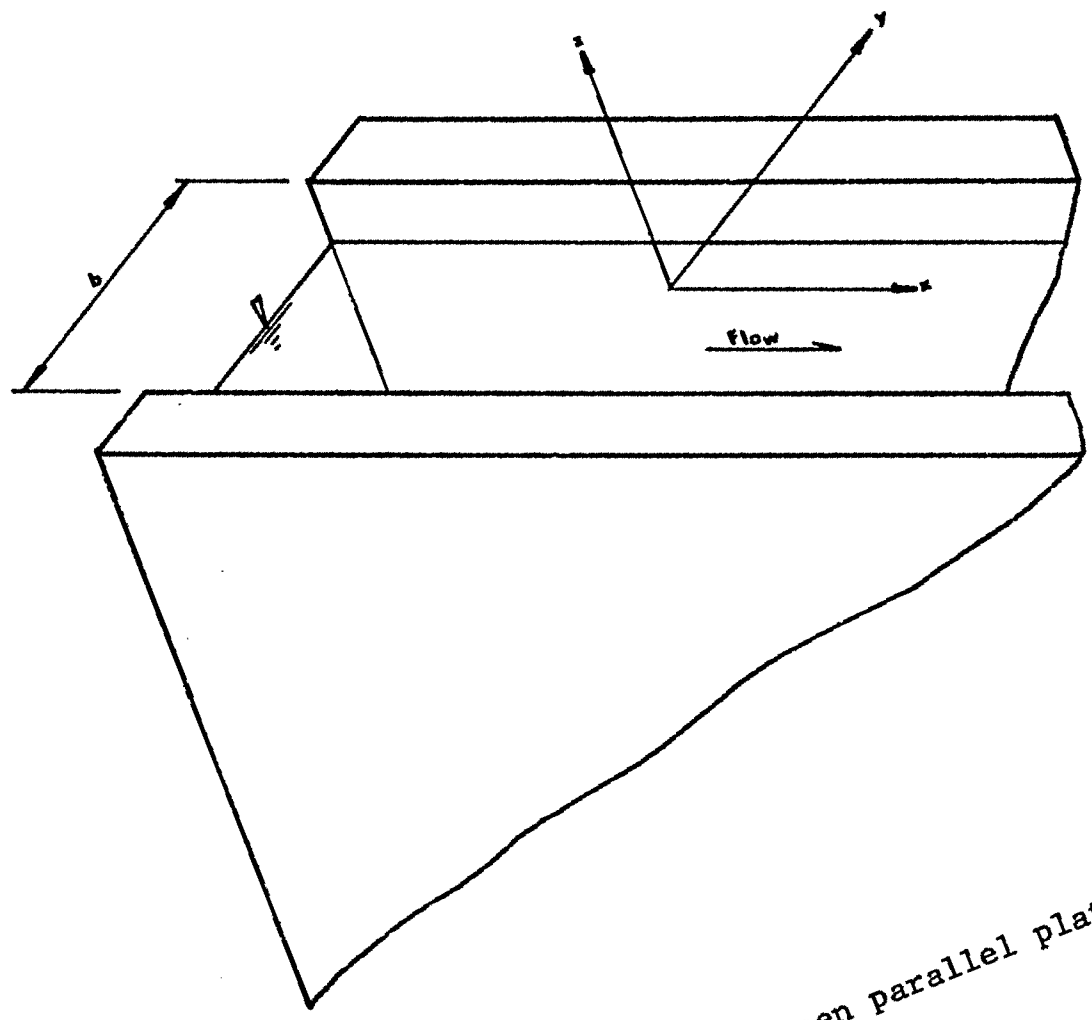

Figure 3.5. Flow between parallel plates.

By integrating the above equation once more with respect to y and dividing the thickness of the flow, the rate of flow per unit area between the plates is obtained as

$$q_i = \frac{1}{b}\int_{-b/2}^{b/2} v_i dy = - \frac{b^2\gamma}{12\mu} \frac{\partial}{\partial x_i}(z + \frac{p}{\gamma}) . \tag{3.39}$$

In general, the sum of the elevation z and the pressure head, called the piezometric head, i.e., $z + p/\gamma$ is denoted by h. The specific discharge is thus given by, for an isotropic porous media,

$$q_i = -K\frac{\partial h}{\partial x_i} . \tag{3.40}$$

By comparison between Equations (3.39) and (3.40), it is realized that the hydraulic conductivity (Bear, 1972) is given by

$$K = \frac{b^2\gamma}{12\mu} . \tag{3.41}$$

This relation can be useful for calibrating the Hele-Shaw model with the aid of an approximate flow field representation such as Dupuit equations or numerical solutions.

CHAPTER 4

FINITE ELEMENT METHOD

Introduction

The finite element method may well be the most common and powerful numerical procedure of all for finding the approximate solutions of partial differential equations (abbreviated here as PDE) which describe many engineering problems.

The finite element formulation, which is a system of linear or non-linear algebraic equations, is obtained by dividing the entire domain into sub-domains which are called elements. The unknowns in each element are then approximated by a polynomial whose order depends on the number of nodal points on the element. For two dimensions a triangular element with three nodes gives a linear spatial variation for the unknowns.

The finite element equation can be derived by several methods. In fact, there are at least two stems from which the fundamentals of the finite element method are derived: the variational approach and the weighted residual methods.

In the variational approach, the virtual work method

Raleigh-Ritz method are important tools for structural engineers to obtain the finite element formulation or approximate numerical formulae. Based on this approach these methods generally require existence of the extremizing function which is formally called "functional." In solid mechanics, the functional describes energy stored in an elastic material. In fluid mechanics, the functional characterizes power since the strain rate, which is the velocity variation in the perpendicular direction to the flow direction, has a unit of $[T^{-1}]$. Any elastic material or fluid flow has the state of minimum energy flux or power, respectively; therefore, the functional must be minimized to achieve the requirements. Also, at the extreme point, the material or the fluid flow should be in equilibrium. Consequently, there must be a relation between the functional and the PDE, which governs the physical phenomenon. As early as in the 18th Century, Euler gave a complete explanation of this subject. It is known today as the Euler-Lagrange equation. Later in this chapter it will be shown how ground water physics is related to this concept.

In the weighted residual method, the error in the integral of any PDE whose unknowns are now replaced by the approximate solutions over the entire domain will be forced to be zero by multiplying the PDE by a weighting function which can be any complete set of functions. Obviously the

functions must be linear or higher order. If the functions are constant values, say one, then the numerical procedure is called the integrated finite difference method. Among the various approaches for representing the weighting function, Galerkin's method is the most famous and widely used by engineers. In the present study, the method will be applied for locating the interface near wells imaged about the interface.

Raleigh-Ritz Method

One of the most useful approximate methods stemming from the variational considerations is the Raleigh-Ritz method. In this section, the method is briefly outlined for the Laplace equation, which is the governing equation for steady isotropic ground water flow.

Let u be the solution of the problem:

$$\nabla^2 u = \frac{\partial^2 u}{\partial x^2} + \frac{\partial^2 u}{\partial y^2} = \frac{\partial^2 y}{\partial x_i^2} = 0 \quad \text{in } \Omega \tag{4.1}$$

$$u = f \text{ on } \Gamma \tag{4.2}$$

where Ω indicates the domain of the problem and Γ is the boundary. Let $v(x,y)$ be any continuously differentiable function in Ω which is continuous to the boundary and has the boundary values:

$$v = f \text{ on } \Gamma. \tag{4.3}$$

Before moving on to the next step, an introduction of two mathematical identifies will ease the proceeding steps (Weinberger, 1965).

$$u\nabla^2 u = \text{div}(u\vec{\nabla}u) - |\vec{\nabla}u|^2 \tag{4.4}$$

and

$$v\nabla^2 u = \text{div}(v\vec{\nabla}u) - \vec{\nabla}v\cdot\vec{\nabla}u \tag{4.5}$$

These equations are easily proven by considering an arbitrary domain and integrating $u\nabla^2 u$ over the domain,

$$\iint_\Omega u\nabla^2 u\,dA = \oint_\Gamma u\vec{\nabla}u\cdot\vec{n}\,d\Gamma - \iint_\Omega \vec{\nabla}u\cdot\vec{\nabla}u\,dA\,. \tag{4.6}$$

Employing the divergence theorem, the line integral in the above equation becomes

$$\oint_\Gamma u\vec{\nabla}u\cdot\vec{n}\,d\Gamma = \iint_\Omega \text{div}(u\vec{\nabla}u)\,dA\,. \tag{4.7}$$

Hence

$$\iint_\Omega u\nabla^2 u\,dA = \iint_\Omega (\text{div}(u\vec{\nabla}u) - \vec{\nabla}u\cdot\vec{\nabla}u)\,dA\,. \tag{4.8}$$

Since the domain is assumed to be arbitrary, it follows that

$$u\nabla^2 u = \text{div}(u\vec{\nabla}u) - |\vec{\nabla}u|^2 \tag{4.9}$$

where

$$|\vec{\nabla}u|^2 = \left(\frac{\partial u}{\partial x}\right)^2 + \left(\frac{\partial u}{\partial y}\right)^2 = \vec{\nabla}u\cdot\vec{\nabla}u \tag{4.10}$$

Subtracting Equation (4.5) from Equation (4.4) yields

$$(u-v)\nabla^2 u = \text{div}((u-v)\vec{\nabla}u) - |\vec{\nabla}u|^2 + \vec{\nabla}u\cdot\vec{\nabla}v \qquad (4.11)$$

Noting that

$$|\vec{\nabla}u - \vec{\nabla}v|^2 = (\vec{\nabla}u - \vec{\nabla}v)\cdot(\vec{\nabla}u - \vec{\nabla}v)$$

$$= |\vec{\nabla}u|^2 - 2\vec{\nabla}u\cdot\vec{\nabla}v + |\vec{\nabla}v|^2 \qquad (4.12)$$

it follows that

$$\vec{\nabla}u\cdot\vec{\nabla}v = \tfrac{1}{2}|\vec{\nabla}u|^2 - \tfrac{1}{2}|\vec{\nabla}u - \vec{\nabla}v|^2 + \tfrac{1}{2}|\vec{\nabla}v|^2 \qquad (4.13)$$

Substituting Equation (4.13) into Equation (4.11) results

$$(u-v)\nabla^2 u = \text{div}((u-v)\vec{\nabla}u) - \tfrac{1}{2}|\vec{\nabla}u|^2 - \tfrac{1}{2}|\vec{\nabla}u-\vec{\nabla}v|^2$$

$$+ \tfrac{1}{2}|\vec{\nabla}v|^2 \qquad (4.14)$$

Integrating both sides of Equation (4.14) over the domain Ω, the left side is zero as defined. Since $u - v = 0$ on Γ, the integral of the first term in the right side of Equation (4.14) is zero by the divergence theorem, and therefore

$$\iint_\Omega \tfrac{1}{2}|\vec{\nabla}v|^2 dA = \iint_\Omega \tfrac{1}{2}|\vec{\nabla}u|^2 dA + \tfrac{1}{2}\iint |\vec{\nabla}(u-v)|^2 dA \qquad (4.15)$$

Since every integration in Equation (4.15) has a positive value,

$$\iint \tfrac{1}{2}|\vec{\nabla}v|^2 dA \geq \iint \tfrac{1}{2}|\vec{\nabla}u|^2 dA \qquad (4.16)$$

for any function v having the same boundary values as u.

Noting that the minimum value of

$$\iint \frac{1}{2} |\vec{\nabla} v|^2 dA \tag{4.17}$$

is

$$\iint \frac{1}{2} |\vec{\nabla} u|^2 dA \tag{4.18}$$

which is given by the exact solution, it is inferred that an approximate solution of $\nabla^2 u = 0$ can be obtained by minimizing Equation (4.17).

Example:

Let v_o be any differentiable function satisfying the boundary condition $v_o = f$ and the approximate function v be

$$v = v_o + \sum_{i=1}^{n} a_i v_i \tag{4.19}$$

where v_i's are a linearly independent complete set of functions; in other words, $v_i \neq$ constant x v_j $j \neq i$. The aim is to find the constants a_i's so that integral of

$$\iint_{\partial} \frac{1}{2} |\vec{\nabla}(v_o + \sum_{i=1}^{n} a_i v_i|^2 dA \tag{4.20}$$

is minimized. Let the integral be I. The unknown a_i's can be determined by imposing the necessary condition for the minimum value of the integral I, hence

$$\frac{\partial I}{\partial a_i} = 0 \quad \text{for} \quad i = 1, 2, \ldots, n. \tag{4.21}$$

This produces n x n simultaneous linear equations.

The Variational Approach

In 1697 Jean Bernoulli I, whose son, Daniel Bernoulli I is famous in fluid mechanics, posed a problem that was to become famous in finding the Calculus of Variations: What is the curve joining two given points such that a particle under the influence of gravity will move along the curve from the upper to the lower point in minimum time? Today, this problem is known as the Brachistochrone. He, with his brother Jacques Bernoulli succeeded in finding the solution. The problem was also sent to Isaac Newton and Gottfried Leibniz. According to John Conduitt (Newton's relative), Newton solved the problem in one evening. The correct curve turns out to be a cycloid, a trace of a point on a wheel rolling on a plane (Beckmann, 1971; Martin and Carey, 1973).

As mentioned earlier, the variational approach is based on physical quantities such as time, length, energy (or work), and temperature. Significantly, the variational approach gives not only the mathematical equations but also an understanding of the physical interpretations. In fluid mechanics, there are two interesting questions: Why is the free surface of a fluid in a stationary container perpendicular to the direction of gravitation? and Why is the trajectory of a free jet parabolic? The crystal clear answers to the questions are given only by the variational approach. In solid and fluid mechanics, energy of energy-per-unit time

is the most convenient quantity for describing the deformations or velocities because any steady state mass has the least energy stored in it.

In this section, the derivation of the Euler-Lagrange equation is presented in one and two dimensions based on the principle of the first variation. An introduction to the virtual work method is also presented.

The point of interest is the determination of the unknown function y(x) which makes the integral

$$I = \int_{x_1}^{x_2} F(x, y, y')dx \tag{4.22}$$

extremitized where the functional F is known and $y' = dy/dx$ (Dym and Shames, 1973). The value of I between points (x_1, y_1) and (x_2 and y_2) will obviously depend on the path chosen between the points. The existence of a path y(x) which extremizes the integral is assumed here with respect to other paths denoted $\bar{y}(x)$

$$\bar{y}(x) = y(x) + ew(x) \tag{4.23}$$

where e is a small parameter and w(x), an arbitrary function, is zero at the limits. An infinite number of varied paths can, therefore, be generated for a given w(x) by adjusting e. In the integral form,

$$\bar{I} = \int_{x_1}^{x_2} F(x, y+ew, y'+ew')dx \tag{4.24}$$

For any w(x) the varied path becomes coincident with the extremizing path when e = 0.

Making use of the Taylor series, $\bar{I}$ near e = 0 can be written as

$$I = (\bar{I}) + (\frac{\partial \bar{I}}{\partial e})de + \text{higher orders} .$$

For I to be extreme or $\bar{I} \rightarrow I$ when e = 0, the necessary condition is

$$(\frac{\partial \bar{I}}{\partial e})_{e=0} = 0 \tag{4.25}$$

which is the equivalent of

$$\int_{x_1}^{x_2} (\frac{\partial F}{\partial \bar{y}} \frac{d\bar{y}}{de} + \frac{\partial F}{\partial \bar{y}'} \frac{d\bar{y}'}{de})_{e=0} dx = 0 \tag{4.26}$$

Noting that $d\bar{y}/de = w$ and $d\bar{y}'/de = w'$, the above equation for e = 0 can be rewritten as

$$\int_{x_1}^{x_2} (\frac{\partial F}{\partial y} w + \frac{\partial F}{\partial y'} w') \, dx = 0 \tag{4.27}$$

Employing integration by parts, it yields

$$\int_{x_1}^{x_2} [\frac{\partial F}{\partial y} - \frac{d}{dx} (\frac{\partial F}{\partial y'})] w \, dx + w \frac{\partial F}{\partial y'} \Big|_{x_1}^{x_2} = 0 \tag{4.28}$$

Since w(x) = 0 at end points, it can be concluded that

$$\frac{d}{dx}\left(\frac{\partial F}{dy'}\right) - \frac{\partial F}{\partial y} = 0 \qquad (4.29)$$

This is the famous Euler-Lagrange equation.

In many problems, however, the boundary values of y(x) are not prescribed. The function w, therefore, need no longer always be zero at the end points. For this case Equation (4.28), which is the Euler-Lagrange equation with the boundary integral attached to it, must be considered. In order to meet the requirement $\partial I/\partial e = 0$. $\partial F/\partial y'$ must be zero on the boundary where y is not prescribed. The condition is called the natural boundary condition.

Example

The functional $F = (y'^2 - uy^2)/2$ satisfies the differential equation $y'' + uy = 0$. This can be shown by substituting the functional into the Euler-Lagrange equation, i.e.,

$$\frac{d}{dx}\left[\frac{\partial}{\partial y'}\left(\frac{1}{2} g'^2 - \frac{1}{2} uy^2\right)\right] - \frac{\partial}{\partial y}\left(\frac{1}{2} y'^2 - \frac{1}{2} uy^2\right) = 0$$

$$= \frac{d}{dx}(y') + uy = 0$$

$$= y'' + uy = 0$$

Two Independent Variables

Many applications in ground water are two-dimensional. However, attention is concentrated on the two-dimensional

ground water system rather than pure mathematical representation.

The minimizing procedure in a two-dimensional aquifer is generally expressible as a double integral of the total potential function h(x,y) and the partial derivatives of h(x,y) in the following form

$$I = \iint_{\Omega} F(x,y,h,\frac{\partial h}{\partial x},\frac{\partial h}{\partial y})\,dA \tag{4.30}$$

where Ω is the area over which the integration is carried out. Using the notation $h_x = \partial h/\partial x$ and $h_y = \partial h/\partial y$, the integration is given as

$$I = \iint_{\Omega} F(x,y,h,h_x,h_y)\,dA \tag{4.31}$$

Although a functional with more than one independent variable must be handled, the procedure for finding the extremizing function is very similar to the one-dimensional case. Starting with a form of

$$\delta I = \iint_{\Omega} [\frac{\partial F}{\partial h}\delta h + \frac{\partial F}{\partial h_x}\delta h_x + \frac{\partial F}{\partial h_y}\delta h_y]\,dA = 0 \tag{4.32}$$

where $\delta I = \bar{I}-I$, $\delta h = \bar{h}-h$, $\delta h_x = \bar{h}_x-h_x$, and $\delta h_y = \bar{h}_y-h_y$, the integration process can be carried out by employing integration by parts in two dimensions that is given as

$$\iint_{\Omega} u\frac{\partial v}{\partial x}dA = \oint_{\Gamma} uv\nu_x d\ell - \iint_{\Omega}\frac{\partial u}{\partial x}vdA \tag{4.33}$$

and

$$\iint_{\Omega} u\frac{\partial v}{\partial y}dA = \oint_{\Gamma} uv\nu_y d\ell - \iint_{\Omega}\frac{\partial u}{\partial y}vdA \tag{4.34}$$

where ν_x and ν_y are the direction cosines. Thus δI becomes

$$\delta I = \iint_{\Omega}[\frac{\partial F}{\partial h} - \frac{\partial}{\partial x}(\frac{\partial F}{\partial h_x}) - \frac{\partial}{\partial y}(\frac{\partial F}{\partial h_y})]\delta h dA + \oint_{\Gamma}\frac{\partial F}{\partial h_n}\delta h d\ell = 0 \tag{4.35}$$

In index notation, it becomes

$$\delta I = \iint_{\Omega}[\frac{\partial F}{\partial h} - \frac{\partial}{\partial x_i}(\frac{\partial F}{\partial h_{,i}})]\delta h dA + \oint \frac{\partial F}{\partial h_{,i}}\nu_i \delta h d\ell = 0 \tag{4.36}$$

The minimizing function for the Laplace equation is given by

$$F = \frac{1}{2}[(\frac{\partial h}{\partial x})^2 + (\frac{\partial h}{\partial y})^2] \tag{4.37}$$

which has been derived by the Raleigh-Ritz method earlier in this chapter. For an anisotropic aquifer system the functional will be given as

$$F = \frac{1}{2}\, q_i\, \frac{\partial h}{\partial x_i} \tag{4.38}$$

where

$$q_i = -K_{ij}\, \frac{\partial h}{\partial x_j} \tag{4.39}$$

K_{ij} is the hydraulic conductivity tensor of an aquifer system.

The minimizing function, derived herein, excludes the effect of boundary conditions. In order to take boundary conditions into account, the line integral must be attached to Equation (4.31), i.e.,

$$I = \iint_{\Omega} F da - \oint_{\Gamma} \tilde{q} h d\ell \tag{4.40}$$

where $\tilde{q}$ is flow occurring through the boundary then

$$\delta I = \iint [\frac{\partial F}{\partial h} - \frac{\partial}{\partial x}(\frac{\partial F}{\partial h_x}) - \frac{\partial}{\partial y}(\frac{\partial F}{\partial h_y})] \delta h dA + \oint_{\Gamma} (\frac{\partial F}{\partial h_n} - \tilde{q}) \delta h d\ell = 0 \tag{4.41}$$

These types of functionals are called Thomson's principle.

The line integral in Equation (4.41) gives the complete boundary conditions to the problem, i.e.,

$$\frac{\partial F}{\partial h_n} = \tilde{q} \quad \text{or h prescribed}$$

Carrying out the Euler-Lagrange equation with the minimizing function (Equation 4.38), the following is obtained.

$$\frac{\partial F}{\partial h} = 0$$

$$\frac{\partial F}{\partial h_{,i}} = \frac{1}{2}(q_i + \frac{\partial q_i}{\partial h_{,i}} \frac{\partial h}{\partial x_i}) = q_i$$

$$\frac{\partial}{\partial x_i}\left(\frac{\partial F}{\partial h_{,i}}\right) = \frac{\partial}{\partial x_i} q_i = \text{div } \vec{q}$$

Thus

$$\delta I = \iint_{\Omega} \text{div } \vec{q}\ \delta h dA + \oint_{\Gamma} (q_n - \tilde{q}) \delta h d\ell = 0 . \qquad (4.42)$$

This implies that div $\vec{q}$ = 0 inside the domain Ω and $q_n = \tilde{q}$ or h must be prescribed on the boundary.

Virtual Work Method

Virtual work is defined as the work done on a particle by all forces acting on the particle as this particle is given a small hypothetical displacement (Shames, 1967). Since work consists of a force and a displacement, there are three possible ways to define the virtual work.

1. Virtual displacement x force.
2. Displacement x virtual force.
3. Combination of (1) and (2).

In ground-water flow systems there will unfortunately be neither forces nor displacements; however, there exists forcing functions of some sort such as sources and flows on the boundary and the potential function h which acts as the "virtual displacement." It should be clear that the "virtual work" for the case would be given as follows:

$$\delta I = \iiint_{\Omega} - P \delta h dV + \oiint_{\Gamma} \bar{q}_n \delta h dA = 0 \qquad (4.43)$$

where P is a source in the domain Ω, and $\bar{q}_n$ is a normal flow to the boundary Γ shown in Figure 4.1. Using Darcy's law and the divergence theorem, the right side of Equation (4.43) can be rewritten as follows.

$$\iiint_{\Omega} - P\delta h d\forall + \oiint_{\Gamma} \bar{q}_n \delta h dA = \iiint_{\Omega} P\delta h d\forall + \oiint_{\Gamma} q_i \nu_i \delta h dA$$

$$= \iiint P\delta h d\forall + \iiint \text{div } \vec{q}\ \delta h d\forall + \iiint q_i \frac{\partial \delta h}{\partial x_i}\, d\forall$$

$$= \iiint (\text{div } \vec{q} - P)\delta h d\forall + \iiint q_i \frac{\partial \delta h}{\delta x_i}\, d\forall \qquad (4.44)$$

At any point in the domain $\text{div}\,\vec{q} - p = 0$ is defined so that the first term on the right side of the above equation vanishes. The resulting equation is then given as follows:

$$\iiint_{\Omega} - P\delta h d\forall + \oiint_{\Gamma} \bar{q}_n \delta h dA = \iiint q_i \frac{\partial \delta h}{\partial x_i}\, d\forall \qquad (4.45)$$

One way of viewing this equation is to consider the left side as applied "virtual work" and the right side as response "virtual work."

Considering a subdomain which is called a finite element, the potential h within the element can be approximated as

$$h = [N]\{h\} \qquad (4.46)$$

where {h} is a vector denoting potential values at nodal

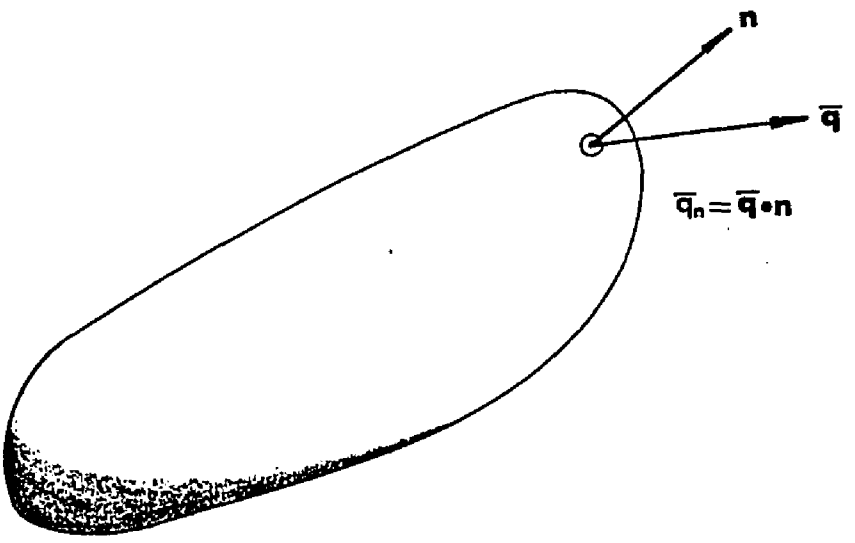

Figure 4.1. Flow around three-dimensional body.

points on the element as shown in Figure 4.2 and [N] is 1 x n matrix whose each entry must be a function of coordinates so that for any given set of coordinates the potential h can continuously be evaluated within the element. Using Equation (4.46) and making use of matrix rules, Equation (4.45) can be reduced to

$$\delta I = \{\delta h\}^T[-\iiint_\Omega [N]^T[N]\{P\}dV + \iint_{\Gamma_2} [M]^T[M]\{\bar{q}\}dA - \iiint_\Omega [B]^T[K][B]dV\{h\}] = 0 \qquad (4.47)$$

where the first row of the matrix [B] consists of the derivatives of [N] with respect to x coordinate and the second row is the same as the first but with respect to the y coordinate, and matrix [M] is the approximate function on the boundary. A detailed treatment of this subject is given in the following section.

Since $\{\delta h\}$ is a non-zero vector by definition, consequently the expression inside the brackets in Equation (4.47) must be zero. This is the basis for the finite element formulation.

In addition to the variational approach, the finite element equation can be obtained by another powerful numerical procedure, the weighted residual method, which is introduced in the next section.

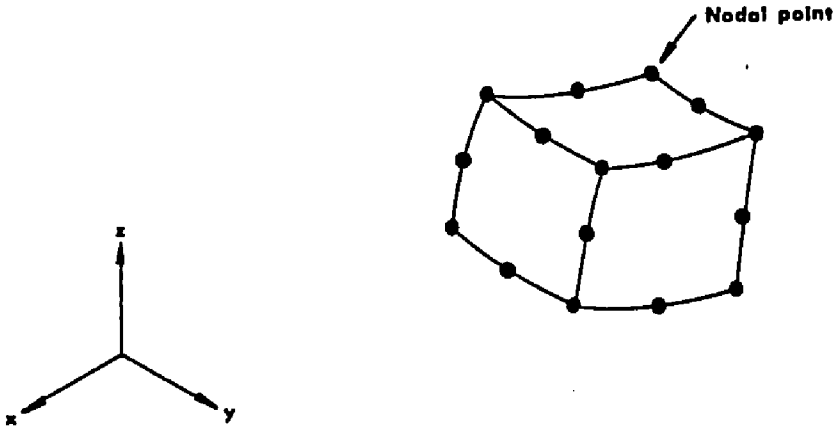

Figure 4.2. A finite element.

Weighted Residual Methods

Methods based on the variational approach require the existence of extremizing functions. The applications are, therefore, limited and there is a need for a more general approach to the numerical procedure. Such a generality is best provided by the weighted residual methods which is briefly reviewed here.

Consider a differential equation

$$L(u_o) = P \text{ in } \Omega \tag{4.48}$$

with proper boundary conditions so that the problem can be well posed. The differential operator L usually denotes a linear differential operator; nevertheless, any differential operator can be employed in the method. The function u_o, which is the exact solution, can be approximated by a set of functions $\phi_i(x)$ in the following manner (Dym and Shames, 1973).

$$u = \sum_{i=1}^{n} a_i \phi_i \tag{4.49}$$

where a_i are constants to be determined and ϕ_i are linearly independent functions (see Appendix A).

By replacing u_o by Equation (4.49), the equation (4.48) yields an error which is here called the residual, i.e.,

$$L(u) - P = R \tag{4.50}$$

The residual R is then forced to be zero, in the average sense, by orthogonalizing (see Appendix A) R with respect to w_i, i.e.,

$$\int R w_i dx = 0 \qquad i = 1, 2, \ldots, n \tag{4.51}$$

where w_i is a set of weighting functions (Gallagher, 1975).

Before the finite element method had become a popular numerical technique for solving many engineering problems, the finite difference method (abbreviated here as FDM) was the major procedure for approximating PDE's. It is important to note that FDM or the integrated finite difference method is a particular form of the weighted residual method. The weighting function w_i for FDM is unity, i.e.,

$$w_i = 1 \tag{4.52}$$

Therefore, the residual R remains as it is. For FDM, the only way to reduce R is to use finer differences. Consequently the convergence of FDM scheme is somewhat slower than one that is derived by the weighted residual method.

In general, the weighting function w_i can be different from the approximating function ϕ_i, and any complete and linearly independent set of functions can be used (see Appendix A). A popular method seen in the next section is the Galerkin's method in which the weighting function is identical to the approximating function.

Galerkin's Method

Galerkin's method is a particular form of the method of weighted residual. As mentioned in the previous section, the weighting function is the same as the approximating function; therefore, the necessary conditions for the weighting function will be automatically satisfied by the characteristics of the approximating function.

Consider a PDE:

$$L(u) - p = 0 \text{ in } D \tag{4.53}$$

and an approximate solution, which satisfies the boundary conditions:

$$u = \sum_{j=1}^{n} a_j \phi_j \tag{4.54}$$

and substituting u into Equation (4.53) yields a residual R. The residual is then orthogonalized with respect to the same approximating function ϕ_i. Hence

$$\int_d \{L(\Sigma a_j \phi_j) - P\}\phi_i dD = 0 \tag{4.55}$$

$$i = 1, 2, \ldots, n$$

Equation (4.55) consists of n individual equations. It is clear that Equation (4.55) gives a system of n linear equations if L is a linear differential operator. Since all ϕ_i's are orthogonalized with the residual R, it is possible to

define a series of arbitrary δa_i coefficients as

$$\delta u = \sum_{i=1}^{n} \delta a_i \phi_i \tag{4.56}$$

The equation (4.55) can be assembled into one equation as (Brebbia, 1978)

$$\int_D (L(u) - P)\delta u dD = 0 \tag{4.57}$$

The above equation is exactly the same as the one which is derived by the "virtual work" method, and taking the derivative of Equation (4.57) with respect to δa_i produces Equation (4.55).

In order to apply the method for the ground water flow equation in an arbitrary domain, the domain should be properly divided into subdomains which are here called finite elements. A typical element having n nodal points is shown in Figure 4.3.

Formulating the finite element expression for this element, the piezometric head within the element is then approximated by

$$h = \sum_{i=1}^{n} \zeta_i h_i = [\zeta_1 \zeta_2 \ . \ . \ . \ \zeta_n] \begin{Bmatrix} h_1 \\ h_2 \\ . \\ . \\ . \\ h_n \end{Bmatrix} = [N]\{h\} \tag{4.58}$$

where n is number of nodes on the element, h_i's are piezo-

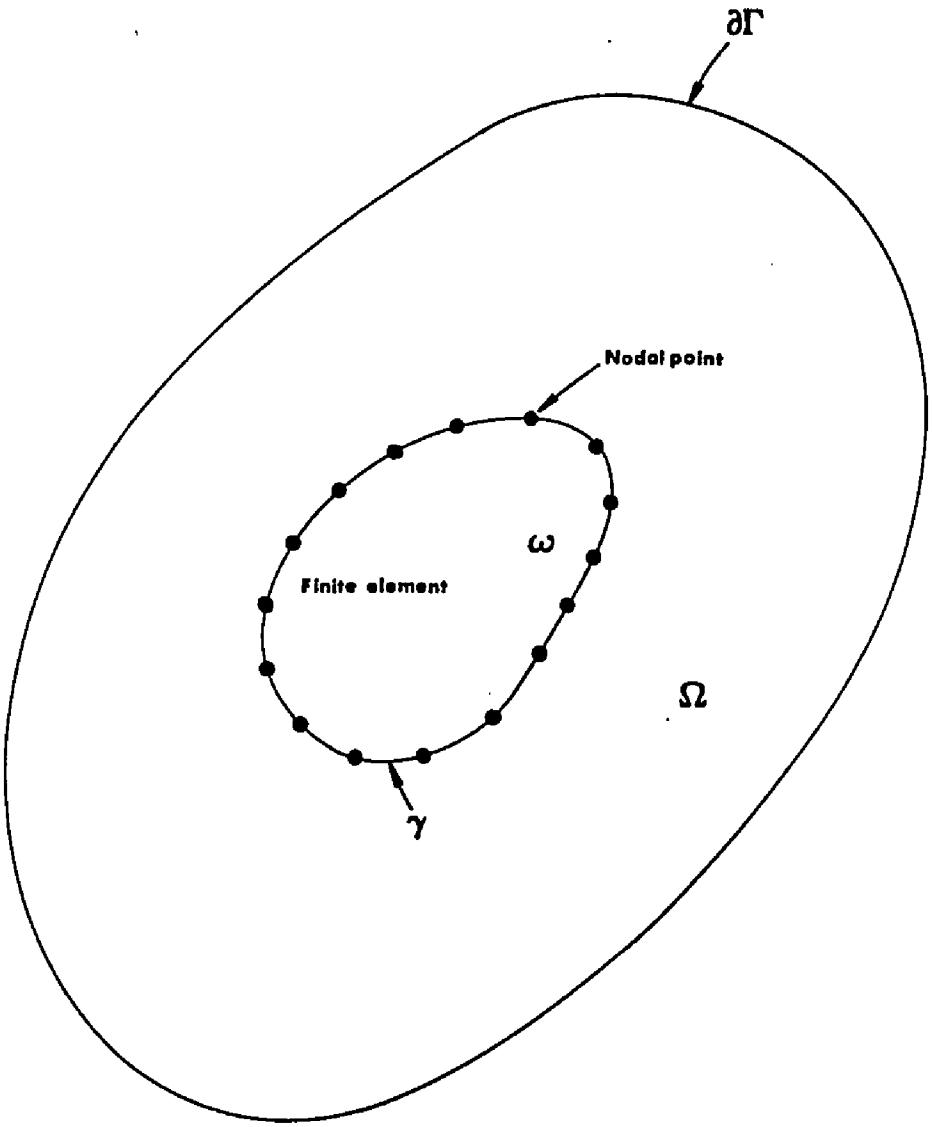

Figure 4.3. Two-dimensional aquifer and typical element.

metric heads at nodal points and ξ_i's are shape function. Applying Galerkin's procedure for the ground water equation and using successively Darcy's law and the divergence theorem,

$$\iint_\omega \left(\frac{\partial q_i}{\partial x_i} - P\right)\delta h dA = 0 \tag{4.59}$$

then

$$\iint_\omega q_i \frac{\partial \delta h}{\partial x_i} dA = \int_\Gamma q_n \delta h d\ell - \iint_\omega P\delta h dA \tag{4.60}$$

where q_n is flow on boundary of the entire domain, $q_i = -K_{ij}\partial h/\partial x_j$, and the symbol ω denotes the domain of the element. Substituting Equation (4.58) into the above equation,

$$\{\delta h\}^T \iint_\omega [B]^T[K][B]dA\{h\}$$

$$= \{\delta h\}^T \int_\gamma [M]^T[m]d\ell\{q_n\} - \{\delta h\}^T \iint_\omega [N]^T[N]dA\{P\} \tag{4.61}$$

where all vectors in { } consist of n entries; for example,

$$\{h\} = \begin{Bmatrix} h_1 \\ h_2 \\ \cdot \\ \cdot \\ \cdot \\ h_n \end{Bmatrix},$$

the matrix [M] is the shape function on the boundary Γ, the matrix [B](2 x n) is defined as

$$[B] = \begin{bmatrix} \frac{\partial \zeta_1}{\partial x} & \frac{\partial \zeta_2}{\partial x} & \cdots & \frac{\partial \zeta_n}{\partial x} \\ \\ \frac{\partial \zeta_1}{\partial y} & \frac{\partial \zeta_2}{\partial y} & \cdots & \frac{\partial \zeta_n}{\partial y} \end{bmatrix}, \tag{4.62}$$

and

$$[K] = \begin{bmatrix} K_{xx} & K_{xy} \\ \\ K_{yx} & K_{yy} \end{bmatrix}.$$

The finite element equation can be obtained by taking the derivative of Equation (4.61) with respect to $\{\delta h\}^T$. It follows that

$$\iint_{\omega} [B]^T[K][B]dA\{h\} = \int_{\Gamma} [M]^T[M]d\ell\{q_n\} - \iint_{\omega} [N]^T[N]dA\{P\} \tag{4.63}$$

The integral in the left side of the above equation is usually called the stiffness matrix in solid mechanics and the integral is here replaced by $[A\omega]$ for an element and [A] for the entire domain. The line integral in the equation (4.63) gives values only for the elements whose sides γ coincide with the boundary Γ where q_n's are prescribed. The line integral, therefore, vanishes for interior elements. The second integral in the right side of Equation (4.63) represents distribution sources or sinks in the element; it does not treat point sources like pumps. The treatment of point sources

will be discussed in the following section. It can also be shown that an entry of the matrix $[A_\omega]$ can be expressed as

$$A\omega_{ij} = K_{pq}\iint_{\omega} \frac{\partial \zeta_i}{\partial x_p} \frac{\partial \zeta_j}{\partial x_q} dA \tag{4.64}$$

in which subscripts i and j are free indices whereas the indices p and q are dummies. The integration for the source term can be written, in matrix form, as $\{S\} = [S\omega]\{P\}$ and an entry of $[S\omega]$ is given as

$$S\omega_{ij} = \iint \zeta_i \zeta_j dA \,. \tag{4.65}$$

Using the shorthand expressions, Equation (4.63) can be summarized for an element as

$$[A\omega]\{h_\omega\} = \{Q\gamma\} - \{S\omega\} \tag{4.66}$$

where

$$\{Q\omega\} = \int_\gamma [M]^T [M] d\ell \{q_n\} \,.$$

For the entire domain,

$$[A]\ \{h\} = \{Q\} - \{S\} \tag{4.67}$$

In general, the hydraulic conductivity tensor is symmetric; it can be shown that the global matrix [A] is also symmetric and the determinant of [A] is zero. This can be easily proved by taking the consideration of a hydrostatic system which results in the condition that the right side of Equation

(4.67) is zero and the piezometric heads are the same everywhere so that {h} can be replaced by a unit vector. Therefore, det [A] must be zero by Cramer's rule, implying necessity Dirichlet boundary condition.

Three-Node Triangular Element

The element consisting of three nodes, each at the apex of a triangle, is found in various engineering applications because it is the simplest and most flexible configuration, as shown in Figure 4.4. Moreover, every entry in the matrix [B] is constant, and it is easy to integrate Equation (4.64).

For the purpose of analyzing the characteristics of the element, a triangular element is first divided into three sub-elements, as shown in Figure 4.5. It is clear that the variation of piezometric head along any straignt line in or on the element is linear; accordingly, the element is classified as the constant strain element in solid mechanics. The shape function [N] is given by

$$[N] = [\xi_i(x,y),\ \xi_j(x,y),\ \xi_k(x,y)] \tag{4.68}$$

which must give

$$h(x,y) = [N] \begin{Bmatrix} h_i \\ h_j \\ h_R \end{Bmatrix} \tag{4.69}$$

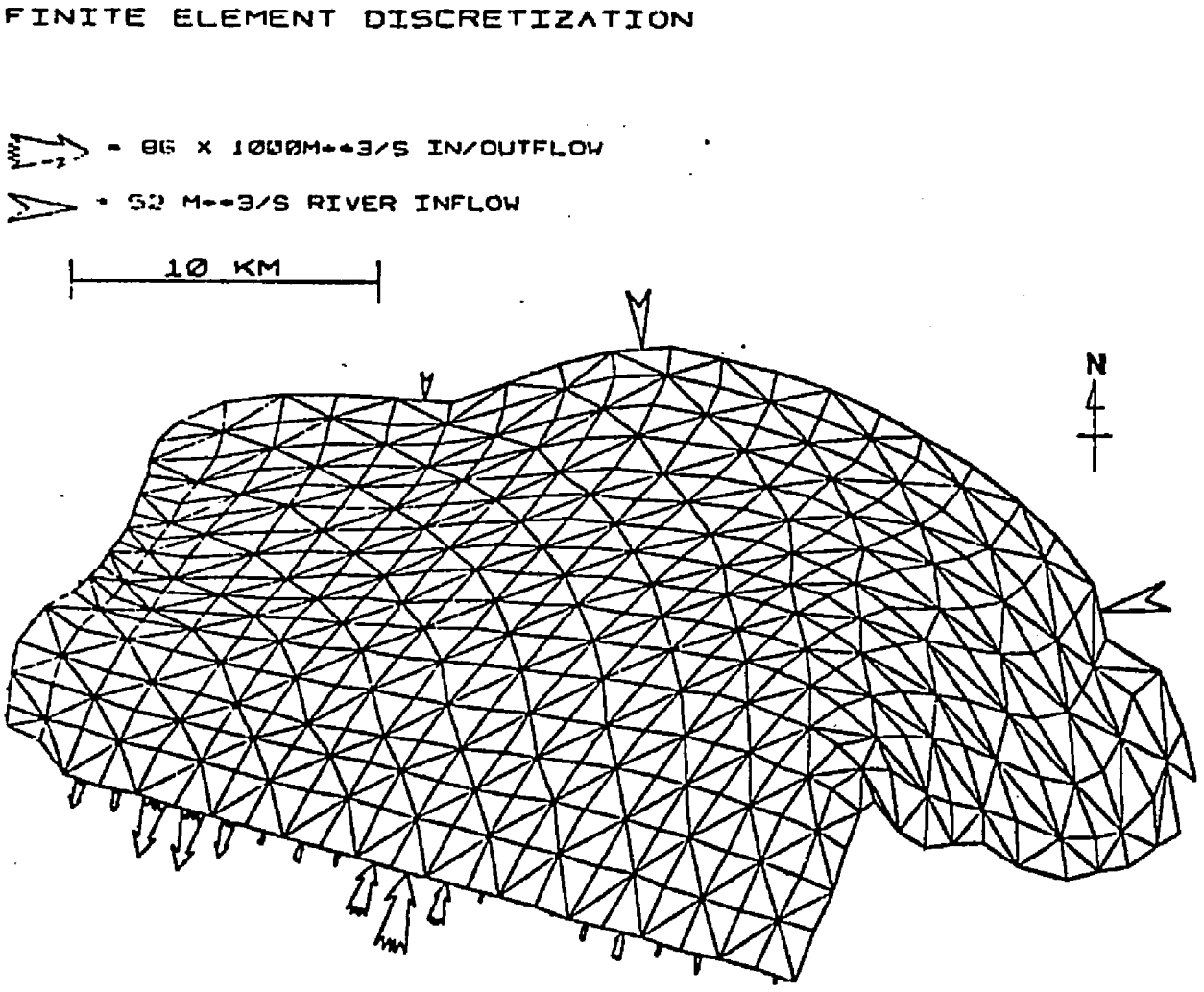

Figure 4.4. Finite element discretization using triangular elements.

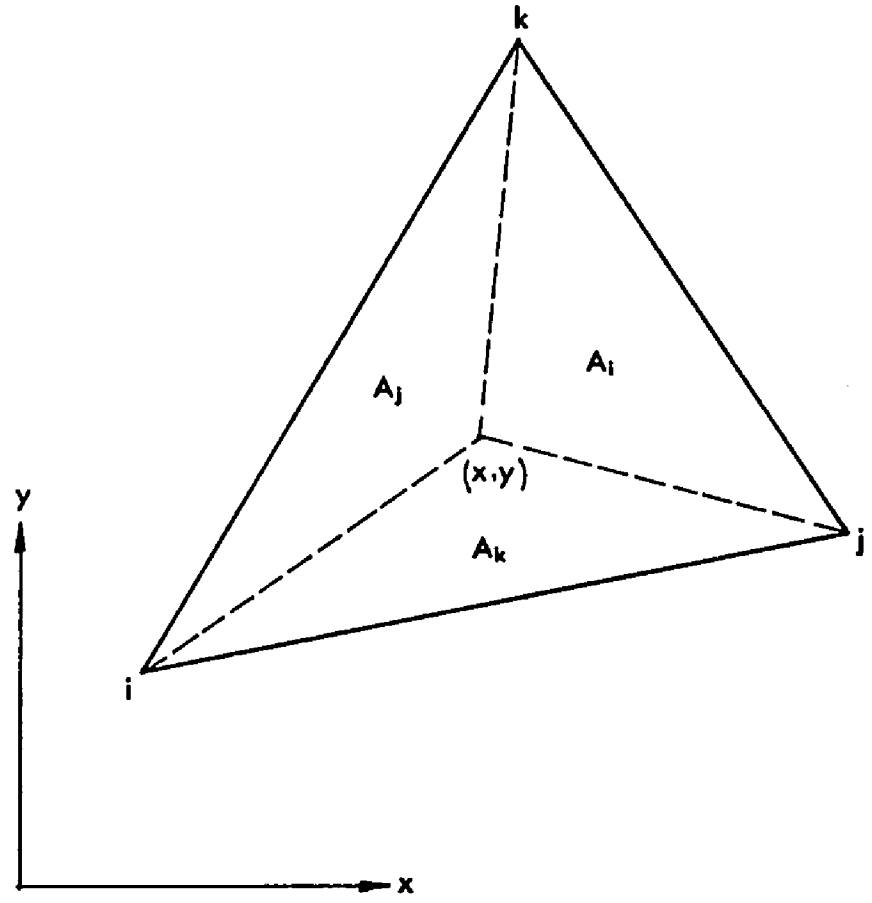

Figure 4.5. Triangular coordinates.

where ξ's are linear interpolation functions. This means that for point i $h(x_i,y_i)$ must be h_i. This results in [N] = [1, 0, 0]. This argument must also be applied for the other two nodel points j and k. For triangular elements the approximating functions ξ's are called the triangular coordinates and are defined as

$$\xi_m = A_m/A\,, \qquad m = i,\ j \text{ or } k \tag{4.70}$$

where A = the area of triangle. The sum of the above three equations always produces one, i.e.,

$$\xi_i + \xi_j + \xi_k = 1 \tag{4.71}$$

It can also be shown that

$$\left.\begin{aligned} \xi_i x_i + \xi_j x_j + \xi_k x_k &= x \\ \xi_i y_i + \xi_j y_j + \xi_k y_k &= y \end{aligned}\right\} \tag{4.72}$$

It is then possible to determine ξ's by solving Equations (4.71) and (4.72) simultaneously. Hence

$$\begin{bmatrix} \xi_i \\ \xi_j \\ \xi_j \end{bmatrix} = \frac{1}{2A} \begin{bmatrix} C_{kj} & b_i & a_i \\ C_{ik} & b_j & a_j \\ C_{ji} & b_k & a_k \end{bmatrix} \begin{bmatrix} 1 \\ x \\ y \end{bmatrix} \tag{4.73}$$

where

$$C_{mn} = y_m x_n - x_m y_n\,,$$

$$b_i = y_j - y_k ,$$
$$b_j = y_k - y_i ,$$
$$b_k = y_i - y_j ,$$
$$a_i = -x_j + x_k ,$$
$$a_j = -x_k + x_i ,$$

and

$$a_k = -x_i + x_j .$$

By replacing ζ in Equation (4.62) by ξ and substituting Equation (4.73) into Equation (4.64),

$$A\omega_{ij} = \frac{1}{4A}(k_{xx}b_ib_j + k_{xy}b_ia_j + k_{yx}a_ib_j + K_{yy}a_ia_j) \tag{4.74}$$

Integrations of ξ_i and $\xi_i\xi_j$ over the area of triangle such as Equation (4.65) are given by the integration equation (Eisenberg and Malvern, 1973; Segerlind, 1976) as

$$\iint_A \xi_i^a \xi_j^b \xi_k^c dA = \frac{a!b!c!}{(a + b + c + 2)!} 2A \tag{4.75}$$

The matrix $[SP] = \int\int [N]^T[N]dA$ then becomes

$$[S] = \frac{A}{12}\begin{bmatrix} 2 & 1 & 1 \\ 1 & 2 & 1 \\ 1 & 1 & 2 \end{bmatrix} \tag{4.76}$$

The first integral in the right side of Equation (4.63) must be evaluated on the boundary of the entire domain. To demonstrate this, a flow on the boundary is considered,

as shown in Figure 4.6. The boundary shape function [M] is given as

$$[M] = [(1 - \frac{\ell}{L}) \quad (\frac{\ell}{L})] \tag{4.77}$$

Thus

$$\int_0^L [M]^T[M]d\ell = \frac{L}{6}\begin{bmatrix} 2 & 1 \\ 1 & 2 \end{bmatrix} \tag{4.78}$$

Then

$$\int_\gamma [M]^T[M]\{q_n\}d\ell = \begin{bmatrix} Lqn_i/3 + Lqn_j/6 \\ Lqn_i/6 + Lqn_j/3 \\ 0 \end{bmatrix} \tag{4.79}$$

This is equivalent to $[Q\gamma]$ in Equation (4.66).

For the case of a point source, the second integral in Equation (4.60) can be rewritten as

$$\iint Q_p \delta(\vec{r} - \vec{r}_p)\delta h dA \tag{4.80}$$

where Q_p, a point source at $\vec{r}_p$, is shown in Figure 4.7. Using the triangular element, the above equation is reduced to

$$\{\delta h\}^T Q_p \iint [N]^T \delta(\vec{r} - \vec{r}_p)dA \tag{4.81}$$

Then

$$\{S_p\} = Q_p \iint \begin{bmatrix} \xi_i \\ \xi_j \\ \xi_k \end{bmatrix} \delta(\vec{r} - \vec{r}_p)dA$$

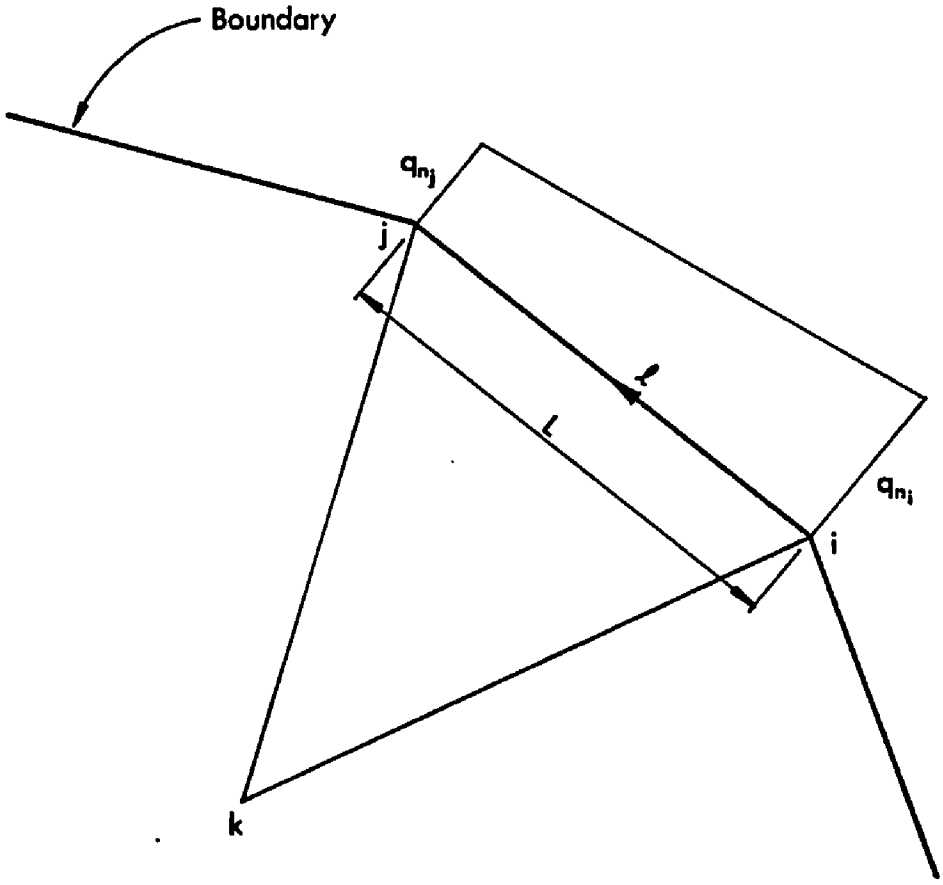

Figure 4.6. A distributed flow on the boundary.

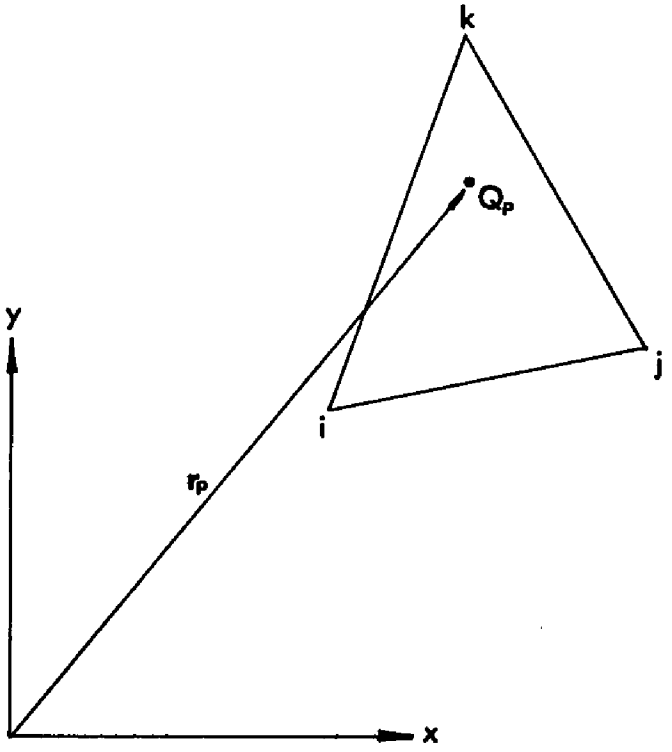

Figure 4.7. A point source in triangular element.

$$= Q_p \begin{Bmatrix} <i\delta> \\ <j\delta> \\ <k\delta> \end{Bmatrix} \tag{4.82}$$

where

$$<i\delta> \equiv \iint \xi_i \delta(\vec{r} - \vec{r}_p) dA .$$

The integral of $\delta(\vec{r} - \vec{r}_p)$ over the domain of the element in Figure 4.7 is unity at the location r_p, and so Equation (4.82) becomes

$$\{S_p\} = Q_p \begin{Bmatrix} \xi_i(\vec{r}_p) \\ \xi_j(\vec{r}_p) \\ \xi_k(\vec{r}_p) \end{Bmatrix} \tag{4.83}$$

The sum of ξ's is always unity by Equation (4.71); hence the magnitude of $\{S_p\}$ is Q_p (Neuman, 1981).

Comment of Finite Elements

It is clear, in general, that higher order elements give better solutions; however, this condition may require an additional analysis such as curvilinear coordinate transformations and complex numerical integrations. In the present study, the flow domain will be divided by sufficiently small triangular elements so that a better approximation can be expected although the simplest element is employed. It is of importance to note here that velocity is constant in

magnitude and direction within each element of this type since the triangular element with three nodes gives a linear variation in the potential field. Thus, the potential is continuous across the element boundaries whereas the velocity field is continuous. A graphic display would show potential lines parallel and equally spaced within any finite element, continuous but with a sudden change in direction and spacing in neighboring elements. The stream lines would also be parallel and equally spaced within any elements, making a square grid pattern with the potential lines. They would not be continuous in neighboring elements. This is undesirable if mass transport analyses are considered in aquifers because problems of these types will require continuous velocity fields otherwise mass will not be conserved. Continuous velocity fields can be accomplished by defining a new approximating solution of the piezometric head h as for the one-dimension case, i.e.,

$$h = \sum_{i=1}^{n} (h_i \zeta_i + h_i' \gamma_i) \tag{4.84}$$

where h_i' is an additional unknown and is the derivative of the head at nodal points. The approximating function of this type is called the Hermite interpolation (Birkhoff, Schultz and Varga, 1968; Huebner, 1975).

One of the important requirements in the finite

element discretization is the interelement continuity, which signifies that the element is joined to the same type of element or to elements with the same shape functions along continguous boundaries of elements.

As mentioned earlier, the triangular element is the simplest and most flexible. This may imply that any triangular-shaped element is acceptable for the discretization of an entire domain. However, it rurns out that the shape of the triangular element is constrained by the inner angles of the triangle in order to retain the stability of the global matrix [A]. The angles should be less than 90 degrees, preferably approaching an equilateral shape (Neuman, 1981).

CHAPTER 5

BOUNDARY ELEMENT METHOD

Fundamentals

After the finite element method was developed, many scientific problems, untouched for years, have been successfully solved using the unique features of the method. Although the finite element method is quite powerful, it requires a large amount of input data, often to a very cumbersome extent. The second numerical method, introduced herein, is the boundary element method which offers many important features. One of the advantages of the method is a considerable reduction in the input data for programming. The method is also well suited to unbounded domain problems which cannot be easily solved by the finite element method.

The analytical approach for the boundary element method (BEM) was introduced by George Green in the 18th century. The method is classified as a weighted residual method since the fundamental solution acts as the weighting function in the formulation.

Consider the Laplace equation $\nabla^2 u = 0$ and a differentiable function V. In order to derive Green's formula (Sokolnikoff and Redheffer, 1966), Green's first identity is used, i.e.,

$$\iiint V\nabla^2 u\,d\forall = \oiint V\frac{\partial u}{\partial n}dA - \iiint \frac{\partial v}{\partial n}\frac{\partial u}{\partial n}d\forall \,. \tag{5.1}$$

The one-dimensional form of the identity is well known as integration by parts. Switching u and v gives

$$\iiint u\nabla^2 v\,d\forall = \oiint u\frac{\partial v}{\partial n}\,dA - \iiint \frac{\partial u}{\partial n}\frac{\partial v}{\partial n}\,d\forall \,. \tag{5.2}$$

Subtracting one from the other, the second term on the right side cancels, leaving the following result:

$$\iiint (v\nabla^2 u - u\nabla^2 v)\,d\forall = \oiint (v\frac{\partial u}{\partial n} - u\frac{\partial v}{\partial n})\,dA \tag{5.3}$$

If the function V satisfies $\nabla^2 v = 0$ in the infinite domain, including the domain where $\nabla^2 u = 0$, except at a point i, as shown in Figure 5.1, and

$$\iiint \nabla^2 v\,d\forall = -1\,, \tag{5.4}$$

then Equation (5.3) becomes

$$u_i = \iint_{\partial D} (V\frac{\partial u}{\partial n} - u\frac{\partial v}{\partial n})\,dA\,. \tag{5.5}$$

Such a function V is called the fundamental solution. In a formal manner, Equation (5.4) can be rewritten as

$$\iiint_D \nabla^2 v\,d\forall = -\iiint_D \delta_i\,d\forall \tag{5.6}$$

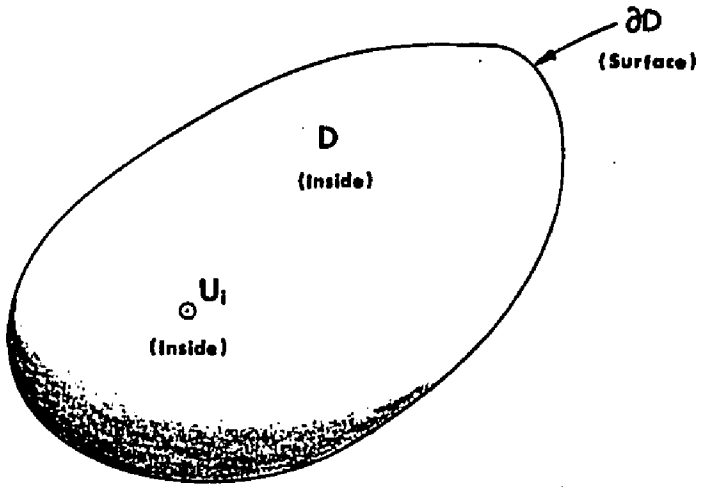

Figure 5.1. A point in a three-dimensional domain.

where δ_i is a Dirac delta function. Since the domain D is arbitrary, it can be shown that

$$\nabla^2 V + \delta_i = 0 \tag{5.7}$$

This is the governing equation for the fundamental equation.

In polar coordinates, Equation (5.7) becomes

$$\frac{\partial^2 v}{\partial r^2} + \frac{2}{r}\frac{\partial v}{\partial r} = \delta(r) \quad \text{(Three dimensions)} \tag{5.8}$$

The fundamental solution, considered here, is symmetric about a point where r = 0. For an isotropic three-dimensional medium the fundamental solution of Equation (5.7) is

$$V = \frac{1}{4\pi r} \tag{5.9}$$

By subsittuting Equation (5.9) into Equation (5.8), the solution is satisfied for any value of r except r = 0. To show that the integration of $\nabla^2 v$ over the domain is equal to minus one, the domain is divided into two subdomains, as shown in Figure 5.2. Making use of the divergence theorem, Equation (5.4) becomes

$$\begin{aligned}\iiint_D \nabla^2 v \, dV &= \iiint_\varepsilon \nabla^2 v \, dV + \iiint_{D-\varepsilon} \nabla^2 v \, dV \\ &= \iint_\varepsilon \frac{\partial v}{\partial n} dA \\ &= \iint_{\partial\varepsilon} \frac{\partial v}{\partial r} dA \end{aligned} \tag{5.10}$$

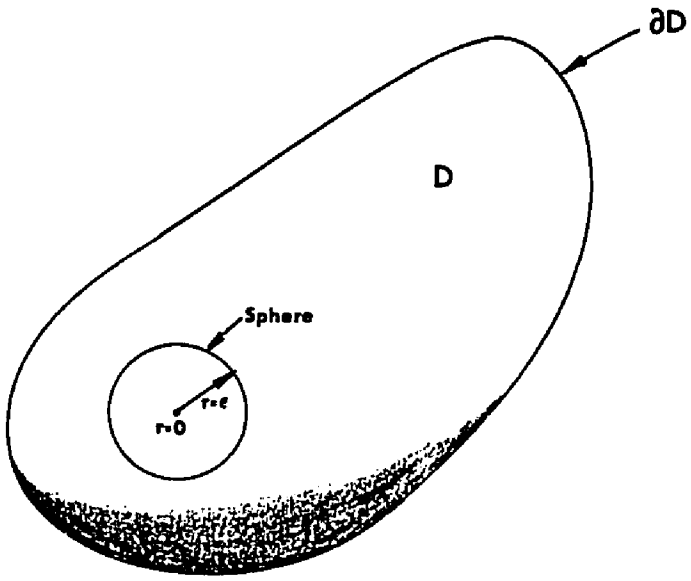

Figure 5.2. A sphere in a three-dimensional domain.

Substituting the fundamental solution Equation (5.9) into Equation (5.10) and letting $dA = r^2 \sin\phi \, d\phi \, d\theta$ for a sphere gives

$$\begin{aligned}
\iint_{\partial\varepsilon} \frac{\partial v}{\partial r} dA &= \int_0^{2\pi}\int_0^{\pi} \frac{\partial}{\partial r}\left(\frac{1}{4\pi r}\right) r^2 \sin\phi \, d\phi \, d\theta \\
&= \frac{1}{4\pi}\int_0^{2\pi}\int_0^{\pi} -\frac{1}{r^2} r^2 \sin\theta \, d\phi \, d\theta \\
&= -\frac{1}{4\pi} 2\pi \int_0^{\pi} \sin\phi \, d\phi \\
&= -\frac{1}{2}[-\cos d]_0^{\pi} \\
&= \frac{1}{2}(\cos\pi - \cos o) = -1
\end{aligned} \tag{5.11}$$

For a two-dimensional medium, such as heat flow in a thin plate or the magnetic field around an electronically activated rod (Ampère's law), the fundamental solution is given by

$$V = \frac{1}{2\pi} \log_e\left(\frac{1}{r}\right) \tag{5.12}$$

where the medium is assumed to be isotropic (a case of an anisotropic medium can be handled by using a different fundamental solution). The fundamental solution should satisfy the integral:

$$\iint_D \nabla^2 v \, dA = -1 \tag{5.13}$$

Using the same procedure as for the three-dimensional case, the two-dimensional domain can be reduced to a circle as

$$\iint_D \nabla^2 v dA = \oint_{\partial D} \frac{\partial v}{\partial n} d\ell = \int_0^{2\pi} - \frac{1}{2\pi r} r d\theta$$

$$= - \frac{1}{2\pi} 2\pi = -1 \qquad (5.14)$$

The Equation on the Boundary

Equation (5.5) is valid for any point in the domain D. In order to formulate the problem as a boundary element method, point i must be taken to the boundary.

Consider a hemisphere on the boundary of a three-dimensional domain, as shown in Figure 5.3. The boundary point is assumed to be at the center of the sphere having a radius of ε (Brebbia, 1978). The radius ε is then reduced to zero by taking the limit. The point will eventually become a boundary point which is resting on a smooth surface. For taking a closer look at the point, the boundary ∂D_2, where $\partial u/\partial n$ is prescribed, is divided into two parts, Equation (5.5) then becomes

$$u_i = \iint_{\partial D_1} (v\frac{\partial u}{\partial n} - u\frac{\partial v}{\partial n}) dA + \iint_{\partial D_2 - \varepsilon} (v\frac{\partial u}{\partial n} - u\frac{\partial v}{\partial n}) dA$$

$$+ \iint_{\partial \varepsilon} (v\frac{\partial u}{\partial n} - u\frac{\partial v}{\partial n}) dA \qquad (5.15)$$

Substituting the fundamental solution (Equation 5.9) into the

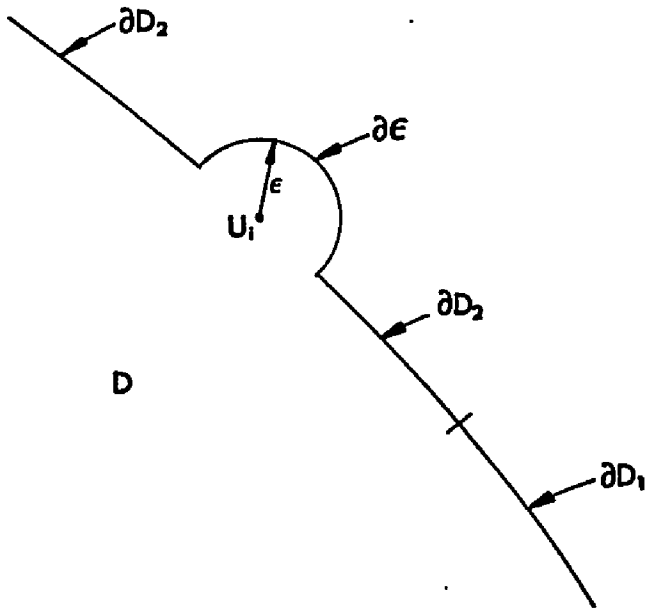

Figure 5.3. Hemisphere on boundary ∂D_2.

third integral of Equation (5.15) and taking the limit as $\varepsilon \to 0$ yields:

$$\lim_{\varepsilon\to 0}\{\iint_{\varepsilon} u\frac{\partial v}{\partial n}dA\} = \lim_{\varepsilon\to 0}\{-\int_0^{2\pi}\int_0^{\pi} u\frac{1}{4\pi\varepsilon^2}\varepsilon^2\sin\phi d\phi d\theta\}$$

$$= \frac{u_i}{2}[-\cos\ ]_0^{\frac{\pi}{2}} = \frac{u_i}{2}[0-1]$$

$$= -\frac{1}{2}u_i \qquad (5.16)$$

and

$$\lim_{\varepsilon\to 0}\{\iint_{\varepsilon} v\frac{\partial u}{\partial n}dA\} = \lim_{\varepsilon\to 0}\{\int_0^{2\pi}\int_0^{\frac{\pi}{2}} \frac{1}{4\pi\varepsilon}(\frac{\partial u}{\partial n})\varepsilon^2\sin\phi d\phi d\theta\}$$

$$= \lim_{\varepsilon\to 0}\frac{\varepsilon}{2}(\frac{\partial u}{\partial n})(\cos o - \cos\frac{\pi}{2})$$

$$= \lim_{\varepsilon\to 0}\{\frac{\varepsilon}{2}(\frac{\partial u}{\partial n})\} = 0\,. \qquad (5.19)$$

As ε is now zero, the boundary $\partial D_2 - \varepsilon$ becomes ∂D_2. Substituting the results into Equation (5.15) gives

1. For three dimensions

$$\frac{1}{2}u_i = \iint_{\partial D}(v\frac{\partial u}{\partial n} - u\frac{\partial v}{\partial n})dA \qquad (5.18)$$

where

$$V = \frac{1}{4\pi r}$$

2. For two dimensions

$$\frac{1}{2}u_i = \int_{\partial D}(v\frac{\partial u}{\partial n} - u\frac{\partial v}{\partial n})d\ell \qquad (5.19)$$

where

$$V = \frac{1}{2\pi} \log_e(\frac{1}{r})$$

It must be emphasized that Equations (5.18) and (5.19) are valid only for smooth boundaries. This becomes an important factor for discretizing the boundary by boundary elements. It is clear that constant elements, as shown in Figure 5.4, give smooth boundaries since the points where the unknown values are considered are assumed to be in the middle of each element. A more detailed treatment of this subject can be found in Brebbia (1978).

For better accuracy in the numerical solution, the boundary will be discretized by linear elements in this study.

Linear Boundary Element

In the present study, the boundary of the domain is approximated by a series of linear segments or linear elements, as shown in Figure 5.5 and the variation of u and $\partial u/\partial n$ are assumed to be linear within each element.

Realizing that the boundary will no longer be smooth as the unknowns are not located at the nodes, Equation (5.19) is rearranged for linear elements are rewritten for non-smooth boundaries as

$$c_i u_i + \sum_{j=1}^{n} \int_{\partial D_j} u \frac{\partial v}{\partial n} d\ell_j = \sum_{j=1}^{n} \int_{\partial D_j} v q d\ell_j \qquad (5.20)$$

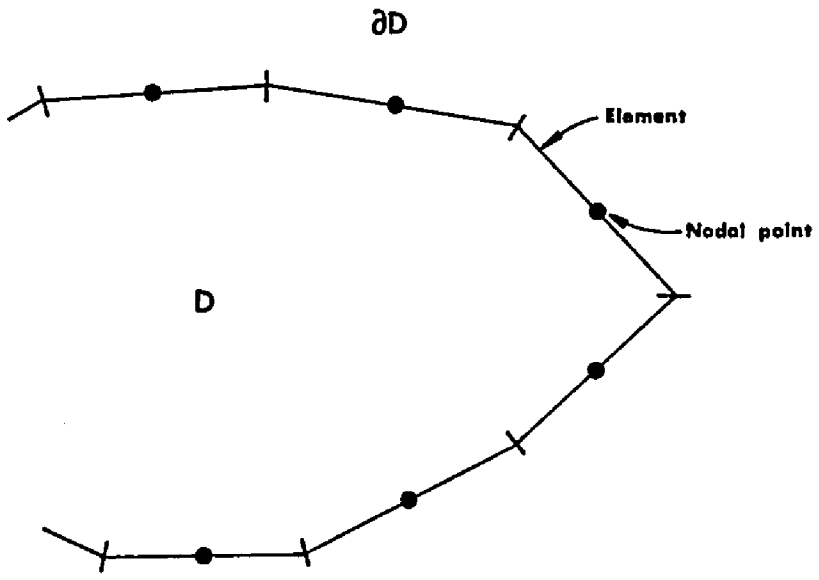

Figure 5.4. Discretization into constant elements.

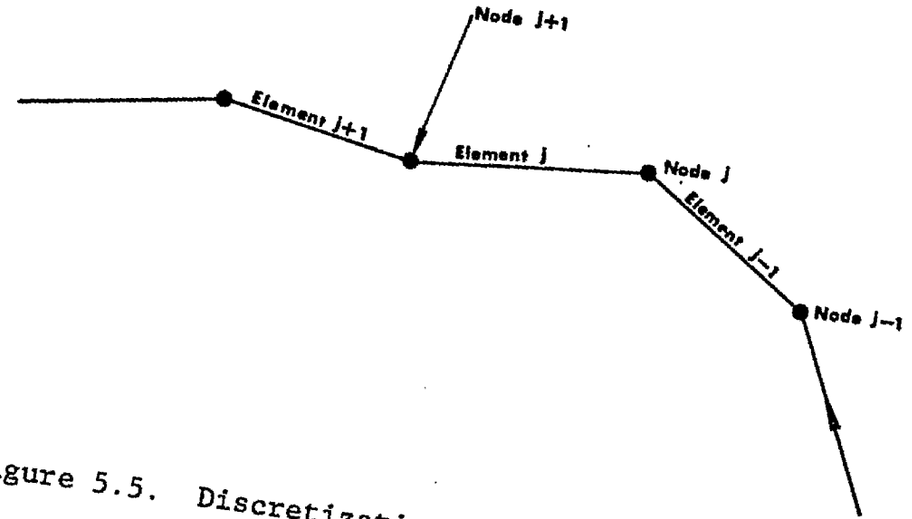

Figure 5.5. Discretization into linear elements.

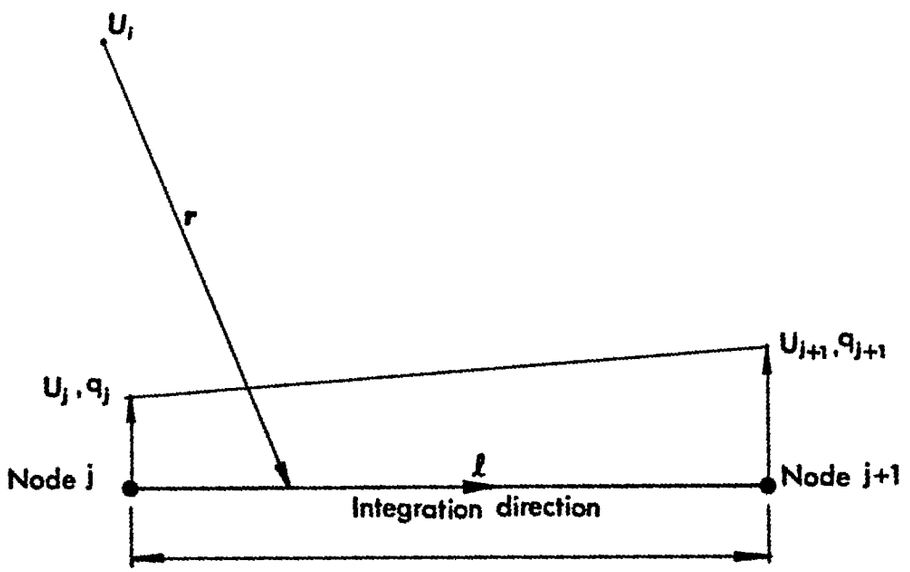

Figure 5.6. A linear element.

where n is number of nodes, $c_i \neq 1/2$, and $q = \partial u/\partial n$.

To evaluate the integral in Equation (5.20), a typical linear element is considered as shown in Figure 5.6. The values of u and q at any point in the element can then be defined in terms of the nodal values as

$$u_j(\ell) = [\phi_1 \ \phi_2]_j \begin{Bmatrix} u_j \\ u_{j+1} \end{Bmatrix}$$

$$q_j(\ell) = [\phi_1 \ \phi_2]_j \begin{Bmatrix} q_j \\ q_{j+1} \end{Bmatrix} \tag{5.21}$$

where

$$\phi_1 = (1 - \frac{\ell}{L_j})$$

and

$$\phi_2 = \frac{\ell}{L_j} .$$

The integrals in Equation (5.20) become

$$\int u \frac{\partial v}{\partial n} \, d\ell_j = \int [\phi_1 \ \phi_2]_j \frac{\partial v}{\partial h} \, d\ell \begin{Bmatrix} u_j \\ u_{j+1} \end{Bmatrix}$$

$$= [h_{ij} \ \bar{h}_{ij}] \begin{Bmatrix} u_j \\ j_{j+1} \end{Bmatrix} \tag{5.22}$$

and

$$\int vqd\ell_j = \int v[\phi_1 \ \phi_1]_j d\ell_j \begin{Bmatrix} q_j \\ q_{j+1} \end{Bmatrix}$$

$$= [g_{ij} \ \bar{g}_{ij}] \begin{Bmatrix} g_j \\ g_{j+1} \end{Bmatrix} \qquad (5.23)$$

where

$$h_{ij} = \int \phi_1 \frac{\partial v}{\partial h} \, d\ell_j, \ \bar{h}_{ij} = \int \phi_2 \frac{\partial v}{\partial n} \, d\ell_j ,$$

$$g_{ij} = \int v\phi_1 d\ell_j , \ \bar{q}_{ij} = \int v\phi_2 \, d\ell_j ,$$

and

$$V = \frac{1}{2\pi} \log_e(\frac{1}{r}) .$$

The evaluation of $\partial v/\partial n$ will be discussed later in this chapter.

Substituting Equations (5.22) and (5.23) into Equation (5.20), the algebraic linear equation for node j is

$$[h'_{i1}h'_{i2}\cdots c_i \cdots h'_{in}] \begin{Bmatrix} u_1 \\ u_2 \\ \vdots \\ u_i \\ \vdots \\ u_n \end{Bmatrix} = [g'_{i1}g'_{i2}\cdots g'_{in}] \begin{Bmatrix} q_1 \\ q_2 \\ \vdots \\ \vdots \\ \vdots \\ q_n \end{Bmatrix} \qquad (5.24)$$

where

$$h'_{ij} = h_{ij} + \bar{h}_{ij-1}$$

and

$$g'_{ij} = g_{ij} + \bar{g}_{ij-1}$$

For elements attached to node i, $\partial v/\partial n$ is absolutely zero since the angle between vector $\vec{r}$ and $\vec{n}$ as in Figure 5.7 is ninety degrees and $\partial v/\partial n$ is given by $(\partial v/\partial r)\cos\theta$. Repeating i from 1 to n gives a n x n system of equations. Hence

$$H\vec{u} = G\vec{Q} \tag{5.25}$$

The boundary ∂D on the domain D consists of two kinds of boundaries; ∂D_1 where u's are prescribed and ∂D_2 where q's are prescribed. This means that the total number of unknowns in Equation (5.25) is still n instead of 2 x n, hence Equation (5.25) can be solved uniquely. For the hydrostatic case, i.e., $\vec{Q} = \vec{0}$, this produces $H\vec{u} = \alpha H\vec{x} = \vec{0}$ where entries of the vector $\vec{x}$ are unity. The constant α can be any number of meaning that the determinant of the matrix H must be zero.

The following two statements can be implicitly defined.

1. $$c_i = h_{ii} = -\sum_{\substack{j=1 \\ j\neq i}}^{n} h_{ij} \tag{5.26}$$

2. At least one of $\vec{u}$ must be prescribed.

The former is easily derived by letting $\vec{u}$ be unity, then solving for h_{ii}. The latter is somewhat difficult to prove; however, engineering intuition can provide a clear-cut explanation to this statement.

It can also be shown that $\vec{Q}$ remains unchanged even if any constant vector $\alpha\vec{x}$ is added to $\vec{u}$, i.e.,

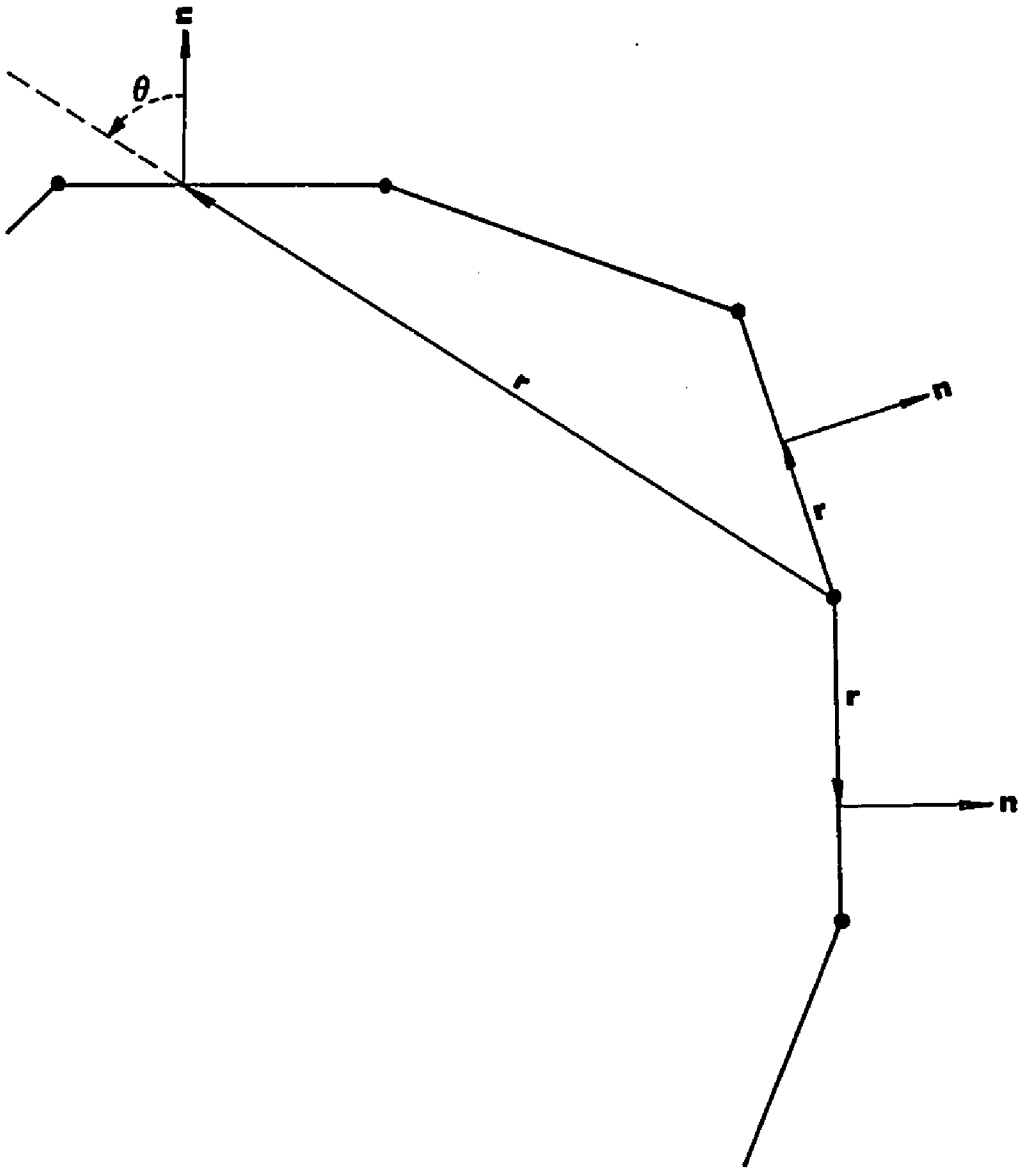

Figure 5.7. Neighboring elements and definition of the angle θ.

$$H(\vec{u} + \alpha\vec{x}) = H\vec{u} + \alpha H\vec{x} = G\vec{Q} .$$

This means that the flow in a pipe between two tanks exists because of difference in head between two tanks, not because of the heights of the tanks. In other words, $\vec{u}$ must be measured from some base or datum line. Therefore, at least one of the entries of vector $\vec{u}$ must be given.

Evaluation of $\partial v/\partial n$

The derivative of the fundamental solution v with respect to the normal direction at any point on the boundary is given by

$$\frac{\partial v}{\partial n} = \frac{\partial v}{\partial r}\frac{dr}{dn} \tag{5.27}$$

where

$$V = \frac{1}{2\pi}\log_e(\frac{1}{r})$$

and

$$\frac{\partial v}{\partial r} = -\frac{1}{2\pi r} .$$

By inspection of the differential triangle in Figure 5.8, $\Delta r \simeq \Delta n \cos\theta$ for $\Delta\theta$. The small incremental length Δr, being in the direction of $\vec{r}$ as shown in Figure 5.8, is not the magnitude of $\Delta\vec{R}$.

Taking the limit of $\Delta r/\Delta n$ as $\Delta\theta \to 0$ leads to

$$\frac{dr}{dn} = \lim_{\Delta\theta\to 0}\frac{\Delta r}{\Delta n} = \cos\theta \tag{5.28}$$

and hence

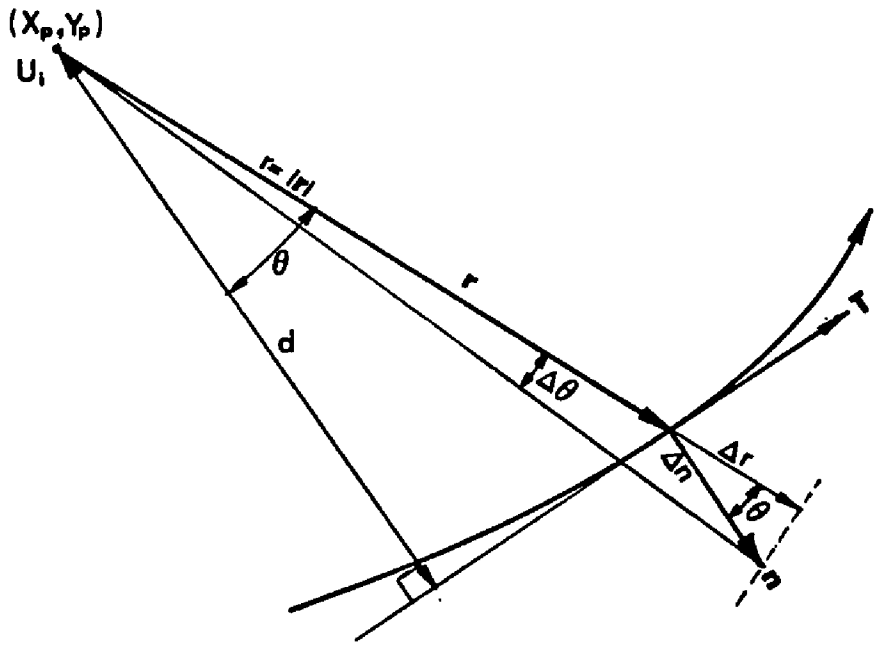

Figure 5.8. Definition of d on a continuous curve.

$$\frac{\partial v}{\partial n} = -\frac{1}{2\pi r}\cos\theta \tag{5.29}$$

The tangent vector at the point where the vector $\vec{r}$ intersects the boundary is defined as

$$\vec{T} = dx\hat{i} + dy\hat{j} .$$

The definition of the normal vector then provides that

$$\vec{n} = dy\hat{i} - dx\hat{j}$$

so that the dot product of two vectors $\vec{T}$ and $\vec{n}$ is zero. Making use of the definition of the dot product, $\cos\theta$ can be interpreted as

$$\vec{n}\cdot\vec{r} = |\vec{n}||\vec{r}|\cos\theta$$

where θ is an angle between $\vec{n}$ and $\vec{r}$. The cosine of θ is also equal to d/r where the length d is the perpendicular distance from the point where r=0 to the tangent line. Therefore, $\partial v/\partial n$ may be expressed as

$$\frac{\partial v}{\partial n} = \frac{\partial v}{\partial n}\cdot\frac{d}{r} \tag{5.30}$$

where

$$d = \vec{n}\cdot\vec{r}/|\vec{n}| .$$

For the purpose of applying the above expression to the numerical solution, the expression is rewritten for the discretized boundary of linear elements.

Referring to Figure 5.9, the normal vector is defined as

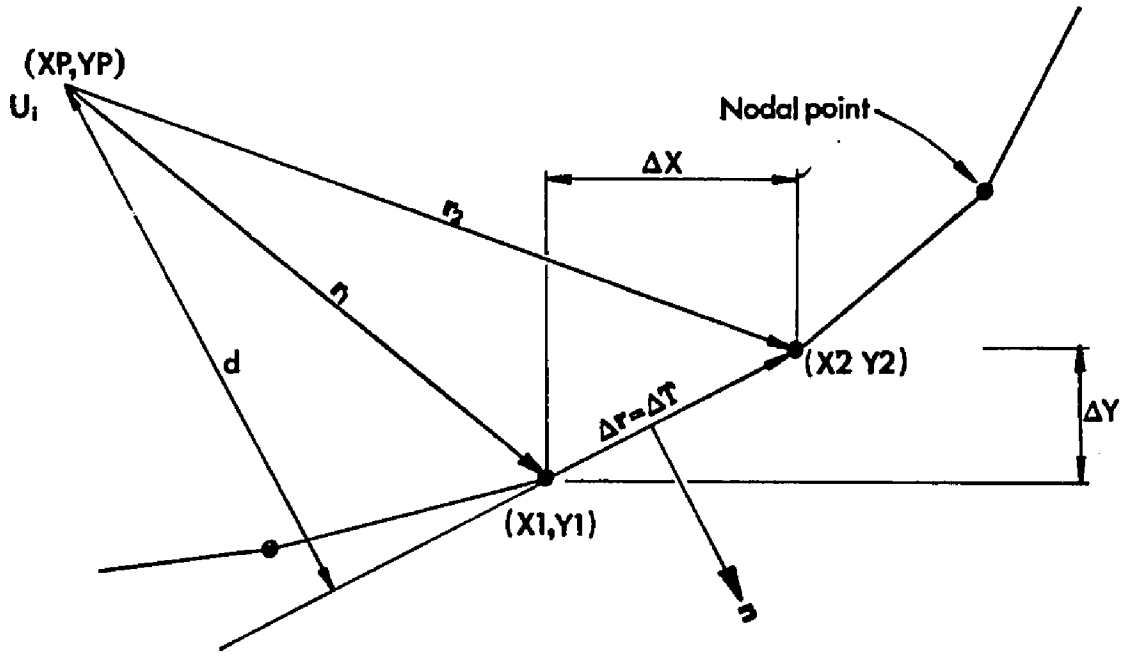

Figure 5.9. Definition of d on a linear element.

$$\vec{n} = \Delta y\hat{i} - \Delta x\hat{j}$$

It is a constant vector within each element so that the choice of $\vec{r}$ (either $\vec{r}_1$ or $\vec{r}_2$) is arbitrary. The vector $\vec{r}_1$ can be expressed as

$$\vec{r}_1 = (x1 - xp)\hat{i} + (y1 - yp)\hat{j} .$$

Hence

$$d = \frac{\vec{n}\cdot\vec{r}}{|\vec{n}|} = \frac{\Delta y(x1 - xp) - \Delta x(y1 - xp)}{L} \qquad (5.31)$$

where L is the length of the element.

The distance d can be found from the following expression,

$$d = \frac{1}{L}\vec{K}\cdot(\vec{r}_1 \times \Delta\vec{r}) .$$

One can show that the above equation is identical to Equation (5.31).

Poisson's Equation

One of the most interesting features of the boundary element method based on Green's function is that it is easy to add point sinks or point sources, as shown in Figure 5.10, to the governing equations.

Consider the governing equation

$$K\nabla^2 u - f = 0 \quad \text{in} \quad D \qquad (5.32)$$

with the boundary conditions:

$$u \text{ specified on } \partial D_1$$

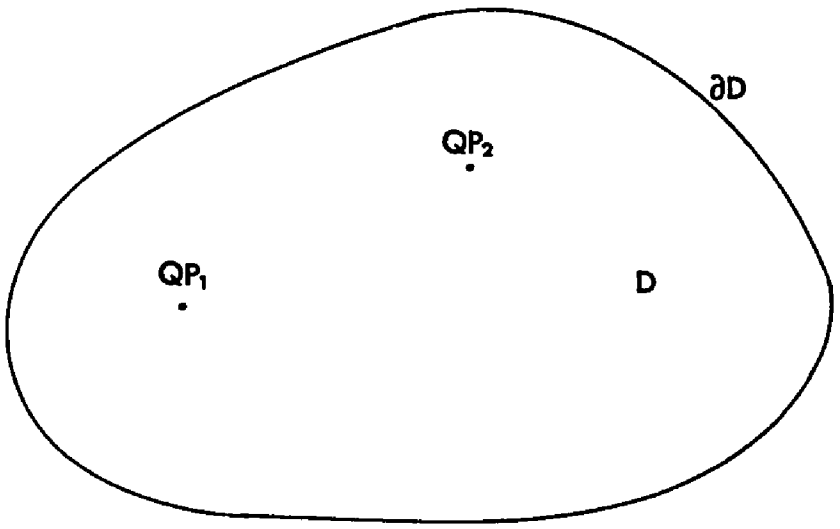

Figure 5.10. Two-dimensional medium with sinks.

and

$$q = K\partial u/\partial n \text{ specified on } \partial D_2$$

where

$K[L^2/T]$ = hydraulic conductivity x constant length

$f[L/T]$ = sink

Since the domain is two-dimensional, the constant K is not exactly the same as defined by hydrologists. It is often called transmissivity if the domain is in a flat plane.

The procedure, used to obtain the boundary equation for Poisson's equation, is exactly the same as that used for the Laplace equation but with an additional term. The procedure starts with the following equations,

$$\iint_D V(K\nabla^2 u - f)\,dA + \oint_{\partial D} vq\,d\ell - \iint_D \frac{\partial v}{\partial x_i} K \frac{\partial u}{\partial x_i}\,dA - \iint_D vf\,dA \tag{5.33}$$

and

$$\iint_D u(k\nabla^2 u)\,dA = \oint_{\partial D} uK\frac{\partial v}{\partial n}\,d\ell - \iint_D K\frac{\partial u}{\partial x_i}\frac{\partial v}{\partial x_i}\,dA \tag{5.34}$$

where

$$V = \frac{1}{2\pi k}\log_e\left(\frac{1}{r}\right).$$

Eliminating common terms in Equations (5.33) and (5.34) and using the property

$$\iint_D K\nabla^2 v = -1 \tag{5.35}$$

$$u_i + \iint_D vf dA = \oint_{\partial D} (vq - uk \frac{\partial v}{\partial n}) d\ell \tag{5.36}$$

The area integral in Equation (5.36) can be reduced to

$$\iint_D vf dA = vf \iint dA = \sum_{k=1}^{m} V(r_{ik}) \times QP_k \tag{5.37}$$

where m is the number of point discharges in the domain, r_{ik} is the distance between the point i and the location of a point discharge (see Figure 5.11), and the rate of point discharge QP_k, has units of $[L^3/T]$ and is defined in the integral form as

$$QP_k = f_k \iint dA = f_k \Delta A \, .$$

Discretization with linear elements results in

$$c_i u_i + \sum_{k=1}^{m} V(r_{rk}) \times QP_k + \sum_{j=1}^{n} \int_{\partial D} u \frac{\partial v}{\partial n} d\ell = \sum_{j=1}^{n} \int_{\partial D} qv d\ell \tag{5.38}$$

which can be rewritten for ith node as

$$B_i + \sum_{j=1}^{n} h'_{ij} u_j = \sum_{j=1}^{n} g'_{ij} q_j \tag{5.39}$$

where

$$B_i = \sum_{k=1}^{m} V(r_{ik}) \times QP_k \, .$$

The entire system of equations for n boundary nodes can be expressed in matrix form as

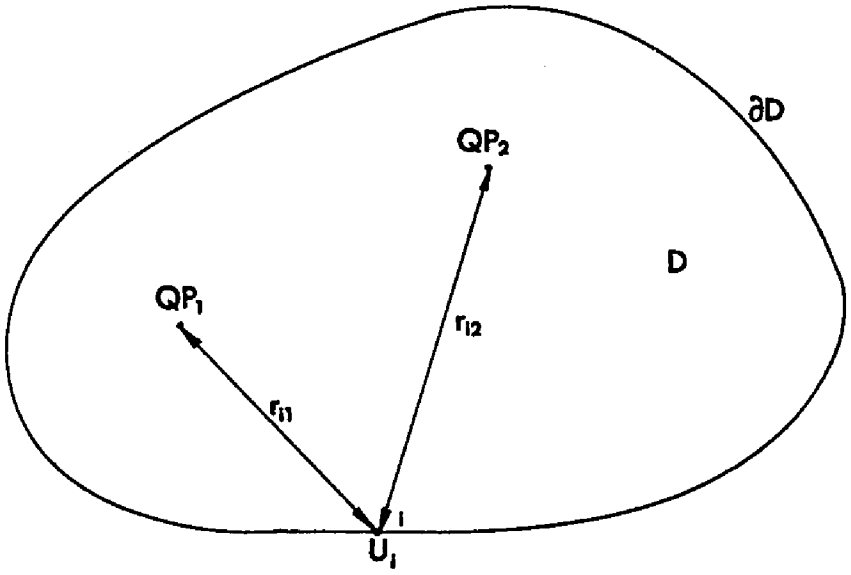

Figure 5.11. Location of sinks.

$$\vec{B} + H\vec{u} = G\vec{Q} \tag{5.40}$$

Since its applicability is comprehensive, the method will be demonstrated with an example.

Numerical Integration

The most common solution method of the numerical integration techniques is Simpson's rule, which was widely used by marine engineers for finding the volume of vessels and tankers before the advent of the computer age. Simpson's rule uses a simple procedure in which the integration limit is first divided into sections (sample points) by equally spaced increments. The only way to achieve a desired accuracy is to increase the number of sections. This type of integration procedure is not generally recommended for a computer solution since the numerical integration must be repeated many times to achieve reasonable accuracies.

The solution technique used in the computer program is the Gauss-Legendre Quadrature or Gauss Quadrature found in most textbooks for computer applications. The sample points in the method are uniquely spaced in order to achieve the greatest accuracy. The integration procedure is given in the form of

$$\int_{-1}^{+1} f(\xi)d\xi \simeq \sum_{m=1}^{p} w_m f(\xi_m) \tag{5.41}$$

where P is the number of integration points whose locations are given by ξ_m, and w_m is the weighting factor.

Before proceeding, the entries of the matrices H and G must first be filled out using numerical integration techniques. The shape function ϕ_1 and ϕ_2 in Equations (5.22) and (5.23) are rewritten in terms of ξ_i,

$$\phi_1 = (1 - \frac{\ell}{L}) = (0.5 - \frac{\xi_m}{2})$$

$$\phi_2 = (\frac{\ell}{L}) = (\frac{\xi_m}{2} + 0.5) \; . \tag{5.42}$$

Making use of Equations (5.41) and (5.42), the h's and g's in Equations (5.23) and (5.24) are approximated by the following expressions:

$$h_{ij} = \frac{L_j}{2} \sum_{m=1}^{P} K(-\frac{1}{2\pi k r_m})(\frac{d}{r_m})(0.5 - \frac{\xi_m}{2})W_m$$

$$\bar{h}_{ij} = \frac{L_j}{2} \sum_{m=1}^{P} K(-\frac{1}{2\pi k r_m})(\frac{d}{r_m})(\frac{\xi_m}{2} + 0.5)W_m$$

$$g_{ij} = \frac{L_j}{2} \sum_{m=1}^{P} (\frac{1}{2\pi k})\log_e(\frac{1}{r_m})(0.5 - \frac{\xi_m}{2})W_m$$

$$\bar{g}_{ij} = \frac{L_j}{2} \sum_{m=1}^{P} (\frac{1}{2\pi k})\log_e(\frac{1}{r_m})(\frac{\xi_m}{2} + 0.5)W_m \tag{5.43}$$

where

$$x_m = \bar{x} + \frac{\Delta x}{2}\xi_m, \; y_m = \bar{y}_m + \frac{\Delta y}{2}\xi_m,$$

$$\Delta x = x_{j+1} - x_j, \; \Delta y = y_{j+1} - y_j,$$

$$\bar{x} = (x_j + x_{j+1})/2, \ \bar{y} = (y_j + y_{j+1})/2$$

and

$$r_m = \sqrt{(x_m - x_i)^2 + (y_m - y_i)^2}$$

Simplifying Equation (5.43), we obtain

$$h_{ij} = \gamma_j \sum_{m=1}^{P} \frac{\alpha_m}{r_m^2}, \ \bar{h}_{ij} = \gamma_j \sum_{m=1}^{P} \frac{\beta_m}{r_m^2},$$

$$g_{ij} = -\delta_j \sum_{m=1}^{P} \alpha_m \log_e r_m, \text{ and } \bar{g}_{ij} = -\delta_j \sum_{m=1}^{P} \beta_m \log_e r_m \tag{5.44}$$

where

$$\gamma_j = \frac{dL_j}{4\pi}, \quad \delta_j = \frac{L_j}{4\pi k},$$

$$\alpha_m = (0.5 - \frac{\xi_m}{2})W_m,$$

and

$$\beta_m = (\frac{\xi_m}{2} + 0.5)W_m.$$

Example: Circular Boundary

Consider the confined aquifer shown in Figure 5.12 having a radius of R = 10 m with a pump at the center of the aquifer and a pumping rate of $Q = 2\pi \ m^3/s$. The transmissivity T is assumed to be unity, i.e., $T = 1 \ m^2/s$. The exact solution is given by

$$QV(r_p) + u_i + \oint u\frac{\partial v}{\partial n}d\ell = \oint qVd\ell$$

where

$q = Q/(2\pi R)$, $u \equiv 0$ on the boundary,

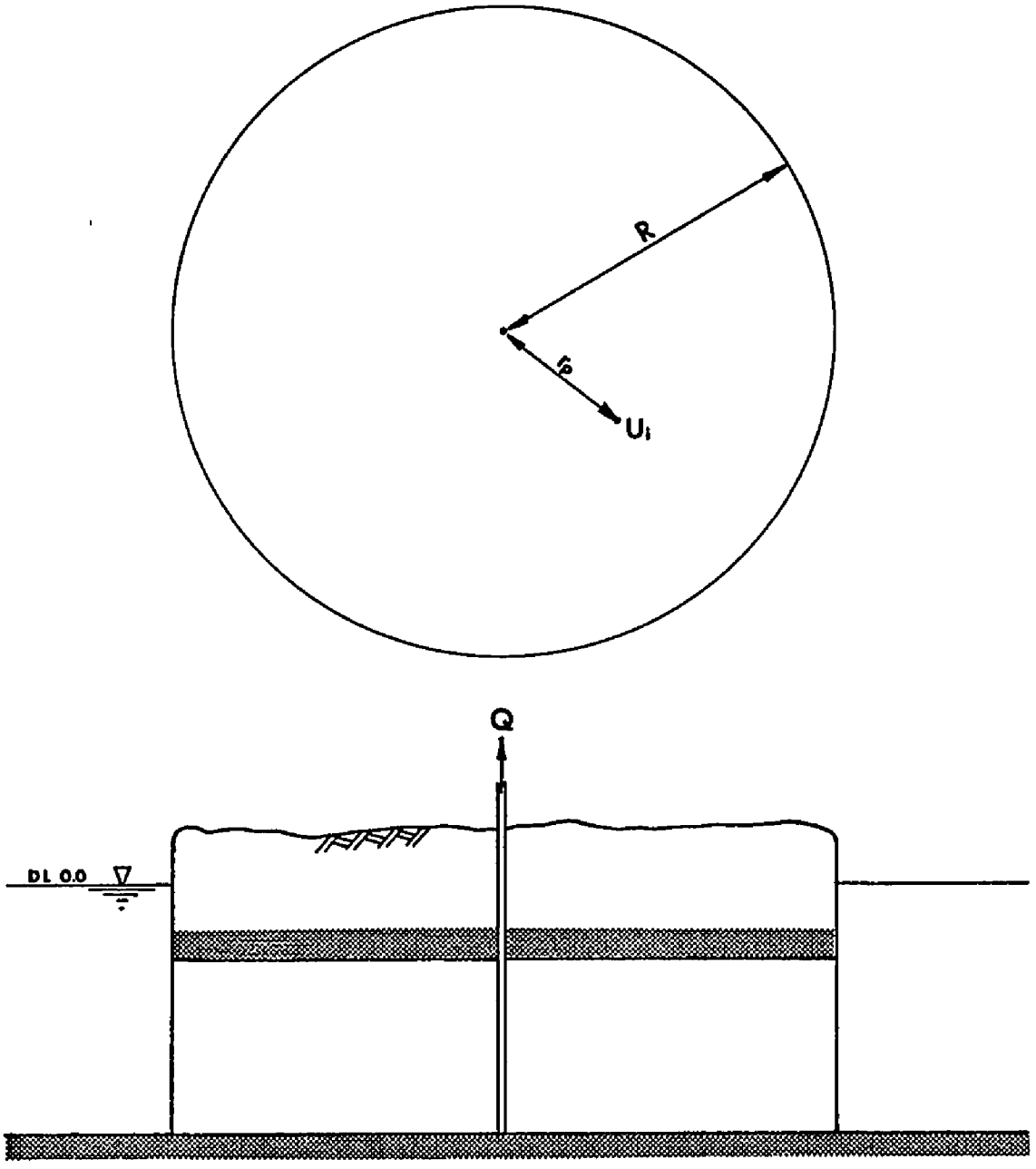

Figure 5.12. Circular island.

$$V = \log_e(1/r)/(2\pi T), \text{ and } d\ell = Rd\theta .$$

It follows that

$$-Q \frac{1}{2\pi T} \log_e r_p + u_i = - \frac{Q}{2\pi T} \log_e R .$$

Hence

$$u_i = \frac{Q}{2\pi T} \log_e(\frac{r_p}{R}) \qquad (5.45)$$

The boundary can be discretized into linear elements, as shown in Figure 5.13. The numerical solution is compared with the exact solution in Figure 5.14. The input data and the simulation results are presented in Tables 5.1 and 5.2, respectively.

If there are several pumps in the aquifer, then the solution is no longer symmetric about the center of the aquifer. An exact solution for this case is much more difficult; however, only minor changes in the input data are required to obtain the approximate solution. This is much simpler than the finite element case, which will require a substantial amount of additional input data to solve the problem of multiple pumps.

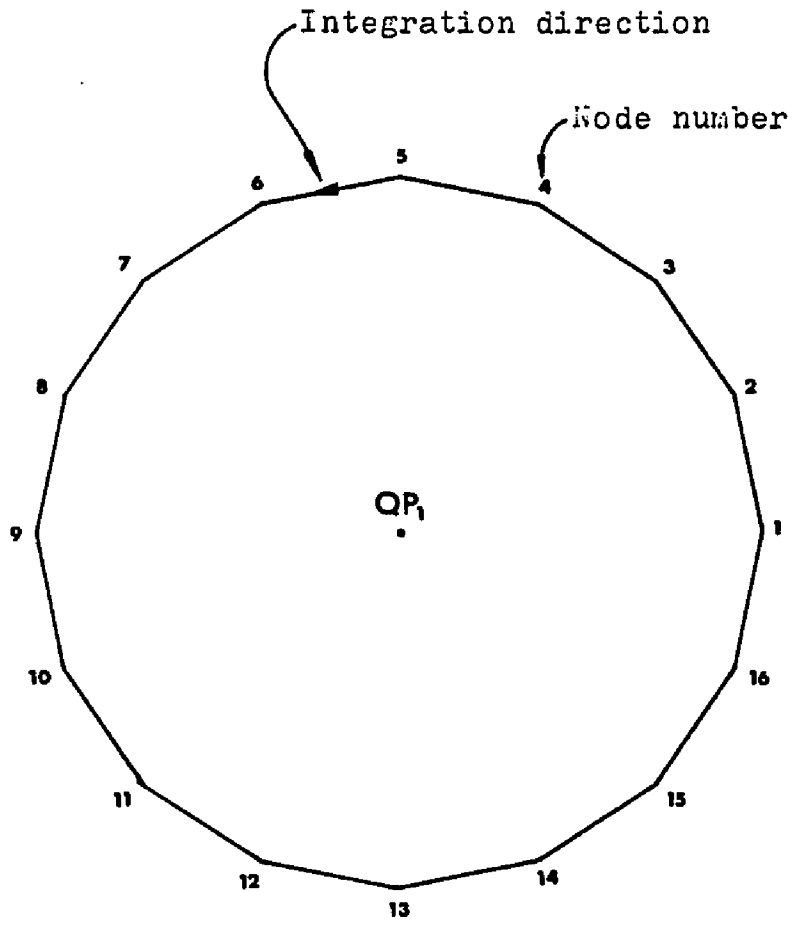

Figure 5.13. Linear elements at the boundary.

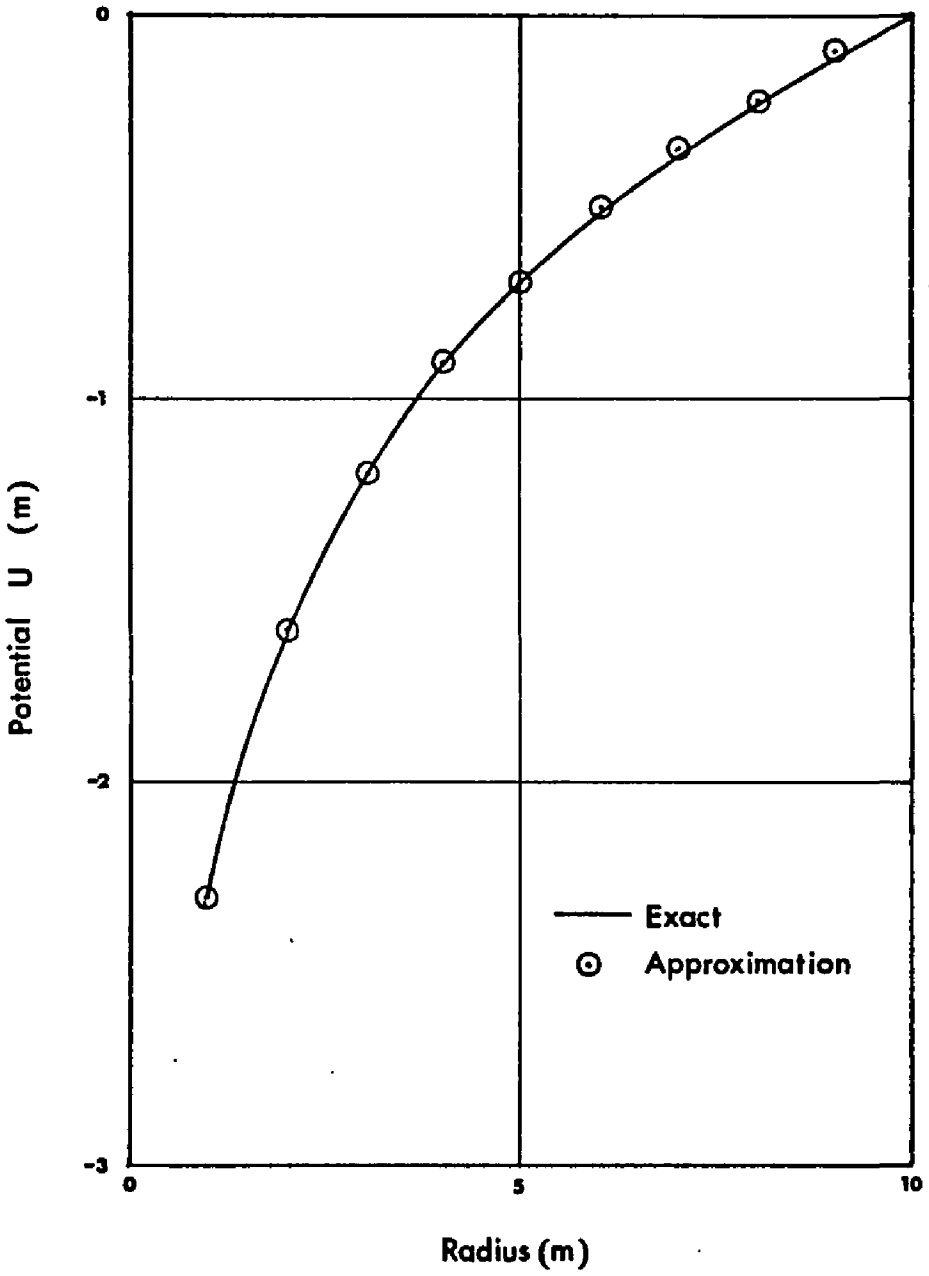

Figure 5.14. Potential versus radius.

Table 5.1. Input data.

EXAMPLE OF CIRCULAR BOUNDARY

HYDRAULIC CONDUCTIVITY = 1.0000000000

INPUT DATA

NUMBER OF BOUNDARY ELEMENTS = 16

COODINATES AND BOUNDARY CONDITIONS OF THE EXTREME POINTS OF THE BOUNDARY ELEMENTS

NODE	CODE	X-COOD	Y-COOD	PRESCRIBED HEAD	VELOCITY
1	0	10.0000	0.0000	0.0000	
2	0	9.2388	3.8268	0.0000	
3	0	7.0711	7.0711	0.0000	
4	0	3.8268	9.2388	0.0000	
5	0	0.0000	10.0000	0.0000	
6	0	-3.8268	9.2388	0.0000	
7	0	-7.0711	7.0711	0.0000	
8	0	-9.2388	3.8268	0.0000	
9	0	-10.0000	0.0000	0.0000	
10	0	-9.2388	-3.8268	0.0000	
11	0	-7.0711	-7.0711	0.0000	
12	0	-3.8268	-9.2388	0.0000	
13	0	0.0000	-10.0000	0.0000	
14	0	3.8268	-9.2388	0.0000	
15	0	7.0711	-7.0711	0.0000	
16	0	9.2388	-3.8268	0.0000	

NUMBER OF INTERNAL POINTS = 9

X	Y
1.0000	0.0000
2.0000	0.0000
3.0000	0.0000
4.0000	0.0000
5.0000	0.0000
6.0000	0.0000
7.0000	0.0000
8.0000	0.0000
9.0000	0.0000

NUMBER OF PUMPS = 1

PUMP	X	Y	DISCHARGE
1	0.0000	0.0000	6.2832

NUMBER OF FREE SURFACE NODE = 0

Table 5.2. Simulation results.

RESULTS

ON BOUNDARY

NODE	X-COORD	Y-COORD	U(X,Y)	DU/DN
1	10.0000	0.0000	0.0000	.1009
2	9.2388	3.8268	0.0000	.1009
3	7.0711	7.0711	0.0000	.1009
4	3.8268	9.2388	0.0000	.1009
5	0.0000	10.0000	0.0000	.1009
6	-3.8268	9.2388	0.0000	.1009
7	-7.0711	7.0711	0.0000	.1009
8	-9.2388	3.8268	0.0000	.1009
9	-10.0000	0.0000	0.0000	.1009
10	-9.2388	-3.8268	0.0000	.1009
11	-7.0711	-7.0711	0.0000	.1009
12	-3.8268	-9.2388	0.0000	.1009
13	0.0000	-10.0000	0.0000	.1009
14	3.8268	-9.2388	0.0000	.1009
15	7.0711	-7.0711	0.0000	.1009
16	9.2388	-3.8268	0.0000	.1009

INTERNAL POINTS

X-COORD	Y-COORD	U(X,Y)
1.0000	0.0000	-2.2958
2.0000	0.0000	-1.6027
3.0000	0.0000	-1.1972
4.0000	0.0000	-.9095
5.0000	0.0000	-.6864
6.0000	0.0000	-.5041
7.0000	0.0000	-.3499
8.0000	0.0000	-.2165
9.0000	0.0000	-.0995

NET FLOW ON BOUNDARY = 6.3000

CHAPTER 6

COMMENTS ON NUMERICAL METHOD

A major difference between the finite difference method (FDM) and the finite element method (FEM) is that the finite element equation can be derived for each element. On the other hand, the finite difference equation requires a consideration of the neighboring cells around the main cell. A comparison between the two methods is shown in Figure 6.1. For FEM, the specific discharge and the hydraulic conductivity are assigned to each element. In the integrated finite difference method (Neuman, 1981), being the general form of FDM, the net flow Q into the main cell shown in Figure 6.1 is defined as

$$Q = b \sum_{i=1}^{5} K'_{oi} \frac{h_i - h_o}{d_i} \ell_i = bS_s \frac{h_o^2 - h_o^1}{\Delta t}. \qquad (6.1)$$

The specific storage in the above equation is given in the cell, but the hydraulic conductivities must be defined between the main cell and neighboring cells. The difficulty is how the hydraulic conductivities should be given. It should be emphasized that FEM does not create this type of problem.

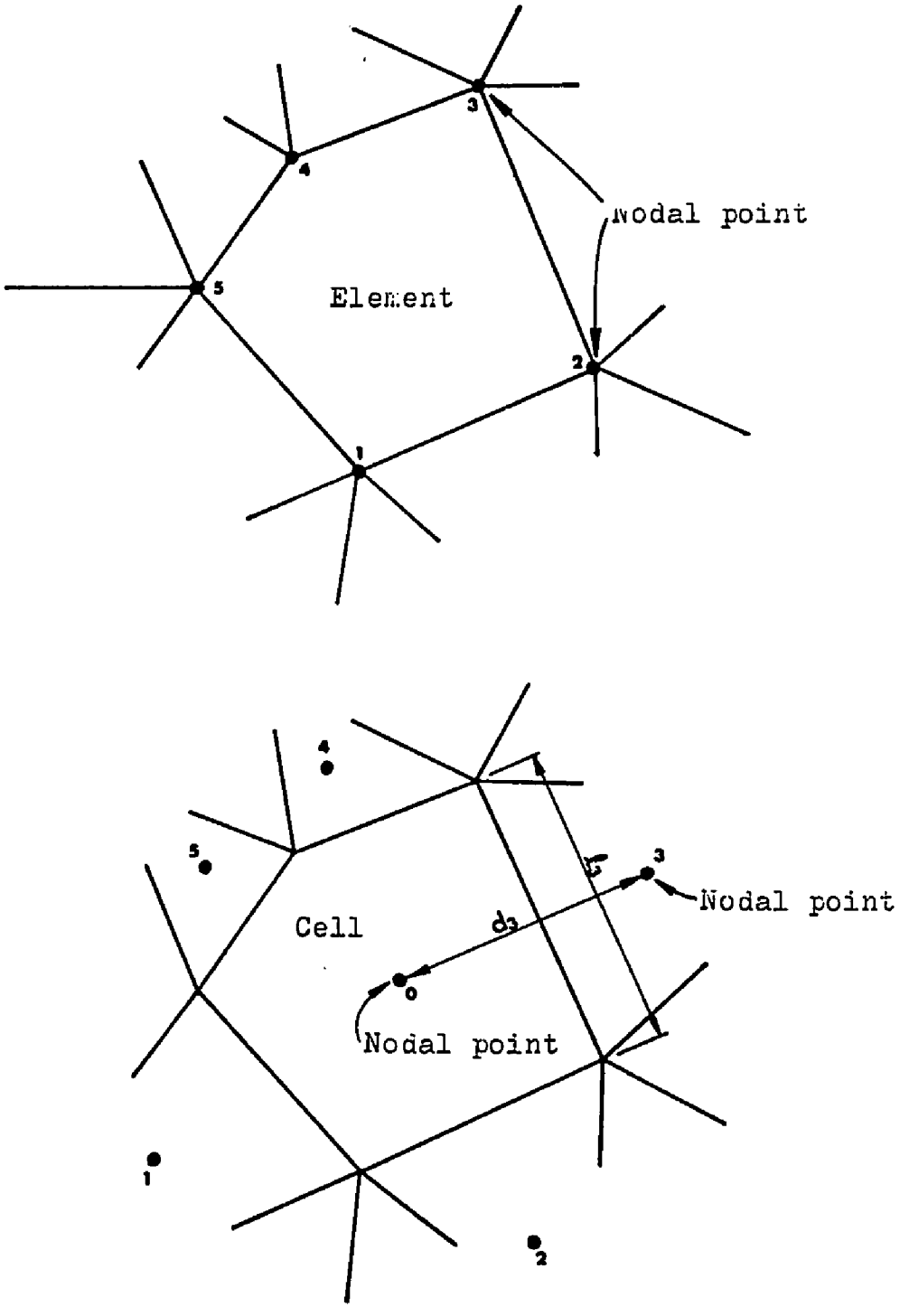

Figure 6.1. Element and cell.

One of the interesting features of both FEM and the boundary element method (BEM) is that the boundary of the domain can be adjusted at any given time. This is known as the moving boundary problem, which is not suitable for FDM. Solving the free surface and the interface locations is also a typical moving boundary problem. In the FEM approach, the nodes on the free surface or the interface are allowed to move according to the conditions such as the requirements related to the free surface and the interface. If the free surface moves upwards, then the areas of the elements whose nodes are on the free surface increase. This may induce unevenly distributed errors in the solution. For preventing such errors, the shape and the size of the elements are usually readjusted before the computation; however, the additional programming adjustment of the elements may cause the entire program to lose the generality of use.

The boundary element method does not have such problems since the unknowns are on the boundary of the domain. However, if distributed sources are applied over the entire domain, then the domain has to be divided into elements as seen in the finite element discretization. The preceeding discussions emphasize that selecting a proper numerical method is the most important task for developing a numerical model in order to achieve maximum efficiency both in terms of program development and execution.

Brebbia (1978) discussed a numerical procedure which uses both FEM and BEM for the entire domain which may be divided into several regions. In this approach, some regions are discretized into boundary elements and others are discretized into finite elements. This technique would be a powerful tool in solving some problems whose domain of interest consists of homogenous and heterogeneous regions.

CHAPTER 7

NUMERICAL DOMAIN

Simplified Domain

For the problem investigated herein it is assumed that the ground water flow behavior around the two-dimensional (horizontal) wells is symmetrical left and right. The constant heads shown in Figure 3.2 in Chapter 3 are arbitrarily chosen for simplifying the aquifer system around the wells. The location of wells is assumed to be halfway between the constant heads. The aquifer is now symmetric about the vertical line on which the two wells are located, and thus the numerical domain is defined as shown in Figure 7.1. In the figure, the horizontal component of the specific discharge at the line of symmetry is zero so that the line can be treated as an impervious wall. The wells are then located on the wall and the pumpage becomes the flow on the boundary, i.e., Neumann-type boundary condition. This system, therefore, simplifies the governing equation to the Laplace equation, and the number of unknowns to solve becomes almost half of the case for the entire domain.

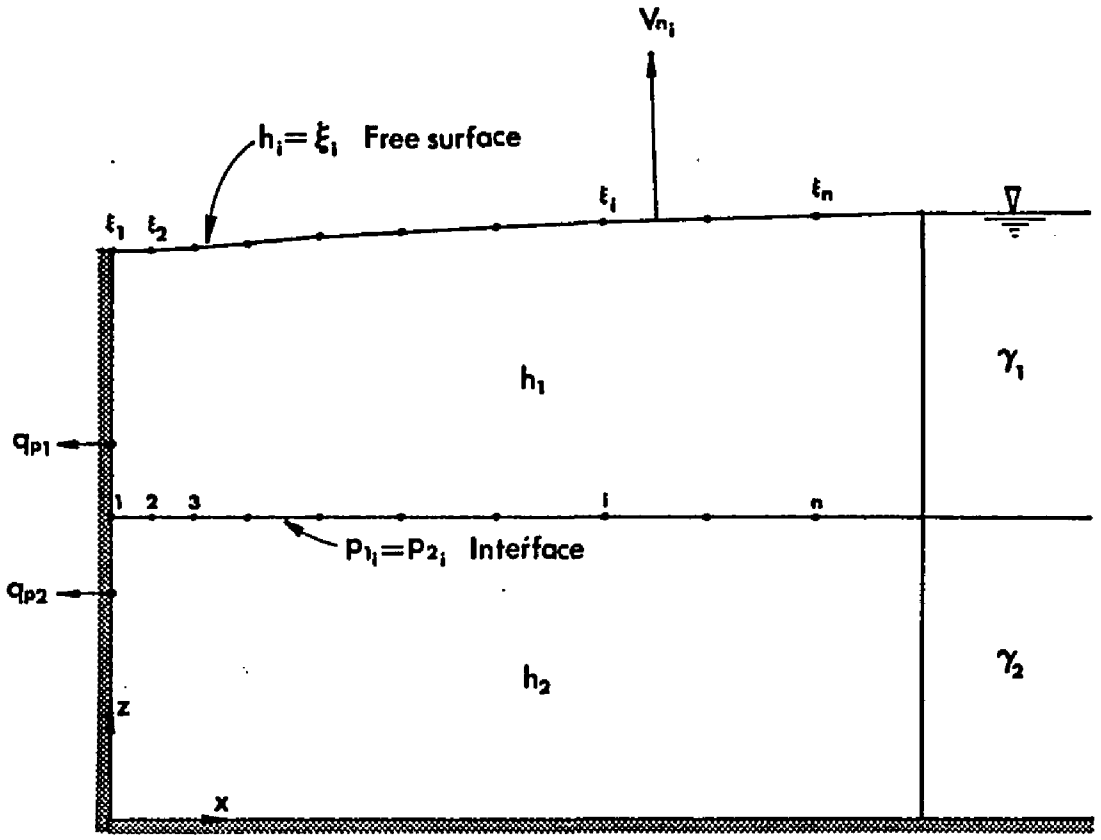

Figure 7.1. Half domain.

Numerical Treatment of Free Surface and Interface

The requirements for the free surface are $V_n = 0$ (if there is no infiltration), and $h = \xi$ where ξ indicates the location of free surface, and V_n is the specific discharge normal to the free surface line, as shown in Figure 7.1. In order to satisfy the requirements, ξ must be determined by a good guess, then the system for the unknowns is solved as if the aquifer were confined. Finally, a check is made on whether the hydraulic head on the guessed free surface is equal to the guessed line. If not, another good guess for ξ is taken and the procedure is repeated. In this procedure, the guessing controls the speed of the convergence. The guessing must be carried out simultaneously because a poorly guessed ξ_i for a node is slows down the convergence. One of the most widely used procedures for this type of iteration is the Newton-Raphson method. To illustrate the procedure, examples for one and two dimensions are considered first. The method for solving the free surface and interface lines is then generalized.

Consider a function $f(x)$ and existence of x_o such that $f(x_o) = 0$. Give a guess x which is assumed to be in the admissible range for finding x_o. Using the Taylor series the function f at x is linearized as

$$f(x + \Delta x) = f(x) + f'(x)\Delta x .$$

where Δx is a small increment that will improve the guess. The next step is to assume $f(x + \Delta x) = 0$ so that Δx can be computed as follows

$$\Delta x = - \frac{f(x)}{f'(x)}$$

The new location of x will be improved by adding Δx to the old x. Repeating the procedure several times, the accuracy of x is successively improved.

For two functions f(x,y) and g(x,y), the aim is to find the position (x_o, y_o) in a two-dimensional plane such that both functions are zero at the point. Using the Taylor series again, the functions f and g can be written as follows

$$0 = f(\vec{R}') = f(\vec{R}) + f_x \Delta x + f_y \Delta y$$

$$0 = f(\vec{R}') = g(\vec{R}) + g_x \Delta x + g_y \Delta y$$

where $\vec{R} = (x,y)$ and $\vec{R}' = (x + \Delta x, y + \Delta y)$.

Values Δx and Δy can be determined by solving the above equations simultaneously as

$$\begin{bmatrix} f_x & f_y \\ g_x & g_y \end{bmatrix} \begin{Bmatrix} \Delta x \\ \Delta y \end{Bmatrix} = - \begin{Bmatrix} f \\ g \end{Bmatrix} .$$

In general the above equations are written for n functions as, in index notation:

$$\frac{\partial f_i}{\partial z_j} \Delta z_j = -f_i \qquad \begin{matrix} i = 1, 2, \ldots, n \\ j = 1, 2, \ldots, n \end{matrix}$$

or in matrix form

$$J\Delta\vec{Z} = -\vec{f}$$

where J is called the Jacobian matrix. In most cases the Newton-Raphson method or Newton's first-order method will result in faster convergence than other available methods. In order to apply the method for the computation of free surface, the functions f_i must be defined as

$$f_i \equiv h_i - \xi_i = 0 \qquad i = 1, 2, \ldots, n$$

where h_i is the hydraulic head of the ith node on the free surface, ξ_i is the elevation of free surface as shown in Figure 7.1, and n is number of moving nodes on the free surface. Experience indicates that a few iterations will be sufficient to obtain a satisfactory accuracy for f_i for the free surface even if a poor initial guess is assigned.

In this method, the evaluation of $\partial F_i/\partial z_i$ turns out to be the most important task if the function f_i consists of unknown parameters. The derivative can be obtained in the following manner. First, $\vec{f}$ is computed with the present condition. For the jth node, ξ_i' is lifted by a small amount ε, then h_i' and f_i' are computed where $f_i' = h_i' - \xi_i'$. The derivative can be approximated by

$$\frac{\partial f_i}{\partial z_j} \simeq \frac{f_i' - f_i}{\varepsilon} \qquad i = 1, 2, \ldots, n$$

The parameter ε should be sufficiently small.

The interface can be analyzed in a similar manner as for the free surface. The function f_i must be redefined as

$$f_i \equiv \gamma_1(h_{1i} - z_i) - \gamma_2(h_{2i} - z_i) = 0$$

where z_i is the elevation of interface at the ith node, γ_1 is the specific gravity in the upper layer and γ_2 in the lower layer. Experience shows that for the interface line computation the Newton-Raphson method does not converge as quickly as it does for the free surface line computation. For a large amount of pumpage of q_{p1} and q_{p2} the method definitely diverges. It has been found that this is due to the small value of $\Delta\gamma$, and in fact, the interface is $\gamma_1/\Delta\gamma$ times as sensitive as the free surface, indicating that if the free surface drops Δh, then the interface rises about $\Delta h \cdot \gamma_1/\Delta\gamma$. In order to assure the convergence, the following procedure has been devised and successfully applied.

$$\Delta\vec{z} = -\alpha J^{-1}\vec{f}$$

The parameter α, which is less than or equal to unity when the interface line is about to settle down, may be a function of $\Delta\gamma$, $\Delta\vec{z}$, and some length. If α is a small value then there will be no divergence but the convergence will be slow. The parameter may be given as

$$\alpha = \frac{\Delta\gamma}{\Delta\gamma + \varepsilon/\beta}$$

where ε is the maximum absolute error in $\Delta\vec{z}$, and β is a constant value for a system. Figure 7.3 shows the rate of convergence for various values of α for the aquifer system given in Figure 7.2. For a value of $\alpha = 0.6$ not shown in Figure 7.3, it requires more iterations than for $\alpha = 0.5$. This indicates that the optimum value for α can be 0.5 for this particular aquifer if a constant value α is to be used. It is known that the Newton-Raphson method has a greater speed of convergence near the exact solution so that a large value α may be accepted when ε is small.

The dotted line in Figure 7.3 is the result based on an empirical expression for α showing an excellent rate of convergence.

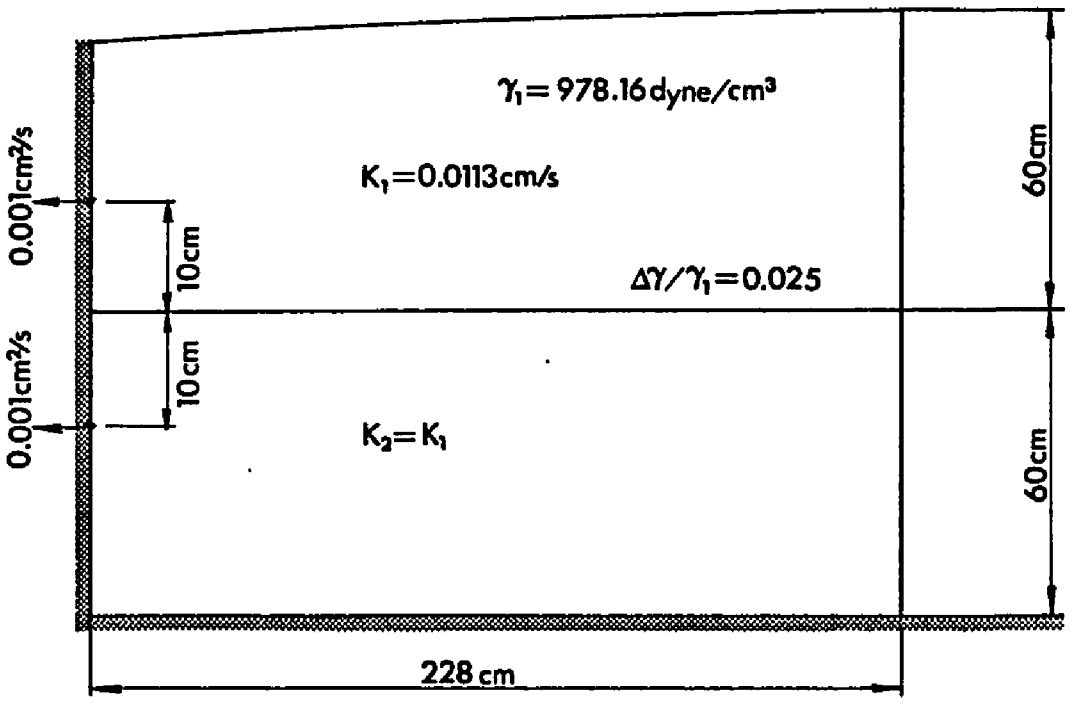

Figure 7.2. Test aquifer.

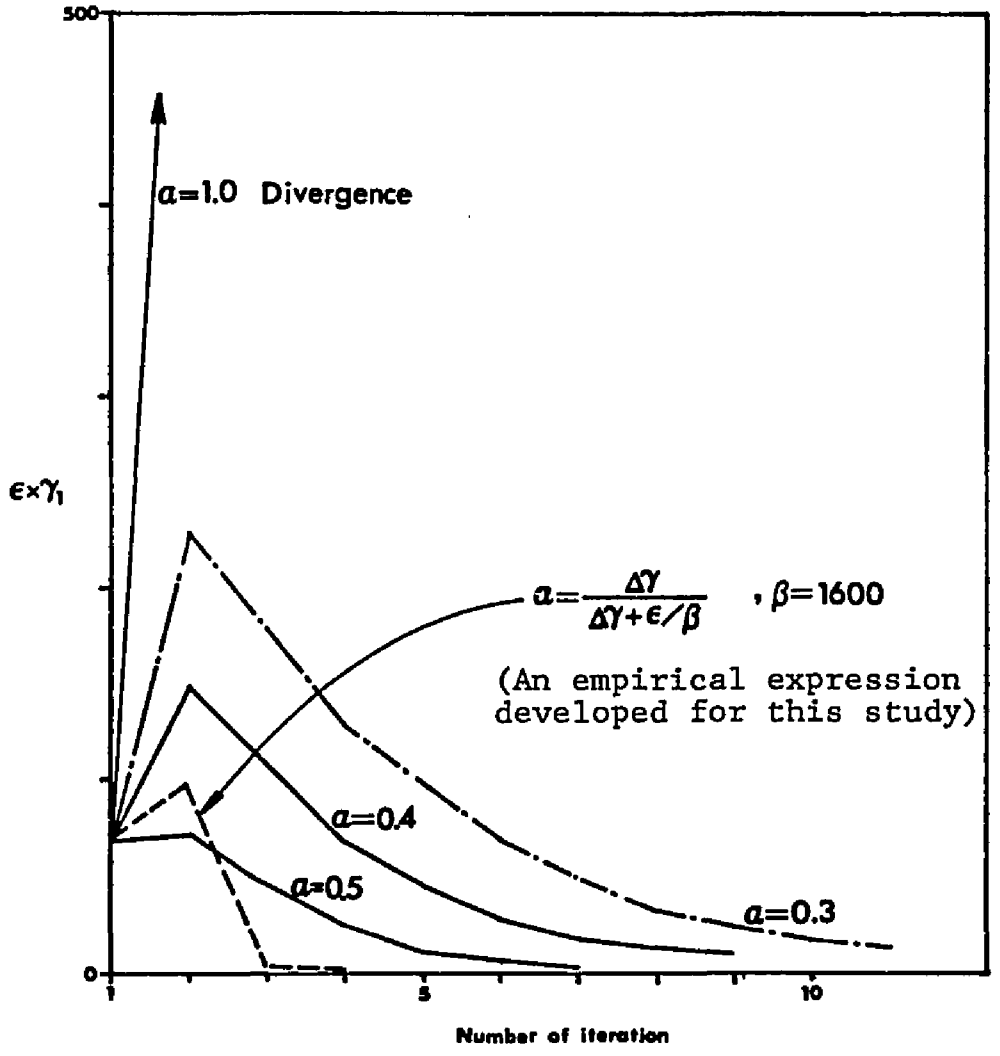

Figure 7.3. Error versus number of iterations.

CHAPTER 8

PRESENTATION OF RESULTS

Introduction

As a preliminary study of multiple wells imaged about the interface of two fluids, the model equations were evaluated for a simplified flow domain. As briefly mentioned in Chapter 7, the simplified flow domain is in the x-y plane and has a unit thickness. Two fully penetrated wells are installed horizontally as shown in Figure 8.1. Although the flow domain is simple, the numerical procedure is quite complex because of the dependent movements of the free surface and the interface.

Single-Fluid Flow

The two-dimensional model behavior of an aquifer subject to pumping was first examined for the single-fluid flow bounded by the free surface and an impermeable layer as shown in Figure 8.2. The model equation for this case was evaluated by both the finite element method and the boundary element method. For the finite element method the domain was discretized into triangular elements as shown in Figure 8.3, and for the boundary element method the boundaries of the entire domain and the half domain were subdivi-

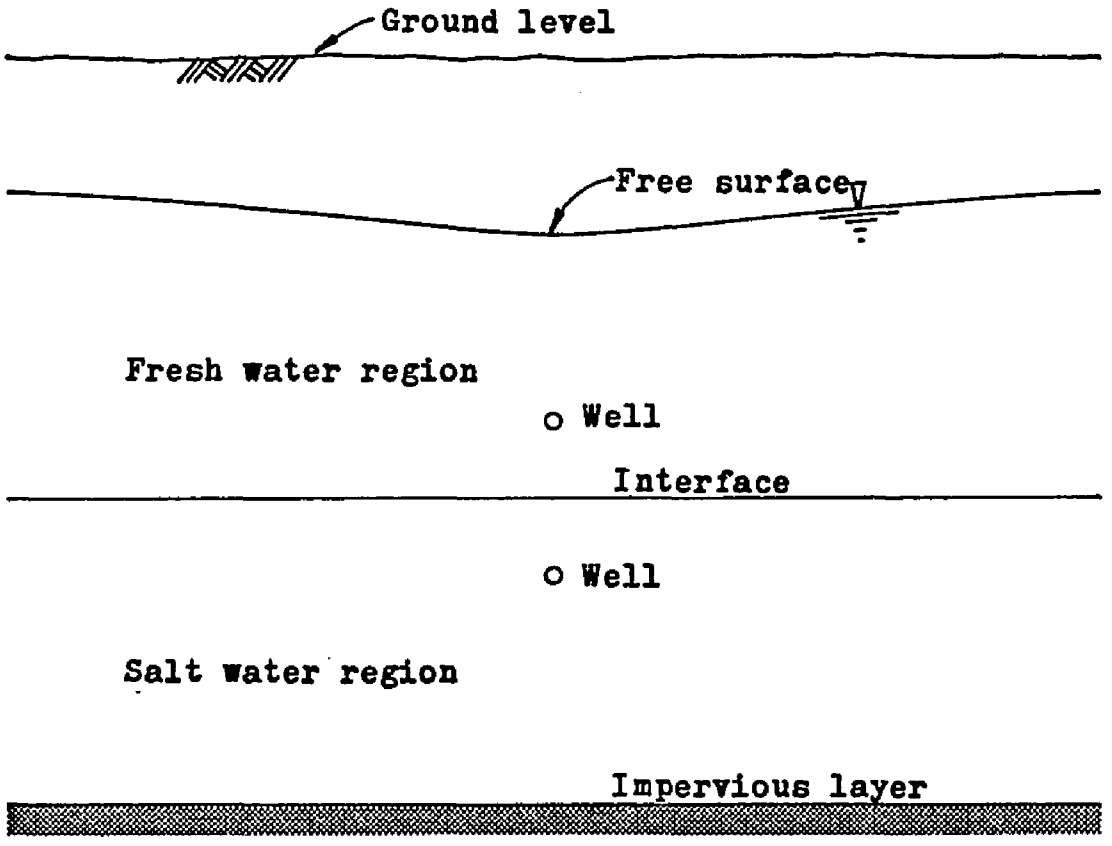

Figure 8.1. Schematic sketch of two-well system.

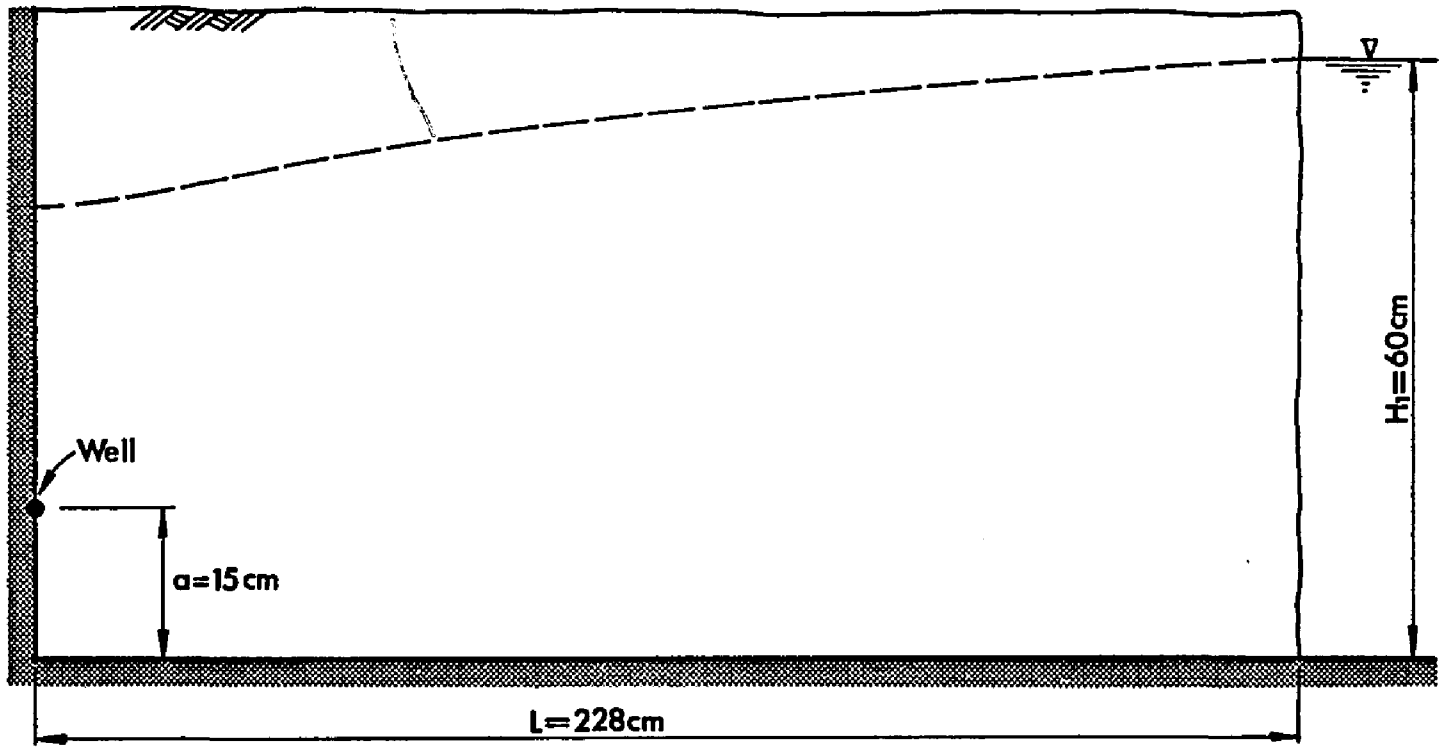

Figure 8.2. Domain for single-fluid flow.

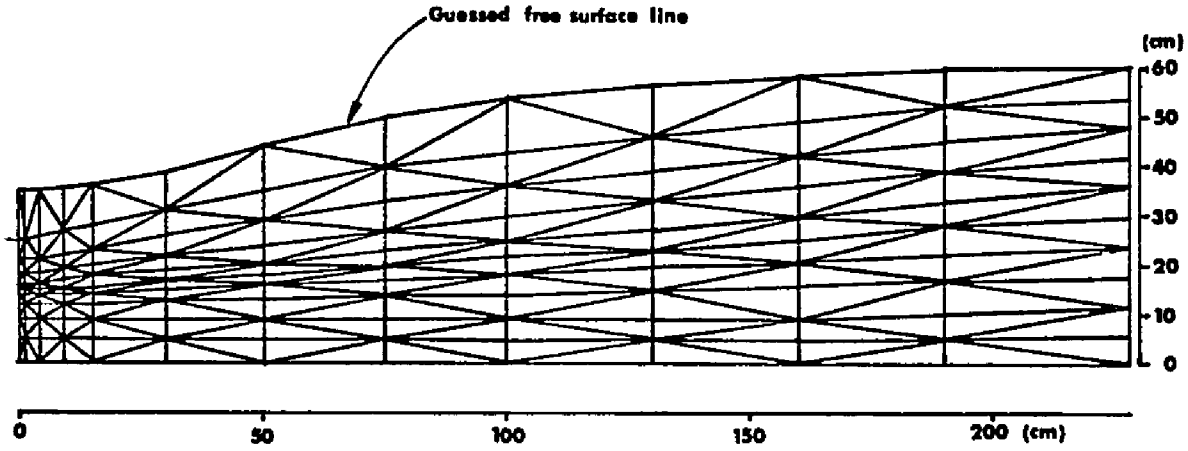

Figure 8.3. Finite element discretization.

ded into linear elements as shown in Figure 8.4. Figure 8.5 shows the formation of the free surface lines for various pumping rates. The following dimensional parameters were used for all the cases.

Horizontal length L = 228 cm

Maximum height H_1 = 60 cm

Thickness of aquifer = 1 cm

Hydraulic conductivity K = 0.678 cm/min

a = 15 cm for q = 1 to 4 cm^2/min

a = 10 cm for q = 5 cm^2/min

Because of the complexity of the free surface formation, flows having a free surface are often approximated by the Dupuit theory, which consists of two assumptions: (1) for small inclinations of the line of seepage the stream lines can be taken as horizontal; and (2) the hydraulic gradient was equal to the slope of the free surface and invariant with depth (Harr, 1962). In the theory, pumps in an unconfined aquifer are treated as fully penetrating vertical wells and the Dupuit assumptions give the following expressions for the single fluid flow:

$$h = \sqrt{h_1^2 - (h_1^2 - h_2^2)\frac{x}{L}} \quad \text{and} \quad q = K\,\frac{h_1^2 - h_2^2}{2L} \qquad (8.1)$$

where h_1 and h_2 are the upstream depth and downstream depth, respectively, and L is the horizontal length of the unconfined

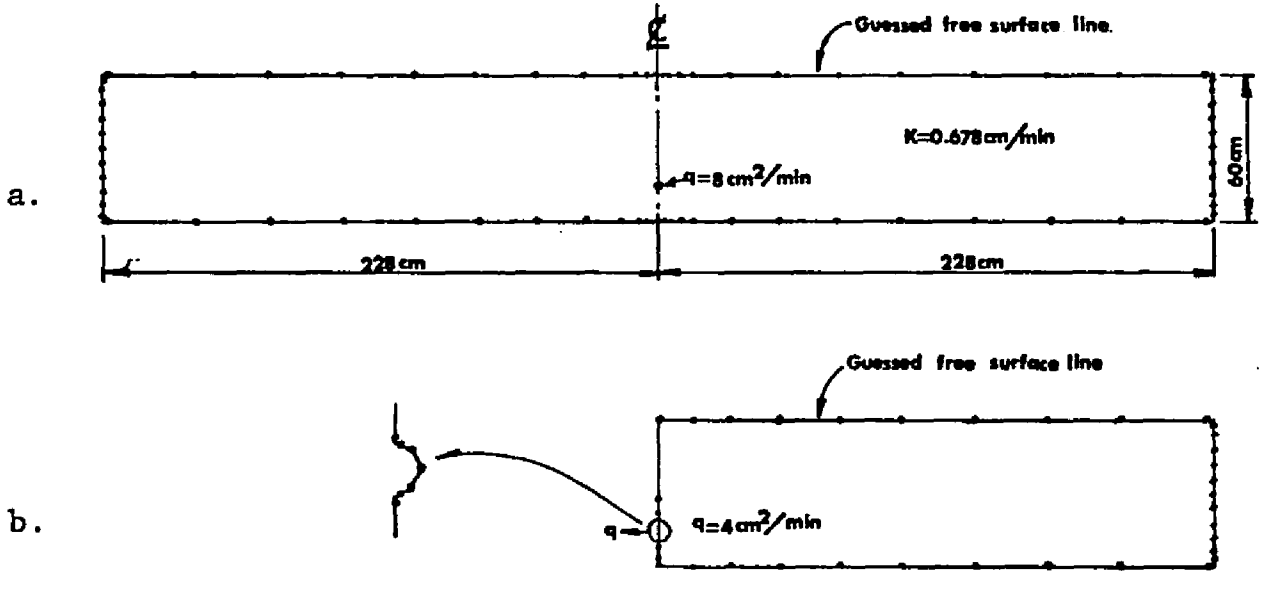

Figure 8.4. Boundary element discretization. -- (a) Entire domain; (b) Half domain.

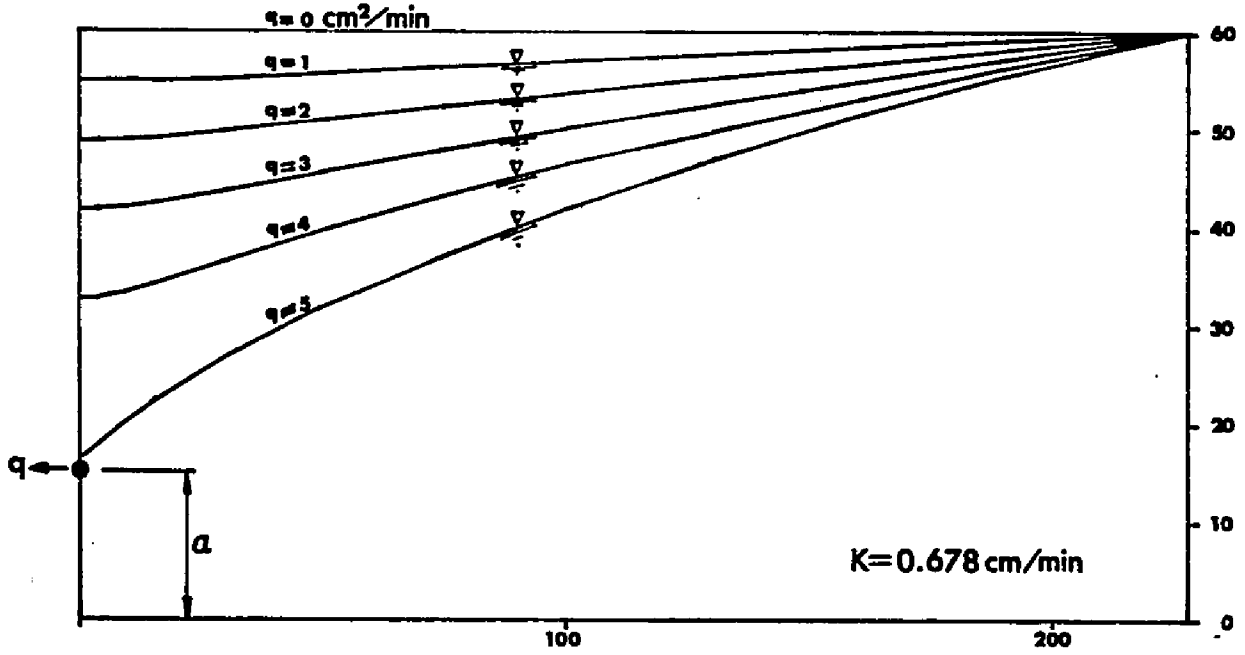

Figure 8.5. Free surface lines for various pumping rates.

aquifer. The comparison of the free surfaces for a pumping rate of $q = 4$ cm^2/min between the solutions by the finite element method and by the Dupuit assumptions is shown in Figure 8.6. It can be concluded that the Dupuit assumptions give reasonable values of h if q is small or the unconfined aquifer is deep. Close to the well the Dupuit solution is not as good as it is far from the well.

As discussed earlier in Chapter 6, the finite element method may give a local error along the free surface due to unevenly discretized elements at the free surface line. Figure 8.7 shows the slight difference in the free surface lines between the two numerical methods. The flow domain in Figure 8.4a was used for the boundary element method. Even though the number of unknowns for the domain in the figure is greater than for the domain in Figure 8.4b, the domain in the former has an advantage in handling the wells, as seen in the example in Chapter 5.

Wells Symmetrically Imaged about the Interface of Two Immiscible Fluids

The difference between the single and the two fluids cases is the additional iterative computation for the interface. As mentioned in Chapter 7, a special numerical treatment was required for the interface prediction to improve the computational efficiency.

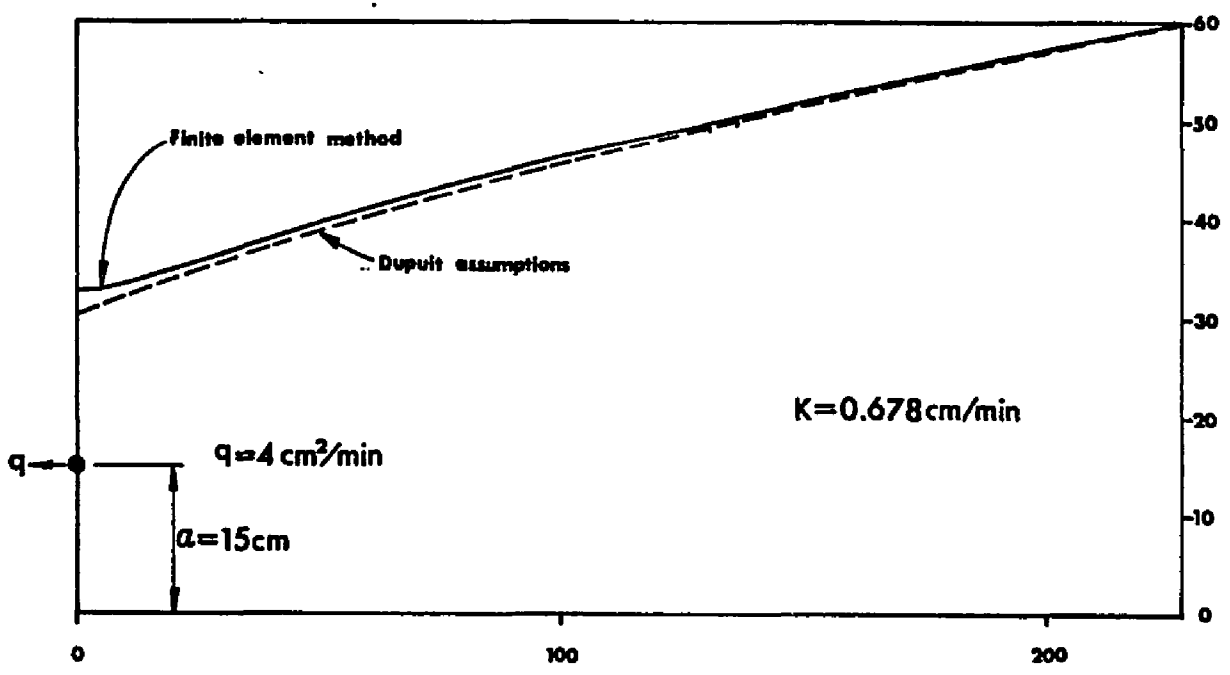

Figure 8.6. Comparison of finite element method with Dupuit assumptions.

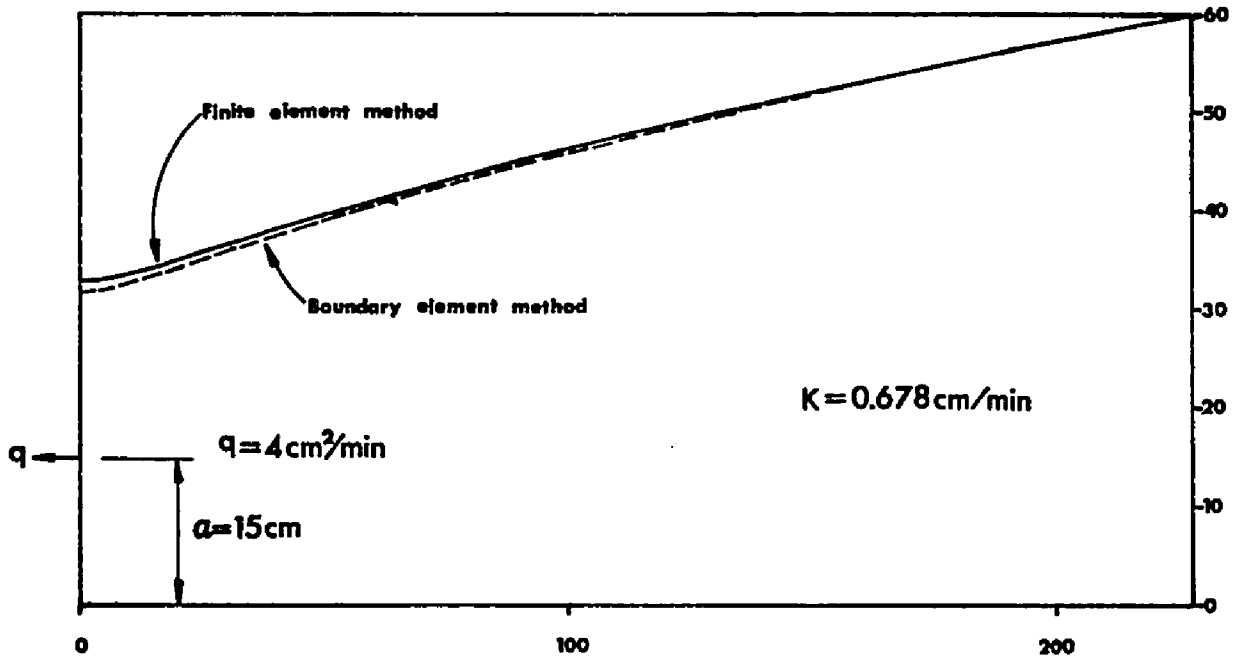

Figure 8.7. Comparison of finite element method with boundary element method.

The model equations were first evaluated for the case shown in Figure 8.8. The pump in the fresh water domain withdraws at a rate of 0.0002 cm^2/sec, the specific density difference between two fluids is $\Delta\gamma / \gamma_1 = 0.025$, and the hydraulic conductivity in the fresh water domain is K = 0.011267 cm/sec. The upconing phenomenon due to the pumpage was demonstrated by the finite element method and plotted in Figure 8.9. Similarly, the downconing can be easily simulated with a few modifications in the input data. The upconing interface may be approximated using the Dupuit assumptions with the consideration of the confined aquifer. The following expression (Rumer, 1980), is given for the situation in Figure 8.10, as

$$y_s = y_{so}^2 + \sqrt{\frac{2q_f}{K\Delta\gamma/\gamma_1}}\,x \qquad (8.2)$$

Figure 8.9 shows that the solution approximated by the Dupuit assumptions is in excellent agreement with the finite element solution.

As discussed earlier, the hydraulic conductivities in the fresh water and salt water regions are different. Although the difference is small, the movement of the interface cannot be easily predicted by the engineering intuition. For the preliminary study it was assumed that the hydraulic conductivities are the same. A value of $\Delta\gamma / \gamma_f = 0.025$ was

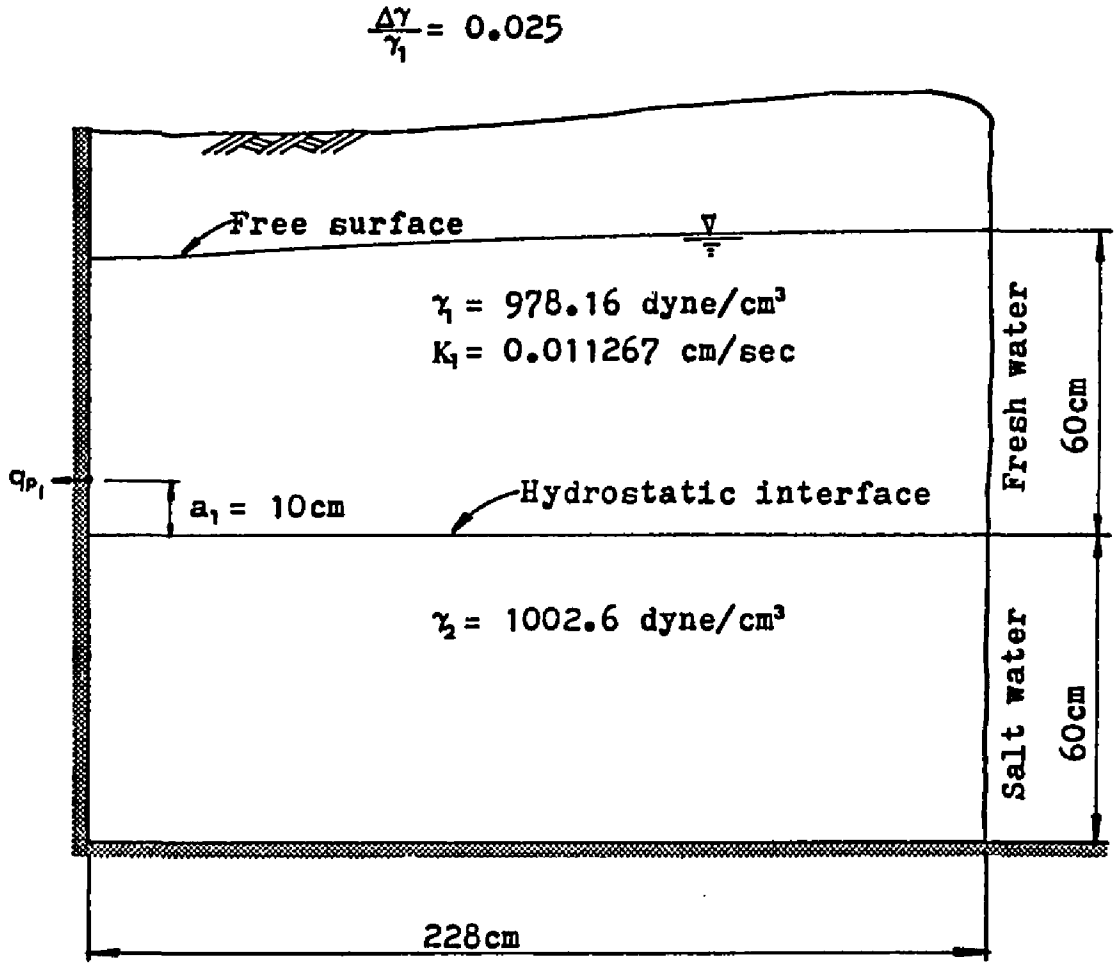

Figure 8.8. Schematic diagram for single-well case.

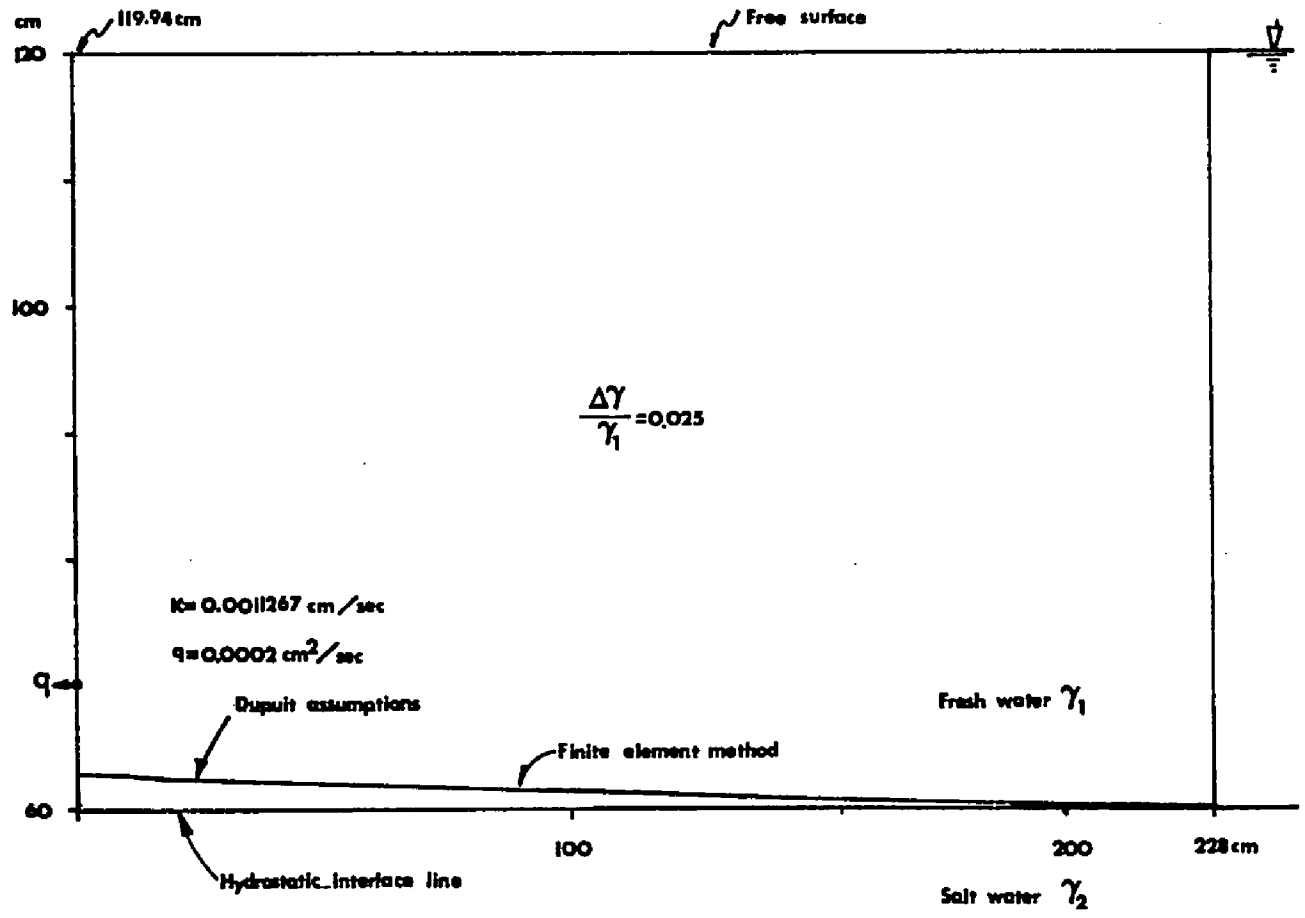

Figure 8.9. Upconing of interface due to fresh-water pumping.

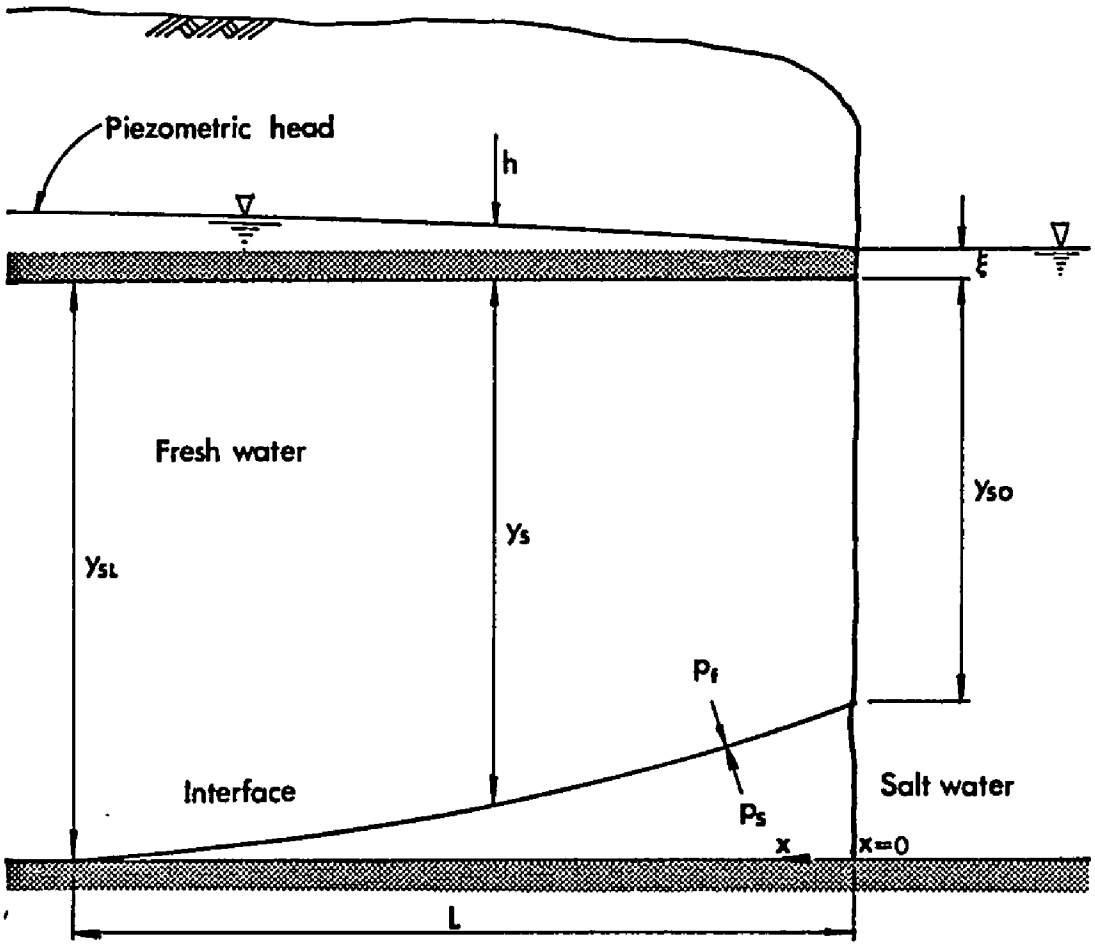

Figure 8.10. Confined aquifer with salt water intrusion.

used as accepted by many engineers. The dimensions and the values of other quantities are shown in Figure 8.11. All solutions for the two-fluid problems were obtained by the finite element method.

Figure 8.12a shows the formation of the interface line at the steady state with $q_{p1} = q_{p2} = 0.001$ cm^2/sec and $a_1 = a_2 = 10$ cm. Due to the small pumpage rate for the fresh water, the free surface dropped only 0.3 cm.

Figure 8.12b indicates that the initial guess of the interface line is almost identical to the computed result for the case of fresh water pumpage at 0.001023 cm^2/sec, i.e., $q_{p1} = q_{p2} \times 1.023$ at $q_{p2} = 0.001$ cm^2/sec. It can be guessed that q_{p2} approaches $(\gamma_1/\gamma_2) \times q_{p1}$ as $q_{p1} \to 0$.

From the study of the single fluid flow the aquifer system was shown to be reasonably approximated by Dupuit theory for small discharges. The theory may be also applicable for wells imaged about the interface for some range of pumpages. Making use of the Dupuit approximations, the specific pumpage, at which the interface remains horizontal, is defined as q_{p2}/q_{p1} and may be expressed as:

$$\frac{q_{p2}}{q_{p1}} = \frac{-K_2 D_2 \frac{dh_2}{dx}}{-K_1 \bar{h}_1 \frac{dh_1}{dx}}$$

$$= \frac{K_2 D_2 \gamma_1}{K_1 \bar{h}_1 \gamma_2} \qquad (8.3)$$

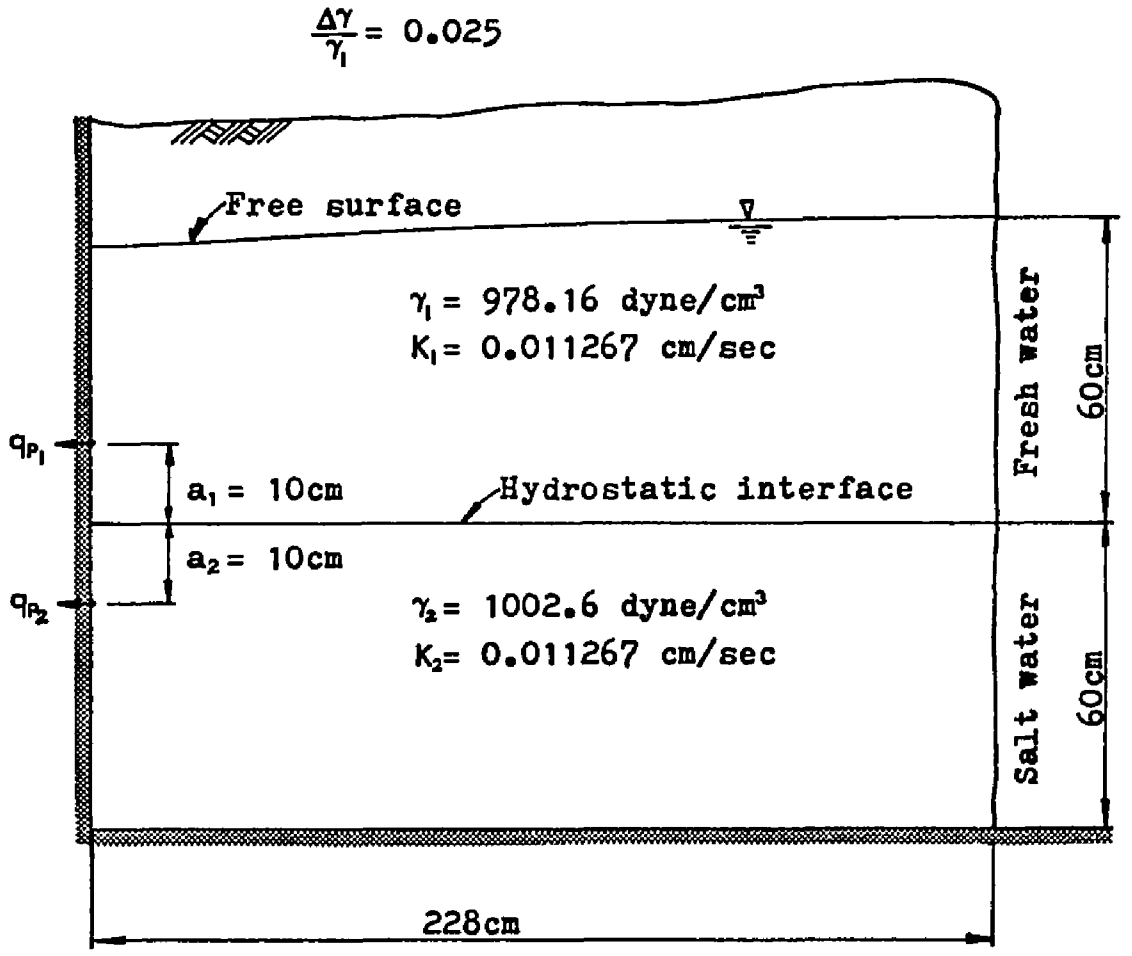

Figure 8.11. Schematic diagram for two wells imaged about the interface of two fluids.

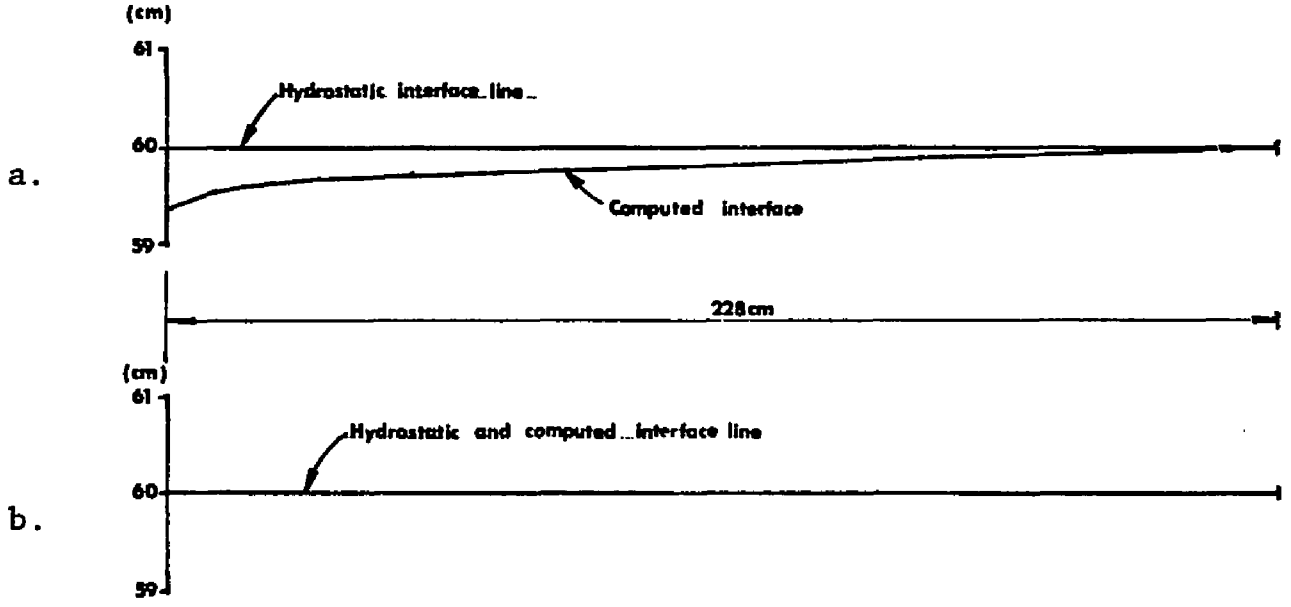

Figure 8.12. Interface lines formed by wells imaged about the interface. -- (a) $q_{p_1} = q_{p_2}$; (b) $q_{p_1} = 1.023 \times q_{p_2}$.

where $h_2 = h_1\gamma_1/\gamma_2$, $\bar{h}_1$ is the average depth of the fresh water aquifer, and D_2 is the average depth of the salt water aquifer. It can be seen that if $K_1 = K_2$ and $\bar{h}_1 = D_2$, then $q_{p2} = q_{p1} \times \gamma_1/\gamma_2$. If the viscosity effect is considered, then the specific pumpage becomes

$$\frac{q_{p2}}{q_{p1}} = \frac{\mu_1 D_2}{\mu_2 \bar{h}_1} \tag{8.4}$$

$$\simeq \frac{1}{1.07} \frac{D_2}{\bar{h}_1}$$

The interesting feature of the wells imaged about the interface for small pumpages is that the specific pumpage depends only on the viscosities and the flow depths, not on the specific weights of the fluids.

A series of cases was examined for various values of q_{p1} and q_{p2} with $K_1 = K_2 = 0.011267$ cm/sec and $a_1 = a_2 = 10$ cm. In order to obtain the combinations of q_{p1} and q_{p2} in Table 8.1, for which the interface remains horizontal, a trial-and-error procedure was used. For characterizing the aquifer system the parameters were nondimensionalized as follows:

$$\begin{aligned} q_r &= q_{p2}/q_{r1} \\ X &= q_{p1}/(\bar{h}_1 K_1) \\ Y &= q_r \times (K_1 \bar{h}_1 \gamma_2)/(K_2 D_2 \gamma_1) \end{aligned} \tag{8.6}$$

Table 8.1. Computed q_{p1}, D_2, and $\bar{h}$.

$q_{p2} \times 10^3$ (cm^2/sec)	$q_{p1} \times 10^3$ (cm^2/sec)	D_2 (cm)	$\bar{h}_1$ (cm)
1	1.023	59.999	59.846
2	2.043	60.029	59.677
3	3.058	59.969	59.552
4	4.071	59.935	59.428
5	5.082	59.993	59.228
6	6.090	59.818	59.158
7	7.097	60.522	58.651

The nondimensional equivalents of values in Table 8.1 are listed in Table 8.2 and the corresponding plots are given in Figures 8.13 and 8.14. It can be seen in Figure 8.13 that the Dupuit assumptions are applicable to the system.

For all computations presented in this study, the hydraulic conductivities are considered as a constant parameter. It is interesting to obtain solutions with different hydraulic conductivities. However, this is not necessary tasks to evaluate the solutions since an expression q_p/K is another parameter in the equation for imaged wells as far as the medium is isotropic. This means that a solution with $(2qp)/(2K)$ is the same as the solution with q_p/K.

Wells Unsymmetrically Imaged about the Interface of Two Immiscible Fluids

In natural aquifers the interface lines are always moving upwards and downwards. This suggests that the location of the wells are not always imaged symmetrically about the interface line.

Consider a situation such that the distance between the interface and the well in the salt water region is doubled, i.e., $a_2 = 2a_1 = 20$ cm. The schematic diagram is shown in Figure 8.15. Unlike the cases of symmetrically imaged wells, the interface line is no longer horizontal. Figure 8.16a shows the computed result for the case $q_{p1} = q_{p2} = 0.001$ cm^2/sec with $a_2 = 2a_1 = 20$ cm. The shape of

Table 8.2. Nondimensional values.

$q_{p2} \times 10^3$ (cm^2/sec)	q_r	$X \times 10^5$	Y
1	0.977	2.52	0.999
2	0.979	5.05	0.997
3	0.981	7.57	0.999
4	0.983	10.10	0.999
5	0.984	12.66	0.996
6	0.985	15.18	0.999
7	0.986	17.85	0.980

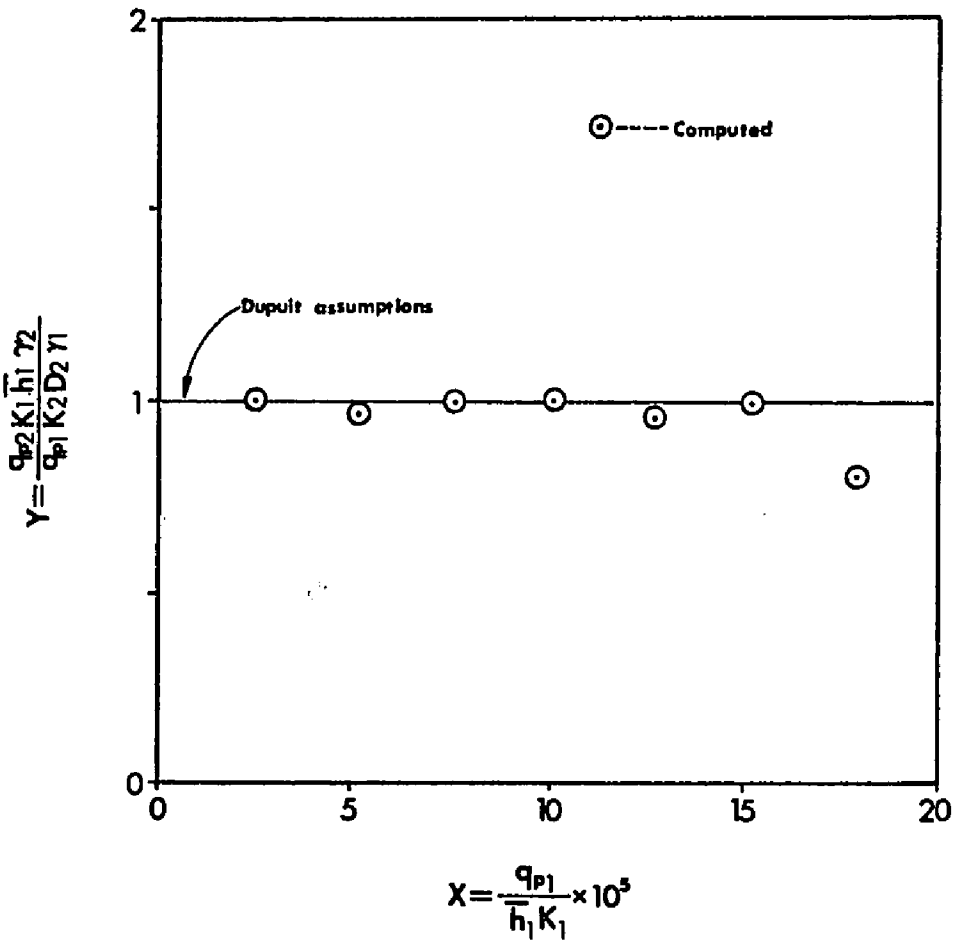

Figure 8.13. Plot of Y against X for wells imaged about the interface.

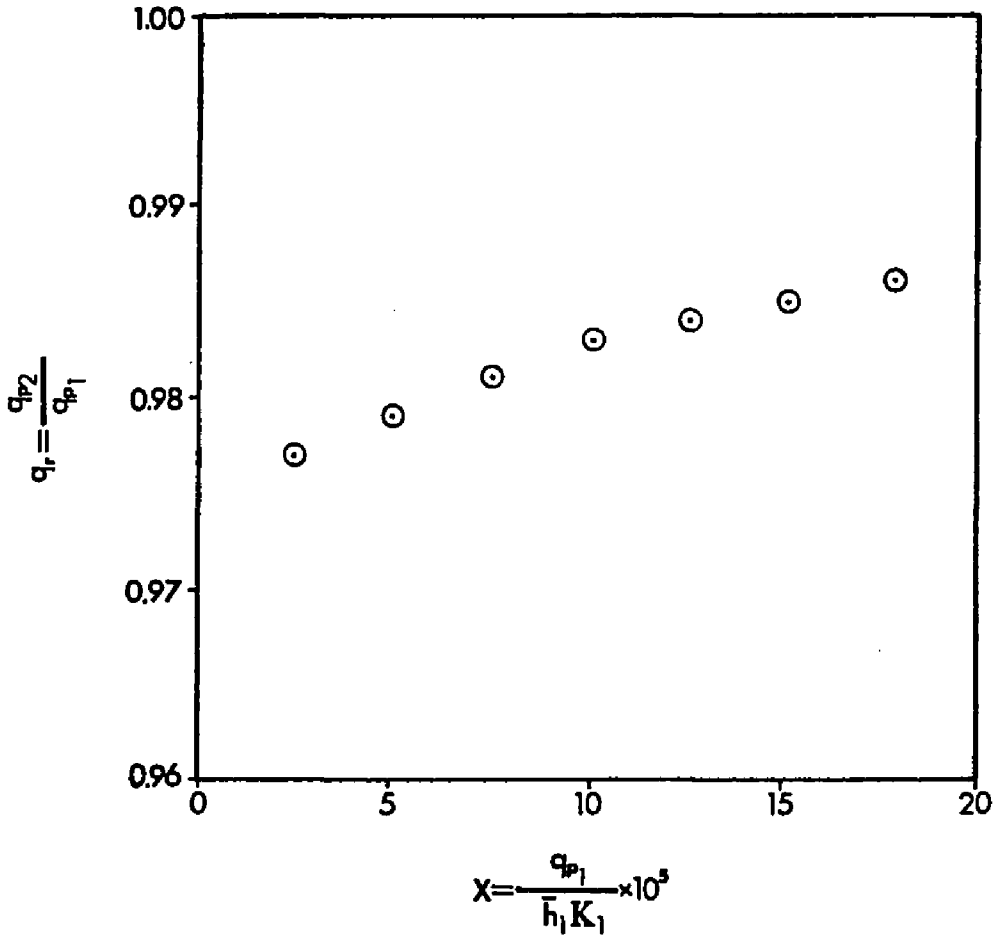

Figure 8.14. Plot of q_r against X for wells imaged about the interface.

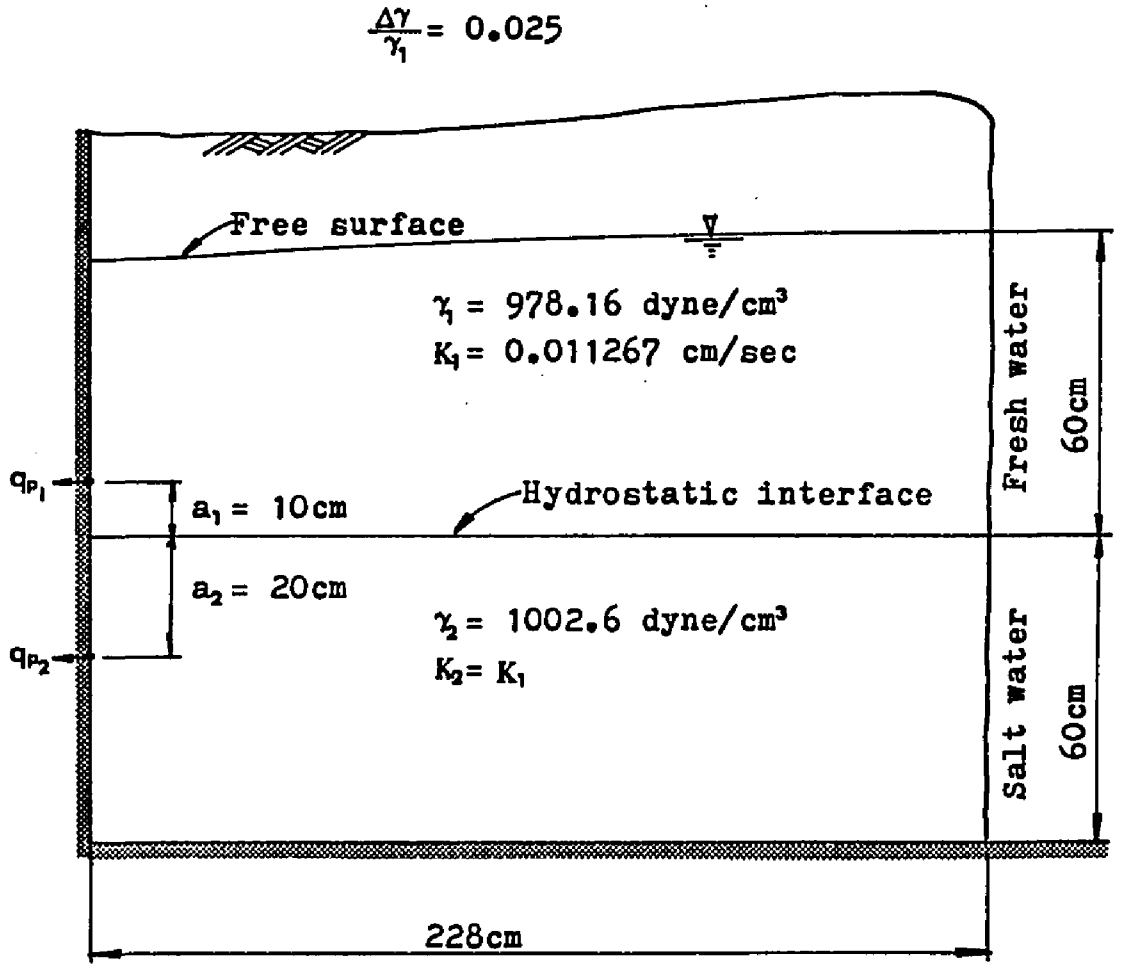

Figure 8.15. Schematic diagram for unsymmetrically imaged wells.

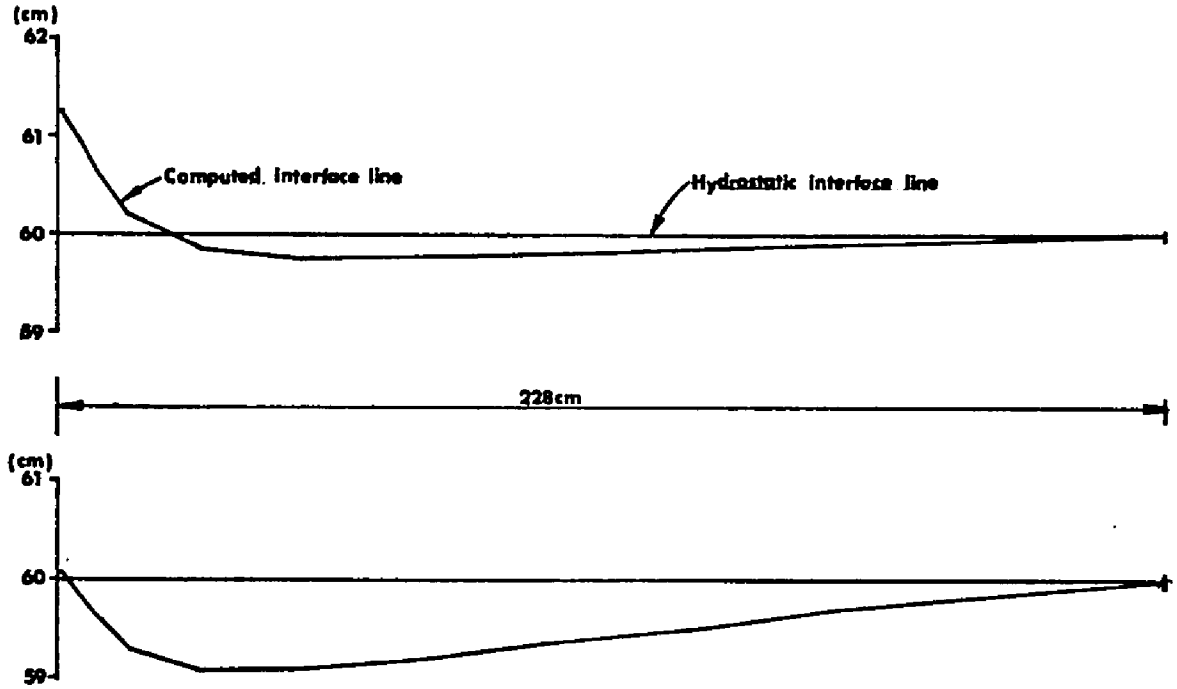

Figure 8.16. Interface lines formed by unsymmetrically imaged wells. -- (a) $q_{p_1} = q_{p_2} = 0.001$ cm^2/sec; (b) $q_{p_1} = 0.001$ cm^2/sec, $q_{p_2} = 1.025 \times q_{p_1}$.

the interface line formed by the unsymmetrically imaged wells is quite different from the imaged case ($a_1 = a_2$). This may be because of asymmetric equipotential lines about the interface line.

For wells unsymmetrically imaged about the interface, a series of cases were computed for various values of q_{p1} and q_{p2}, and the similar analysis to the cases of symmetrically imaged wells was performed. Figure 8.17 shows that the computed results differ significantly from the line diverged from the Dupuit assumptions. The average value of Y was 1.08. It is desirable to obtain a convenient expression similar to Equation 8.3 for the case of unsymmetrically imaged wells. Such an attempt, however, would require an excessive computational commitment in view of the numerous combinations for a_1 and a_2 as well as the much greater computation time per case for the unsymmetrically imaged wells than for the symmetrically imaged wells. It is evident, however, that as a_2 becomes greater than a_1, the value of specific pumpage also increases. The tendencies of the computer results in Figures 8.14 and 8.18 suggest that there exists a certain combination of a_1 and a_2 which gives the constant specific pumpage for any given X. This further indicates that the following type of equation may be considered:

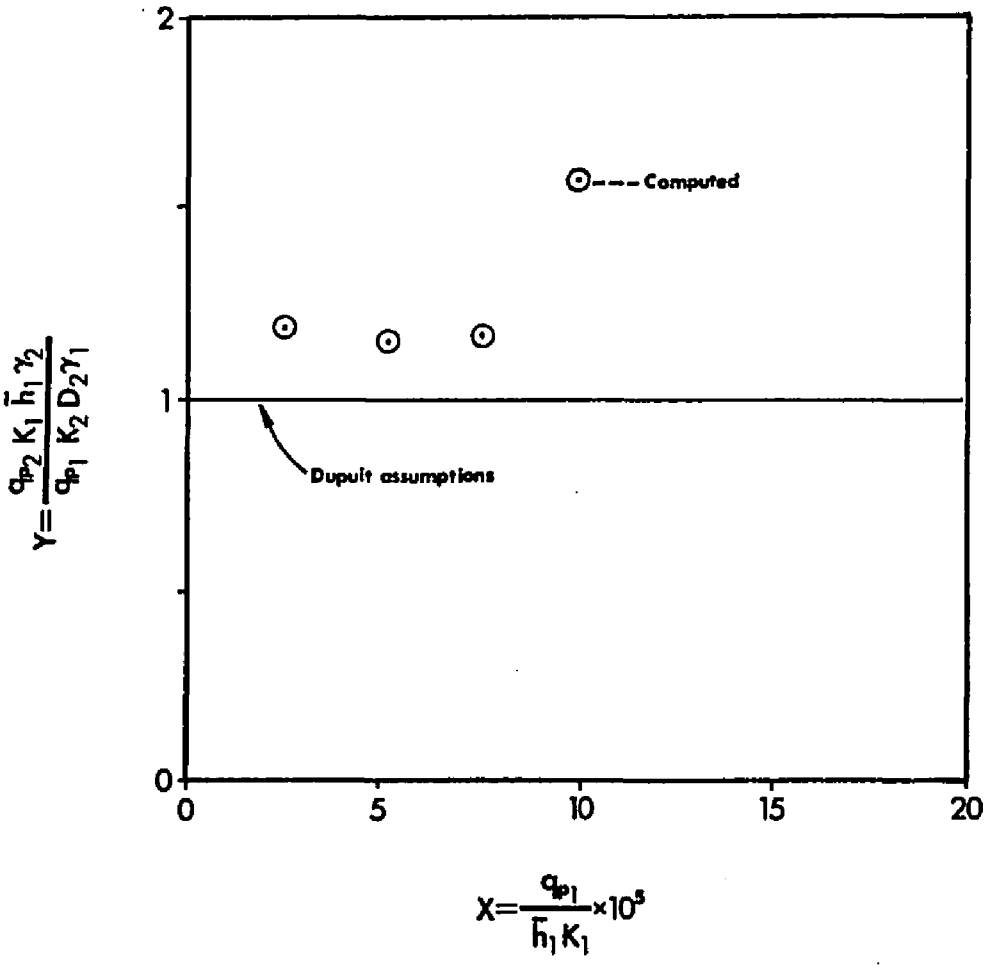

Figure 8.17. Plot of Y against X for wells unsymmetrically imaged about the interface.

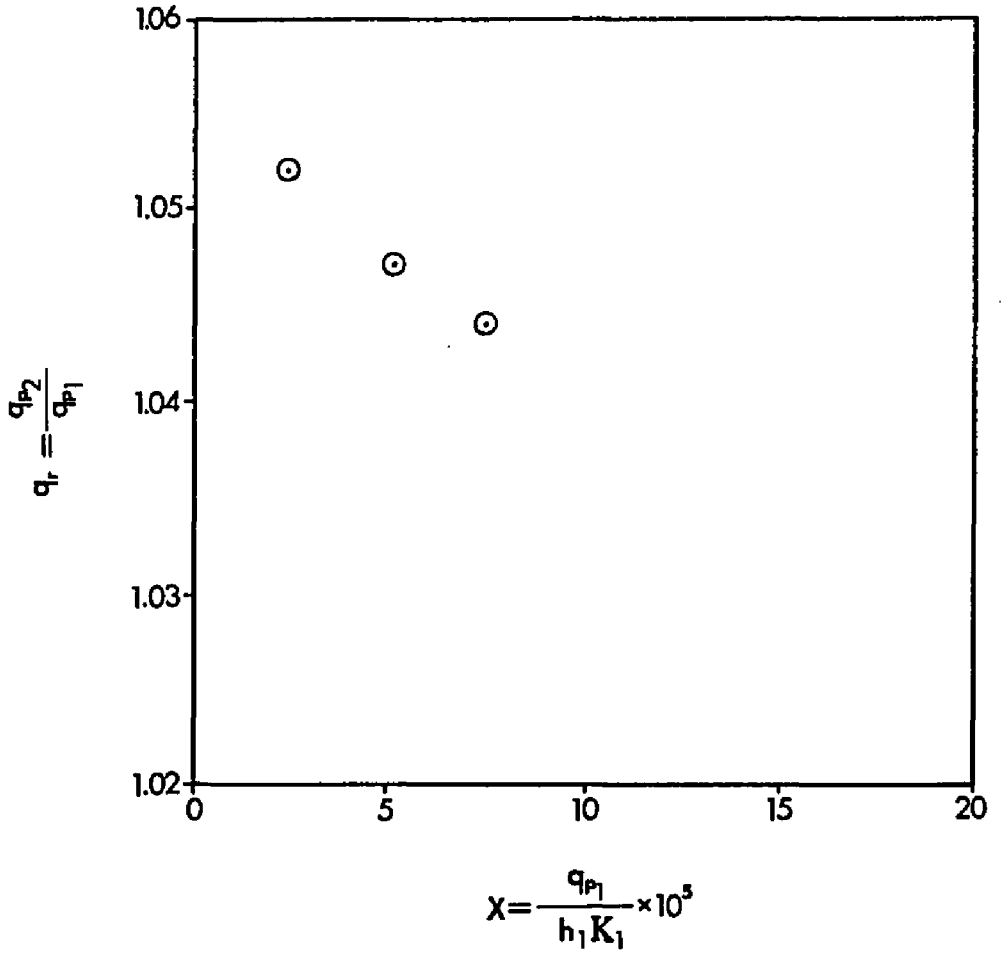

Figure 8.18. Plot of q_r against X for wells unsummetrically imaged about the interface.

$$\frac{dq_r}{dX} = \lambda\left(\frac{a_2}{a_1} - \alpha\right)^{\beta}(q_r - q_{r\infty}) \qquad (8.7)$$

where α is a value of a_2/a_1, giving the constnat specific pumpage, β and λ are constant values which may be a function of K_1, K_2, γ_1, γ_2 and so on, and $q_{r\infty}$ is the specific pumpage which q_r approaches asymptotically. It must be emphasized that Equation (8.7) is an empirical expression and, therefore, an enormous amount of systematic computations will be required to determine the constants

CHAPTER 9

SUMMARY AND CONCLUSIONS

The location of the interface line between two wells is governed by the properties of fluids and aquifers, the pumpage rates, and the location of the wells. Governing equations for wells imaged about the interface line can be derived by the concept of mass conservation provided that Darcy's law is valid throughout the flow domain. Although the flow very near the wells may not be represented exactly by the law, the well hydraulics should not bother the solution for the aquifer flow. There may also be a high degree of mixing of two fluids near the wells when, especially the rate of pumpage is substantial, and this phenomenon needs to be investigated. Although the notion of the two-well system for coastal aquifers seems to have been recognized to some extent, no mathematical modeling effort has been made prior to the present study. Since the model equations are nonlinear, involving non-fixed boundaries of the free surface and the interface, they cannot be solved in closed form. The solution requires a complex numerical procedure, including an iterative technique in order to locate the interface and the free surface. It has been found that the convergence rate

for the interface computation is much slower than that for the free surface computation. Also, it has been found that the repeated free surface computation is normally unnecessary for the successive iterations of the interface computation. This clearly indicates that the free surface movement is not as sensitive to the pumpage rate as the interface fluctuation.

The computed results for the single-fluid case show that the location of the free surface line approximated by the Dupuit assumptions is below the location predicted by the numerical solutions. With the two numerical methods, the results were slightly different. The free surface line computed by the boundary element method lies between the location computed by the finite element method and the line approximated by the Dupuit assumptions. In general, the Dupuit assumptions are expected to be useful for small withdrawal rates or far from the wells. For larger withdrawal rates, considdrable errors will likely occur, particularly near the well.

For an aquifer system having two wells symmetrically imaged about the interface of two fluids, it has been shown that the interface line at the steady state remains almost horizontal for a certain combination of pumpage rates. Also, the results suggest that the Dupuit assumptions are valid and applicable to the two-well system as long as the wells are imaged about the interface line.

Two numerical methods have been used for solving the

mathematical model equations. Although the finite element method is efficient in terms of the computation time, it requires a substantially large amount of the input data compared to the boundary element method. The accuracy of the boundary element method with linear element depends only on the number of the Gaussian integration points. Normally, four integration points have been found to be sufficient for most applications.

Three numerical models have been developed for the present study and coded in CDC FORTRAN IV as general-purpose programs. Two of the programs for the single-fluid flow simulation have been written using two different numerical approaches: the finite element method and the boundary element method. The comparison of results indicates that the finite element method may be better suited for the present purposes. For the two-fluid flow with an interface, only the finite element method has been applied. The performance of the models is generally satisfactory, and the analytically expected results have been well reproduced.

In summary, the mathematical and numerical model study presented in this thesis shows the possibility of practical applications. Extensive field and laboratory experiments, as well as further model refinements, are needed before the model can serve as a practical tool for the analysis of two-well aquifer system.

CHAPTER 10

RECOMMENDATIONS FOR FUTURE WORK

One of the significant assumptions employed in the present study is to consider no mixing zone between the the two stratified fluids. This may be a reasonable assumption if the mixing zone is narrow and the motion is small. However, it is generally known that coastal aquifers can have thick mixing zones depending on the degrees of tidal influences. The upconing, due to the withdrawal from a single well, does not necessarily indicate the rising of the salt water region. It is generally an expansion of the mixing zone in the entire aquifer. The explicit consideration of the mixing zone in the mathematical formulation would, therefore, greatly enhance the model applicability and reliability. Such a model would have to include the time-dependent tidal influences.

Among the various numerical techniques, the finite element method is the best choice for such a problem since the method is particularly suited for handling transient transport problems.

The two-dimensional case solved in this study could be extended to cases:

1. In which the aquifer is non-isotropic and non-homogeneous.
2. In which the fresh water comes from one side and the salt water from the other side.

The axisymmetric case of standard wells should be similar to this two-dimensional case.

The effect of imaged pumping on salt water intrusion some distance from the wells should be solvable.

The three-dimensional case both far and near the wells might be too "big" to be feasible. Perhaps the simpler cases will permit approximate solutions which will be sufficient for engineering purposes.

APPENDIX

SOME MATHEMATICAL DEFINITIONS

It is said that two functions ϕ and ψ are orthogonal on the limits of the integration if

$$\int_{\Omega} \phi\psi d\Omega = 0 .$$

A collection of functions $\{\phi_1, \phi_2, \ldots, \phi_n\}$ in a scalar field is said to be linearly independent if

$$\sum_{i=1}^{n} a_i \phi_i = 0$$

which can be accomplished when all a_i are zero. (This is not true if one of the functions is made of others.)

The linearly independent function is said to be complete if there is no break in the scalar field.

REFERENCES

Abed, Sami A. A., (1982), Wells Imaged about an Interface: Hele-Shaw Model, M.S. Thesis, University of Arizona, Tucson, Arizona.

Bear, Jacob, (1972), Dynamics of Fluids in Porous Media, American Elsevier Publishing Co., Inc., New York, N.Y.

Bear, Jacob, (1979), Hydraulics of Groundwater, McGraw-Hill Inc., New York, N.Y.

Beckmann, Petr, (1971), A History of π (PI), St. Martin's Press, New York, N.Y.

Birkhoff, G., M. H. Schultz, and R. S. Varga, "Piecewise Hermite Interpolation in One and Two Variables with Applications to Partial Differential Equations," Numerische Mathematik, Vol. II, pp. 232-256.

Brebbia, C. A., (1978), The Boundary Element Method for Engineers, John Wiley & Sons, New York, N.Y.

Dym, C. L. and I. H. Shames, (1973), Solid Mechanics: A Variational Approach, McGraw-Hill Book Co., Inc., New York, N.Y.

Eisenberg, M. A. and L. E. Malvern, (1973), On Finite Element Integration in Natural Coordinates, International Journal for Numerical Methods in Engineering, Vol. 7, pp. 574-575.

Fader, S. W., (1957), An Analysis of Contour Maps of 1955 Water Levels, with a Discussion of Salt-Water Problems in Southwestern Louisiana, Department of Conservation Louisiana Geological Survey and Louisiana Department of Public Works, Water Resources Pamphlet No. 4, pp. 16-21.

Freeze, R. A. and J. A. Cherry, (1979), Groundwater, Prentice-Hall, Inc., Englewood Cliffs, N.J.

Gallagher, Richard H., (1975), Finite Element Analysis Fundamentals, Prentice-Hall, Inc., Englewood Cliffs, N.J.

Harr, H. E., (1962), Groundwater and Seepage, McGraw-Hill Book Co., Inc., New York, N.Y.

Hubbert, M. K., (1940), Theory of Groundwater Motion, J. Geol., 48, pp. 785-822.

Huebner, K. H., (1975), The Finite Element Method for Engineers, John Wiley & Sons, New York, N.Y.

Lee, J. H., (1981), "Boundary Integral Equation Solutions to Moving Interface Between Two Fluids in Porous Media," Water Resources Research, Vol. 17, No. 5, pp. 1445-1452.

Long, R. A., (1965), Feasibility of a Scavenger Well System as a Solution of the Problem of Vertical Salt-Water Encroachment, Department of Conservation Louisiana Geological Survey and Louisiana Department of Public Works, Water Resources Pamphlet No. 15, pp. 1-22.

Martin, H. C. and Carey, G. F., (1973), Introduction to Finite Element Analysis, McGraw-Hill Book Co., Inc., New York, N.Y.

Mathes, G. M., (1982), "Spilled Petroleum Recovered from Atop Water Table of Mississippi Aquifer," ASCE, pp. 58-59, (June).

Neuman, S. P., (1981), Numerical Methods in Subsurface Hydrology (Lecture Note from Hydrology 504), Hydrology Department, University of Arizona, Tucson, Arizona, (Spring).

Neuman, S. P. and P. A. Witherspoon, "Finite Element Method of Analyzing Steady Seepage with a Free Surface," Water Resources Research, Vol. 6, No. 3, pp. 889-957

Potter, M. C. and J. F. Foss, (1975), Fluid Mechanics, The Ronald Press Company, New York, N.Y.

Rumer, R. R., (1980), Flow in Porous Media (Lecture Note), State University of New York at Buffalo, Buffalo, N.Y.

Segerlind, L. J., (1976), Applied Finite Element Analysis, John Wiley & Sons, Inc., New York, N.Y.

Shames, I. H., (1962), Mechanics of Fluids, McGraw-Hill Book Co., Inc., New York, N.Y.

Shames, I. H., (1967), Engineering Mechanics: Statics and Dynamics, Prentice-Hall, Inc., Englewood Cliffs, N.J.

Sokolnikoff, I. S. and R. M. Redheffer, (1966), Mathematics of Physics and Modern Engineering, McGraw-Hill Book Co., New York, N.Y.

Underhill, H. W. and M. J. Atherton, (1964), "A Coastal Ground Water Study in Libya and a Discussion of a Double Pumping Technique," Journal of Hydrology, Vol. 2, pp. 52-64.

Weinberger, H. F., (1965), A First Course in Partial Differential Equations, John Wiley & Sons, Inc., New York, N.Y.

Wickersham, G., (1977), "Review of C. E. Jacob's Doublet Well," Ground Water, Vol. 15, No. 5, pp. 344-347.